ELUCIDATION OF THE CONFORMATIONS OF BIOLOGICAL COMPOUNDS BY NUCLEAR MAGNETIC RESONANCE SPECTROSCOPY

by

ROXANNE DESLAURIERS

A thesis submitted to the University of Ottawa in partial fulfilment of the requirements for the degree of Doctor of Philosophy.

April 1972

ELUCIDATION OF THE CONFORMATIONS OF BIOLOGICAL COMPOUNDS BY NUCLEAR MAGNETIC RESONANCE SPECTROSCOPY

by
Roxanne Deslauriers.

SUMMARY

This thesis deals with the applications of NMR spectroscopy to the study of conformations of biologically active molecules. The first three chapters are intended as a brief introduction to the principles of NMR spectroscopy. Chapters 4 and 5 deal with the conformational analysis of small molecules such as amphetamines and nucleosides. In Chapter 6 applications of NMR spectroscopy to the study of peptides such as oxytocin and vasopressin are discussed. The isolation of porcine neurophysin for the purpose of NMR study is described. In Chapter 7, the newer technique of ^{13}C NMR is used to study oxytocin and related protected peptides.

Conformational Studies on Amphetamines.

The NMR spectra of amphetamine (α-methyl-β-phenylethylamine) and amphetamine derivatives (N-methyl amphetamine, o-methoxy methamphetamine and N-benzyl-N,α-dimethylphenethylamine in aqueous solutions have been analyzed. The methyl and methylene protons give rise to ABC type spectra, which have been analyzed by a first-order approach and by use of the computer program LAOCOON II. The spectrum of amphetamine.HCl is 'deceptively' simple. Studies in mixed solvents of DMSO-d_6

and D_2O have allowed an estimate of the methyl and methylene proton chemical shifts and coupling constants. Free rotation about the ethane linkage is possible in these compounds. The preferred rotamer in all cases is the trans phenyl-amino rotamer.

NMR Studies of Rare Nucleosides found in Transfer RNA.

A) Conformation of Dihydrouridine in Aqueous Solution.

The conformation of dihydrouridine in aqueous solution has been analyzed. The base is in the anti conformation with respect to the ribose ring. The ribose ring is not in any of the classical ring conformations. The ribose ring is interconverting rapidly between various conformations. The equilibrium is shifted towards the C_2' endo and C_3' exo conformational equilibrium. Raising the temperature to 60°C does not change the ring conformation. Rapid rotation about the exocyclic C_4'-C_5' bond occurs but the gauche-gauche rotamer is preferred. At 60°C this preference is less, as expected.

B)Conformation of β-pseudouridine at Basic pD.

It has been proposed that the anomalous U.V. spectrum of β-pseudouridine at basic pH could be caused by a hydrogen bond between the C_5'-OH of the exocyclic hydroxymethyl group and the C_4 oxygen of the base. It has been demonstrated by NMR that this is not the case because the base is in the anti conformation, therefore, the C_4 oxygen is not available for hydrogen bonding. A hydrogen bond between the OH of the exocyclic hydroxymethyl group and the C-5,C-6 double bond on the

base remains possible, as proposed from infra red studies on model compounds in carbon tetrachloride.

C) Conformation of Rare Nucleosides in Dimethyl Sulfoxide and Water.

The conformations of the nucleosides, uridine, β-pseudouridine and dihydrouridine in dimethyl sulfoxide have been analyzed and the OH couplings reported. No large conformational difference in any of the molecules can be seen in D_2O and DMSO-d_6. No changes in the sugar-base torsion angle were detected. Measurement of the hydroxyl proton couplings have allowed an estimate of the rotamer populations about the C-O bonds.

NMR Studies of Neurohypophyseal Hormones: Oxytocin and Lysine Vasopressin.

Comparison of spectra of lysine vasopressin and oxytocin in aqueous solution shows an upfield shift in the aromatic resonances from lysine vasopressin. Such upfield shifts are not present in 4-Pro,8-Ile oxytocin or 4-Pro,8-Gln oxytocin either. The upfield shifts of the Tyr and Phe aromatic resonances are attributed to stacking of the aromatic rings. The aromatic dipeptides L-tyrosyl-L-tyrosine, L-tyrosyl-L-phenylalanine, L-phenylalanyl-L-phenylalanine and L-phenylalanyl-L-tyrosine were examined in D_2O solutions. Upfield shifts in the dipeptides, when compared to the corresponding monomers, indicate that the time-average

conformation of the dipeptide is more that of a stacked dipeptide than an unstacked dipeptide. The tendency to stack is however smaller than that observed in lysine vasopressin. The positions of the aromatic resonances in the dipeptides are strongly pH dependent.

^{13}C NMR Studies on Oxytocin and Related Protected Peptides.

^{13}C NMR spectra were obtained from protected precursor peptides of oxytocin in DMSO-d_6 solutions. Protected tri-, tetra-, penta-, hexa-, hepta-, octa- and nonapeptides were examined. All the carbon resonances in the peptides were assigned. A number of changes occur in the spectra when the protected nonapeptide is cyclized to form oxytocin. The α carbon resonances of the cyclic moiety move downfield while the β-carbon resonances move upfield by various amounts. Essentially no changes are seen in the terminal tripeptide. ^{13}C NMR is shown to be useful in detecting cis and trans isomers of Pro in peptides. The spectrum of 1-deamino lysine vasopressin was also examined and compared to that of oxytocin.

ACKNOWLEDGEMENTS.

I am grateful to Drs B. Belleau and D.S. Layne of the Biochemistry Department for the kind assistance they provided during the course of my graduate studies.

I wish to thank Dr. R.R. Fraser of the Chemistry Department for the use of his Varian HA-100 NMR spectrometer and helpful suggestions.

I am indebted to Dr. I.C.P. Smith of the National Research Council of Canada for the use of his laboratory, the equipement therein and for continuous guidance in the course of my research. I wish to express my appreciation to Dr. R.D. Lapper for the use of his computer programs, for reading my thesis and offering constructive criticism. I am grateful to Dr. R.L. Somorjai for reading and correcting my thesis and also the time he spent in explaining the physical aspects of NMR.

I acknowledge the National Research Council of Canada, le Ministère de l'Education du Québec and the Ontario-Québec Permanent Commission for financial support during my years as a graduate student.

The Biochemistry Division of the National Research Council allowed me to use its laboratory facilities, for which I am very grateful.

FOREWORD

This thesis deals with the applications of NMR spectroscopy to the study of conformations of biologically active molecules. Because the chapters cover essentially different topics, references are placed at the end of each chapter. In this way each chapter constitutes a seperate entity.

The first three chapters are intended as a brief introduction to the principles of NMR spectroscopy. Chapters 4 and 5 deal with conformational analysis of small molecules such as amphetamine and dihydrouridine. In Chapter 6 applications of NMR spectroscopy to the study of peptides and proteins are discussed. In Chapter 7, the newer technique of ^{13}C NMR spectroscopy is used to study oxytocin and protected precursor peptides of oxytocin.

TABLE OF CONTENTS

LIST OF TABLES

LIST OF FIGURES.

CHAPTER 1.

PRINCIPLES OF NUCLEAR MAGNETIC RESONANCE (NMR).

1.1 Phenomenological Description of NMR.

1.2 Characteristics of an NMR Spectrum.

1.2.1 The Chemical Shift.

1. Definition
2. Factors Influencing the Chemical Shift of a Nucleus in a Molecule.
3. Hydrogen-Bonding.
4. Solvent Effects.

1.2.2. The Intensity of Resonance Lines.

1.2.3. Spin-spin Splitting.

1.3 Note on ^{13}C NMR Spectroscopy.

1.4 References.

1.1 Phenomenological Description of NMR.

A number of textbooks have been written which deal with various aspects of the NMR phenomenon (1 - 10). In view of this, I will only outline the principles of NMR. I will mention mainly the facts which are needed in order to interpret the spectra of compounds I have studied.

The proton has a spin quantum number, I, of 1/2 as does the neutron and the electron. For nuclei other than hydrogen the spin angular momenta of the neutrons and the protons couple to give an observable total spin. The total spin of the nucleus can be integral, half integral or zero. The NMR phenomenon depends on the existence of nuclear spin; nuclei with a spin quantum number equal to zero, such as ^{12}C and ^{16}O do not give rise to resonance. This greatly simplifies the spectra of organic compounds. The nucleus most commonly studied in organic compounds is ^{1}H.

Proton magnetic resonance arises in the following manner:

The hydrogen nucleus, which has a spin of 1/2, behaves as if it were a spinning body and therefore possesses an angular momentum $\vec{P}$. This angular momentum can be calculated as if it were an orbital angular

momentum. For instance, (Fig. 1.1A) a mass m, orbiting about a centre with a velocity $\vec{v}$ at a distance $\vec{r}$ from the centre will have an angular momentum which is the product of the velocity and the radius

$$\vec{P} = m \vec{v} \times \vec{r}$$

$\vec{P}$ is a vector which is directed perpendicularly to the plane of $\vec{v}$ and $\vec{r}$.

The nucleus also behaves as a spinning charge q and therefore possesses a magnetic moment $\vec{\mu}$ (Fig. 1.1B). A charge q circulating at a distance r from a central point with a velocity v, generates a current i.

$$i = q \text{ (frequency of rotation)}$$

$$\text{Freq. of rot.} = \frac{v}{2\pi r}$$

The magnitude of the magnetic moment μ is equal to the product of the current and the area A covered by the rotation of the spinning charge.

$$\mu = i A$$

therefore

$$\mu = (q) \frac{v}{2\pi r} (\pi r^2)$$

Figure 1.1A

Angular momentum associated with a spinning mass.

Figure 1.1B

Magnetic moment associated with a spinning charge.

A

m = mass

$\vec{r}$ = radius

$\vec{v}$ = angular velocity

$\vec{P}$ = angular momentum

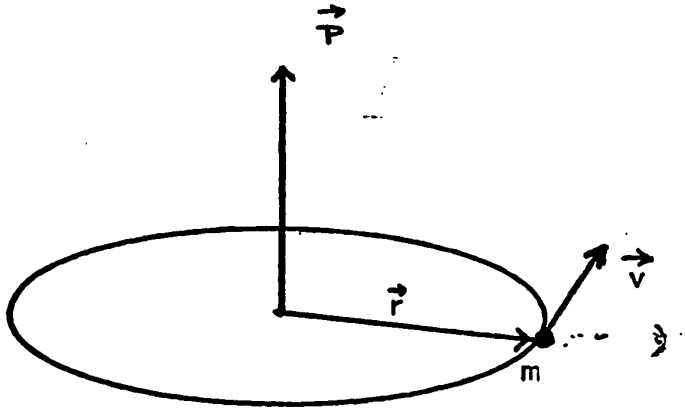

$$\vec{P} = m\,\vec{v} \times \vec{r}$$

B

q = charge

$\vec{r}$ = radius

$\vec{V}$ = angular velocity

A = area of orbit

i = current

$\vec{\mu}$ = magnetic moment

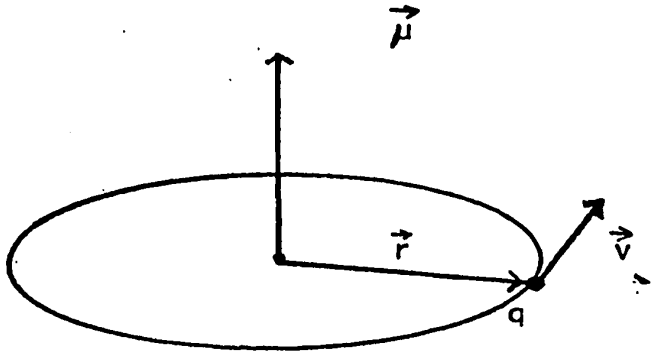

$$\mu = i\ A$$

$$i = q\,\frac{v}{2\pi r}$$

$$\mu = \frac{q\,v\,r}{2}$$

$$\mu = \frac{q\ v\ r}{2}$$

$\vec{\mu}$ is a vector and, like $\vec{P}$, is also perpendicular to the plane formed by $\vec{v}$ and $\vec{r}$. $\vec{P}$ and $\vec{\mu}$ are proportional to each other following the relationship

$$\vec{\mu} = g \frac{q}{2m} \vec{P}$$

the g is introduced because we are dealing with spin motion and not orbital motion.

When the nucleus is placed in a magnetic field it precesses. This is because it possesses both angular momentum and magnetic moment. A magnetic moment $\vec{\mu}$ in an applied field $\vec{B}_o$ feels a torque $\vec{\tau}$ equal to

$$\vec{\tau} = \vec{\mu} \times \vec{B_o}$$

The torque tries to align the magnetic moment with the field.

The angular momentum causes the nucleus to behave like a gyroscope and keeps the magnetic moment from aligning with the field. The magnetic nucleus will precess about an axis parallel to the applied field (Fig. 1.2)

Figure 1.2

Precession of a magnetic nucleus about the direction of an applied magnetic field.

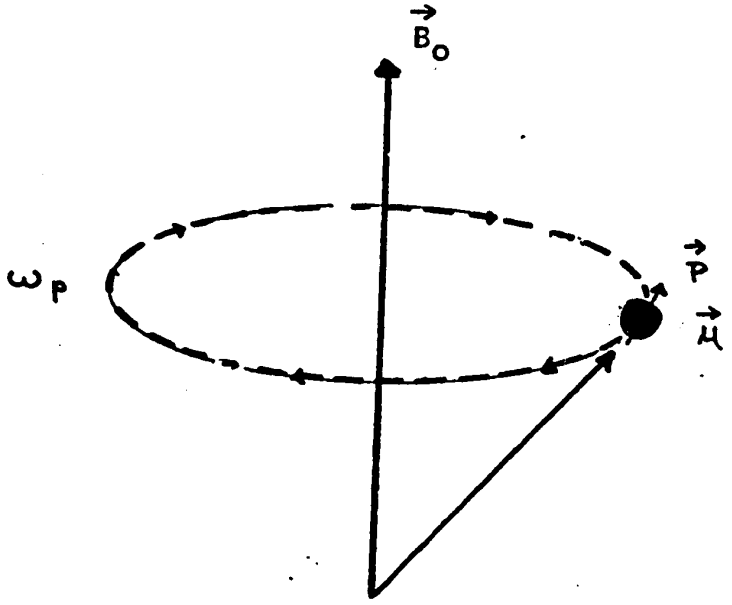

$\vec{B}_o$ = applied magnetic field

$\vec{\mu}$ = magnetic moment

$\vec{p}$ = angular momentum

$\vec{\tau}$ = torque

ω_p = precession velocity

$$\vec{\tau} = \vec{\mu} \times \vec{B}_o$$

q = charge

m = mass of proton

g = nuclear g factor

$$\omega_p = \frac{\mu}{p} B_o = g\left(\frac{q}{2m}\right) B_o$$

The angular velocity of precession ω_p, is proportional to the applied field $\vec{B}_o$. The relationship is described in the following formula:

$$\omega_p = \frac{\mu}{P} B_o$$

The ratio of the magnetic moment $\vec{\mu}$ to the angular momentum $\vec{P}$ is called the magnetogyric ratio, γ. The preceeding equation can be rewritten as

$$\omega_p = \gamma B_o$$

The corresponding frequency, known as the Larmor frequency, is

$$\nu_p = \frac{\gamma}{2\pi} B_o$$

Because the proton has a spin of 1/2 it has two possible energy states. In the presence of an applied magnetic field the spin can align with or against the field (Fig. 1.3). In a sample of ^1H nuclei there will be slightly more protons in their lower energy states, with their moments parallel to the field. The number of protons in each of the two possible states follows

Figure 1.3

Conditions required for an oscillating magnetic field to induce transitions between the two possible energy states of protons.

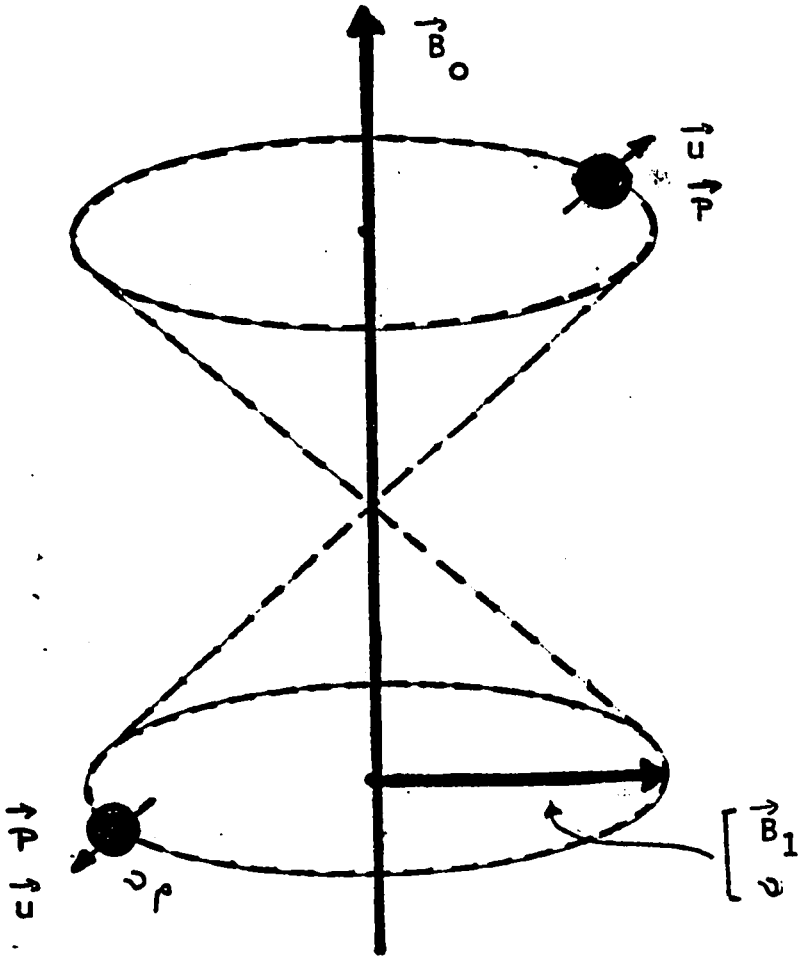

$\vec{B}_1$ = oscillating magnetic field

υ = frequency of oscillating magnetic field

$\vec{B}_0$ = applied magnetic field

υ_p = precession frequency of nucleus

RESONANCE CONDITION:

$$\upsilon = \upsilon_p = g\left(\frac{q}{2m}\right) B_o$$

a Boltzmann distribution. The difference between the number of protons with spin up and spin down is only 1 part in 10^5. This difference in population depends on temperature and magnetic field strength.

If a small, variable, oscillating field ($\vec{B}_1$) is applied perpendicularly to $\vec{B}_o$ it can, under well-defined conditions, induce transitions between the two energy states. Induced transitions will occur when the field $\vec{B}_1$ is made to oscillate at the frequency υ_p, the previously-mentioned precession frequency (Fig. 1.3)

The transfer of the proton from its lower energy state to the higher energy state is due to an absorption of energy. When the proton drops fron the higher energy state to the lower energy state there will be a release of energy. Since there are more protons in the lower energy state there will be a net absorption of energy.

The energy absorption will occur only when the oscillating field is in resonance, i.e. when the frequency of the oscillating field $\overrightarrow{B_1}$ is the same as the precession frequency of the magnetic nucleus about the direction of the applied field $\overrightarrow{B_o}$.

Recording of spectra can be done by measuring the change in power that occurs when resonance takes place, i.e. the absorption of energy that takes place when the nucleus 'flips' from one state to the other. Resonance can be achieved in two ways, either by keeping the magnetic field constant and varying the the oscillating field until the resonance condition is produced or, alternatively, by keeping the oscillating frequency constant and varying the magnetic field until resonance occurs. Both procedures give the same result.

As can be seen from an NMR spectrum, not all protons in a compound resonate at the same frequency. This is because the magnetic field felt by a nucleus depends on the chemical environment of that nucleus. The following section deals with the characteristics of an NMR spectrum and describes qualitatively their origins.

1.2 Characteristics of an NMR Spectrum.

When examining a proton NMR spectrum a number of features are present which aid in structure and conformation determination. These are:

1) Chemical shift.
2) Intensity of resonance lines.
3) Spin-spin splitting.
4) Line width.

1.2.1. The Chemical Shift.

1.2.1.1. Definition.

The chemical shift of a resonance line is the difference in position between the resonance line and a virtually invariant line position provided by a standard reference sample. Tetramethylsilane (TMS) is a common reference substance used for non-aqueous solutions. For aqueous solutions the main references used are: hexamethyldisiloxane (HMS or HMDS), sodium,2,2-dimethyl-2-silapentane-5-sulfonate (DSS) and sodium 3-trimethylsilylpropionate (TSP).

Chemical shifts are usually reported in parts per million (p.p.m.) from the reference. The chemical

shift on this scale is symbolized by δ. In frequency-swept spectrometers δ is defined as

$$\delta = \frac{\upsilon - \upsilon_R}{\upsilon_o} \times 10^6$$

where υ is the resonance frequency (in Hertz) of the observed line in a particular magnetic field, υ_R is the resonance frequency of the reference compound in the same magnetic field and υ_o is the operating frequency of the spectrometer.

1.2.1.2 Factors Influencing the Chemical Shift of a Nucleus in a Molecule.

A) Fields produced by surrounding electrons.

The chemical environment of a given nucleus influences the frequency at which it resonates because the surrounding electrons, which constitute the chemical environment, shield the nucleus from the applied magnetic field.

The applied magnetic field sets up a circulating current in the electron orbits around the nucleus (Fig. 1.4). This produces a slight field $\Delta\vec{B}$ at the nucleus which opposes the incident field $\vec{B_o}$. The effective magnetic field is ($\vec{B_o} - \Delta\vec{B}$). Because resonance frequency depends on the field strength at the nucleus the applied field will have to be increased so as to

Figure 1.4

Circulation of current in the electron orbitals surrounding a nucleus in a magnetic field.

N = nucleus

e^- = electron

$\vec{B}_o$ = applied magnetic field

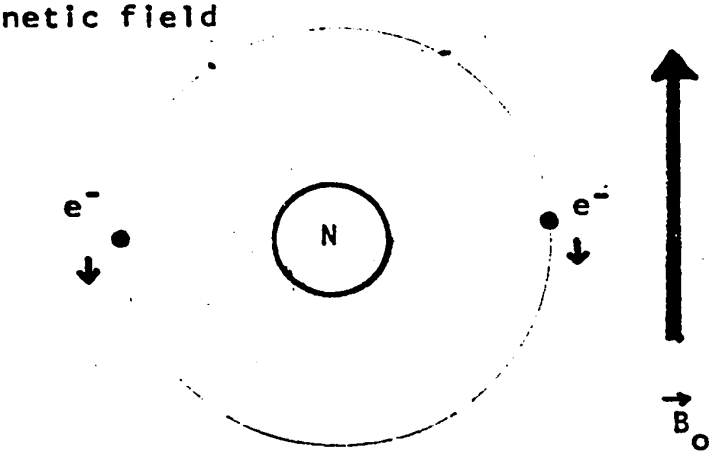

$\vec{\Delta B}$ = Induced field due to electrons.

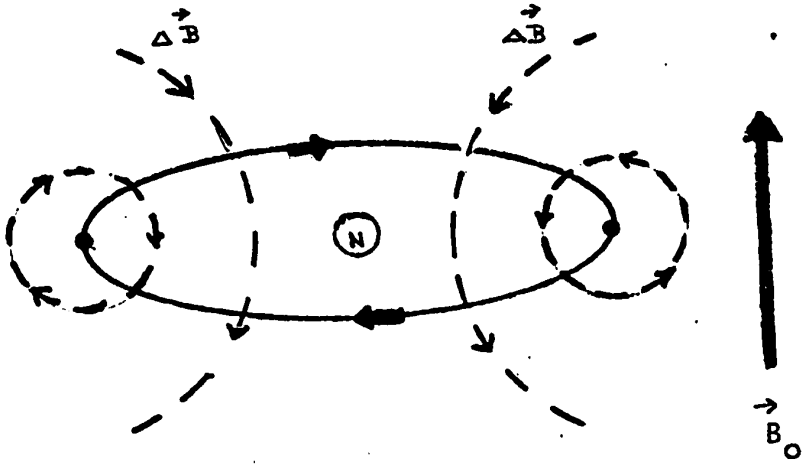

EFFECTIVE MAGNETIC FIELD: $(\vec{B}_o - \vec{\Delta B})$

produce the required field at the nucleus.

B) Electronegativity of neighbouring atoms.

Neighbouring atoms can also cause changes in the shielding of the nucleus under study. For example the spectrum of a methyl halide reflects the electronegativity of the halogen. The halogen decreases electron density around the hydrogens in the methyl group. The halogen deshields the methyl group, it partially removes the electron shielding effect. The hydrogen nuclei are more exposed to the applied field and resonate at a lower value of the applied field $\overrightarrow{B_o}$. The reverse also occurs; electron-donating groups increase the electron density around the nucleus and therefore are said to shield the nucleus. The nucleus is less exposed to the applied field and the field strength must be increased in order to produce resonance at a given frequency. Resonance is said to occur at higher field.

C) Fields produced by anisotropic groups.

A second shielding mechanism is the local diamagnetic circulation in anisotropic groups. In molecules, electrons are distributed over bonding orbitals which are not spherically symmetric. Such molecules are said to be anisotropic (they exhibit

different properties or effects when tested with respect to different axes).An applied magnetic field produces a current in the electron orbitals. This current induces a secondary magnetic field which can shield or deshield adjacent nuclei depending on the orientation of the induced field with respect to the bond.

For instance, Figure 1.5 depicts the effect of a magnetic field $\vec{B}_o$ on the electrons of an atom A. The magnetic field induces a current in the electron orbital. This current produces a secondary field which can affect the neighbouring nucleus X. When the A-X bond axis is perpendicular to the applied magnetic field, the field produced by the current in the electron orbitals deshields the X nucleus. When the A-X bond is parallel to B_o, X is shielded.

D) Fields produced by aromatic rings.

Shielding also occurs when interatomic diamagnetic currents are induced in aromatic rings. Aromatic rings, such as those in tyrosine and phenylalanine have cylindrically delocalized π electrons which circulate in parallel planes above and below the plane of the ring atoms (Fig. 1.6). The presence of a strong magnetic field induces a ring current. Associated with the ring current is a large magnetic field, which is a strong source of shielding and deshielding. The shielding

Figure 1.5

Effect of a magnetic field $\vec{B}_o$ on anisotropic groups.

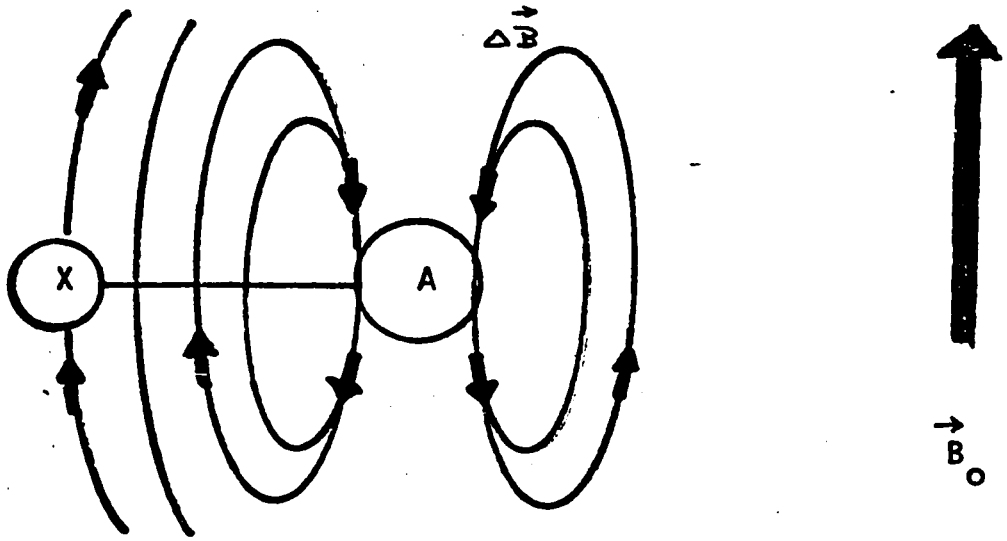

X DESHIELDED

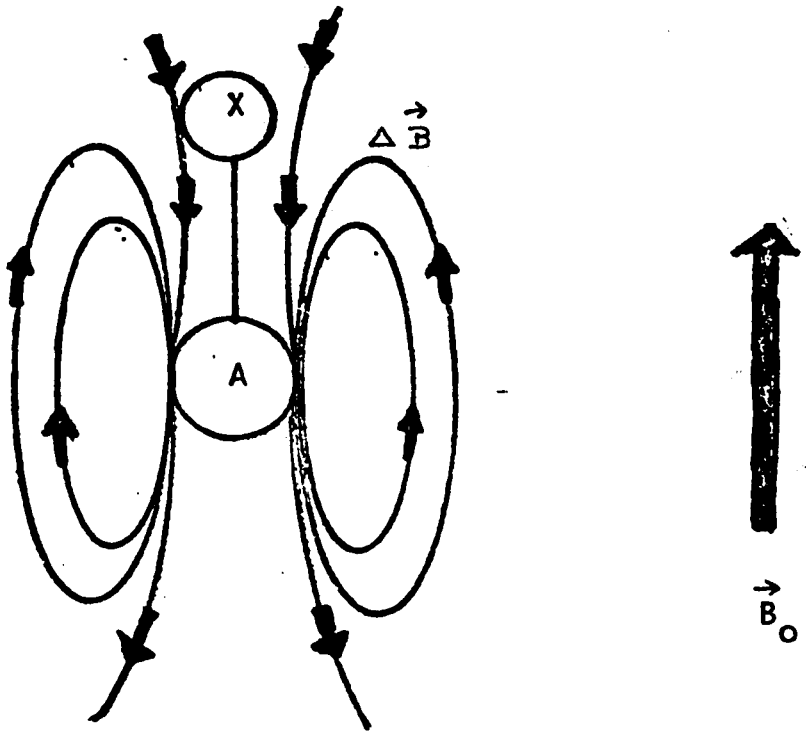

X SHIELDED

or deshielding effect depends on the position of the nucleus under study with respect to the ring. Above and below the ring shielding occurs. On either side of the aromatic ring, deshielding occurs (Fig. 1.6)

1.2.1.3 Effect of Hydrogen-Bonding on the Chemical Shift.

Chemical shifts can yield information about the presence or absence of hydrogen bonds in compounds. The resonance of a proton involved in a hydrogen bond is shifted to low field. This implies that a hydrogen-bonded proton is deshielded as compared to a non-hydrogen-bonded proton.

No clear-cut theoretical interpretation has been given to explain the observed downfield shifts of hydrogen-bonded protons. Pople, Schneider and Bernstein (2) consider two effects when examining a hydrogen bond formed between a molecule H-X and a donor atom,Y, in another molecule.

1°) The anisotropy of Y. Currents induced in the Y atom will change the magnetic field experienced by the hydrogen atom in X-H. This gives rise to upfield shifts rather than downfield shifts, this however is only a small effect.

2°) The electrostatic nature of the hydrogen bond. Both X and Y are electronegative and therefore

Figure 1.6

Production of zones of shielding and de-shielding in aromatic rings by an applied magnetic field.

DELOCALIZED π ELECTRONS IN AROMATIC RINGS.

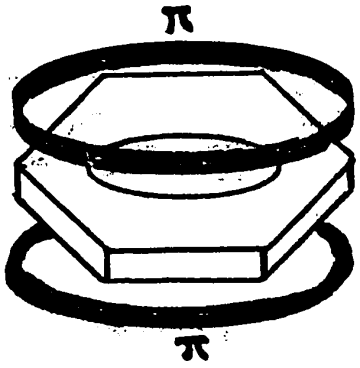

PRESENCE OF STRONG MAGNETIC FIELD B_o INDUCES RING CURRENT

LARGE MAGNETIC FIELDS ARE ASSOSCIATED WITH THE RING CURRENTS. INDUCED MAGNETIC FIELD OPPOSES APPLIED MAGNETIC FIELD.

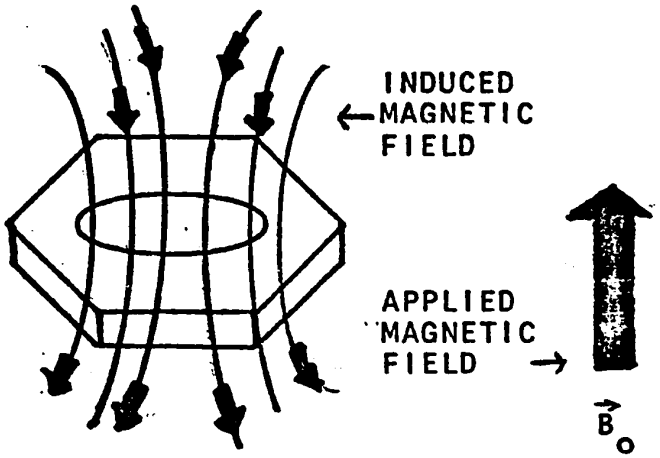

INDUCED MAGNETIC FIELD IS STRONG SOURCE OF LONG RANGE SHIELDING AND DESHIELDING

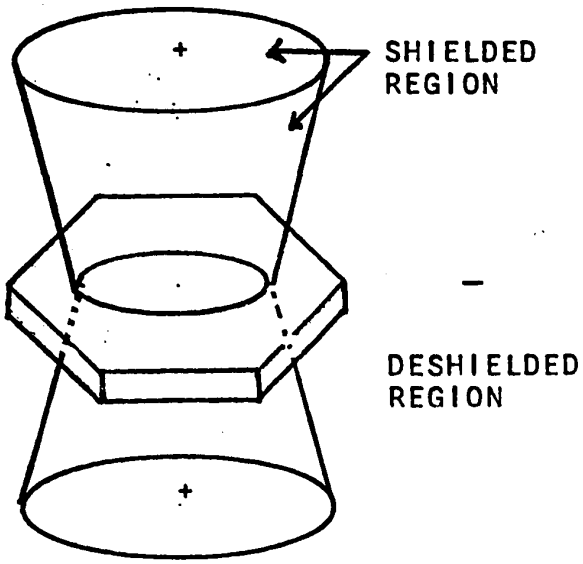

tend to decrease the electron density around the proton. The shielding normally caused by the surrounding electrons decreases and the resonance moves to lower field.

Lynden-Bell and Harris (3) point out that, in actual fact, electron density around a hydrogen-bonded proton is probably greater than around a non-hydrogen bonded proton. As an example, they offer the O-H ··· O bond where the O,O distance is smaller then the van der Waals diameter of the O. This implies that the hydrogen-bonded proton is shielded by the electrons of both O atoms. Therefore resonance should occur at higher field.

In spite of the lack of explanation as to the cause of the downfield shifts which occur in hydrogen-bonded protons, the phenomenon does yield valuable conformational information. This has been demonstrated in the study of cyclic antibiotics in particular (11 - 12).

Hydrogen-bonded and non-hydrogen bonded protons can be observed in the same spectrum if the lifetime in each state is larger than 1/H bond shift (measured in Hertz). Values of 10^{-2}, 10^{-3} seconds are usually found. The two separate signals observed correspond to the two environments in which the proton can be found.

When only a single sharp line is seen it implies that the lifetimes in each state are considerably shorter than 10^{-2} seconds. An average resonance for hydrogen-bonded and non-hydrogen bonded species is observed.

Measurement of hydrogen bonds.

A method now common for studying hydrogen bonds in peptides involves the effect of temperature and dilution on hydrogen-bonded systems. The proposed hydrogen bonded structure for gramicidin -S (11), valinomycin (12), oxytocin (13) and lysine vasopressin (14) are supported by temperature studies of the amide proton resonances

In solvents such as dimethyl sulfoxide (DMSO) hydrogen bonds could be formed intramolecularly or intermolecularly. Intermolecular bonds could be either to the solvent molecules or the solute molecules. Intermolecular bonds to solute molecules can be minimized by using dilute solutions. Intramolecular hydrogen bonds and intermolecular hydrogen bonds between solute and solvent are distinguished by their response to temperature changes. In solvents such as dimethyl sulfoxide, water, methanol, it appears that increases in temperature cause intermolecularly-bonded amide resonances to shift to higher fields than intramolecularly hydrogen bonded amides.

1.2.1.4 Solvent Effects.

One often finds that the chemical shift of a proton in a molecule changes from solvent to solvent. In fact, this change in chemical shift is the difference in the effect of the solvent on the solute molecules and on the internal reference. Solvent effects can be divided into three categories (3): polar solvent effects, solvent magnetic anisotropy effects and specific interactions between solute and solvent.

Polar solvent molecules form 'solvent cages' around polar solutes. The solvent molecules change the shielding of the solute molecules by an electric field effect. The polar solvents increase the inductive effect of electronegative substituents in the solute molecules. Therefore, the protons in solute molecules will be deshielded. Non-polar solutes are less affected by polar solvents. A proton of a polar solute will be affected differently from a proton in a non-polar reference compound when the solvent is polar and when the solvent is non-polar. This causes the 'solvent shift' .

Solvents such as benzene create large effects on the resonance positions of solutes which are not spherically symmetric. This is due to the magnetic anisotropy of the aromatic ring. There is a preferred orientation of solute

and solvent molecules with respect to one another. The ring current effect of benzene will shield or deshield specific parts of solute molecules depending on their orientation with respect to the plane of the ring.

Specific interactions can occur between solute and solvent or between two solute molecules. Intermolecular hydrogen-bonding is an example of such phenomena. The extent of intermolecular hydrogen-bonding between solute molecules can however be measured by dilution studies, as mentionned in section 1.2.1.3.

1.2.2 Intensity of Resonance Lines.

A readily observable parameter in an NMR spectrum is the relative intensity of the peaks. The intensity of a peak involves only the number of nuclei associated with a particular chemical shift and is independent of the nature of the chemical environment. Because peaks are not infinitely narrow, a more accurate measurement of the number of protons causing a particular resonance is gained from measuring the area under a peak, this is called the integrated intensity.

1.2.3. Spin-spin Splitting.

Spin-spin coupling is responsible for the fine structure associated with the individual resonances. It occurs because of mutual interaction between nuclei in the same molecule via the intervening electrons. Spin-spin coupling can sometimes occur via a through-space mechanisn.

The spin-spin splitting is measured in Hertz and is independent of the strength of the applied field. The magnitude of the splitting is a function of the geometry of the molecule.

The spin-spin coupling usually decreases as the distance between the two coupled nuclei increases.

Figure 1.7 illustrates how spin-spin coupling arises. In this example a nucleus of spin 1/2 (^1H) is chemically bonded to a nucleus of spin 1 (^2D). In both atoms the single electron associated with each nucleus will tend to align itself so that its magnetic moment vector lies parallel to the nuclear magnetic moment vector. In addition to this nucleus-electron interaction, these two electrons which constitute the H-D bond interact with each other so that their magnetic moment vectors tend to be antiparallel. As a result it can be seen in Figure 1.7 that the magnetic moment vectors of the two nuclei are antiparallel. This is the stable configuration for the system.

The above gives a path by which the spin-spin coupling interaction between nuclei can be transmitted. However as an explanation it cannot yield the existence of more than one energy level. Taking into account the existence of excited states

Figure 1.7

One mechanism of spin-spin coupling.

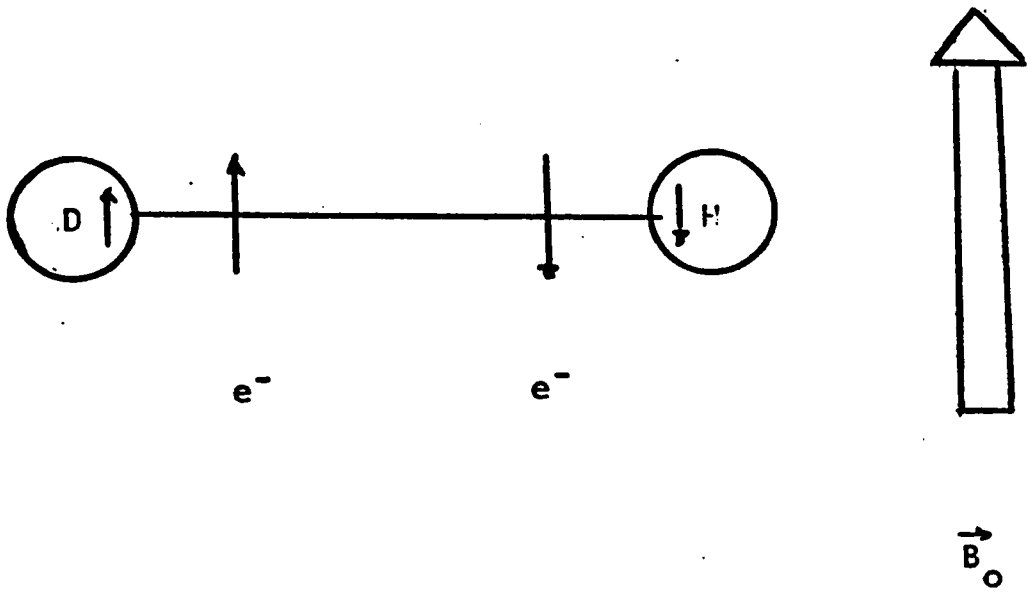

NOTE: Arrows indicate the direction of the nuclear and electronic magnetic moments.

of the electrons it is possible to have the magnetic moments of the nuclei parallel to each other.

When the hydrogen nuclear magnetic moment is parallel to the applied field, it reinforces the applied field, therefore the deuterium resonance will occur at lower field. When the hydrogen nuclear magnetic moment is antiparallel to the applied field it decreases the field and the deuterium resonance occurs at higher field. The deuterium resonance will not therefore be a single line but a double line, a doublet. The separation between the lines is the coupling constant which is measured in Hertz.

The interaction between nuclei is reciprocal and the hydrogen resonance will also be a doublet, with the same splitting between the lines.

1,1 dibromoethane provides a classical example of spin-spin splitting (Fig.1.8). The methyl resonance is split into a doublet by the two possible orientations of the spin of the methine proton. The methine resonance is a quartet where the ratio of the line intensities is 1:3:3:1. This occurs because there are three times as many ways of orienting two nuclei in one direction and one nucleus in another direction as there are ways of orienting three nuclei in one direction.

From this spectrum it can be seen that the number of lines associated with a particular nucleus is

Figure 1.8

Idealized spectrum of 1,1 dibromoethane.

SPECTRUM OF 1,1 DIBROMOETHANE

$Br_2CH - CH_3$

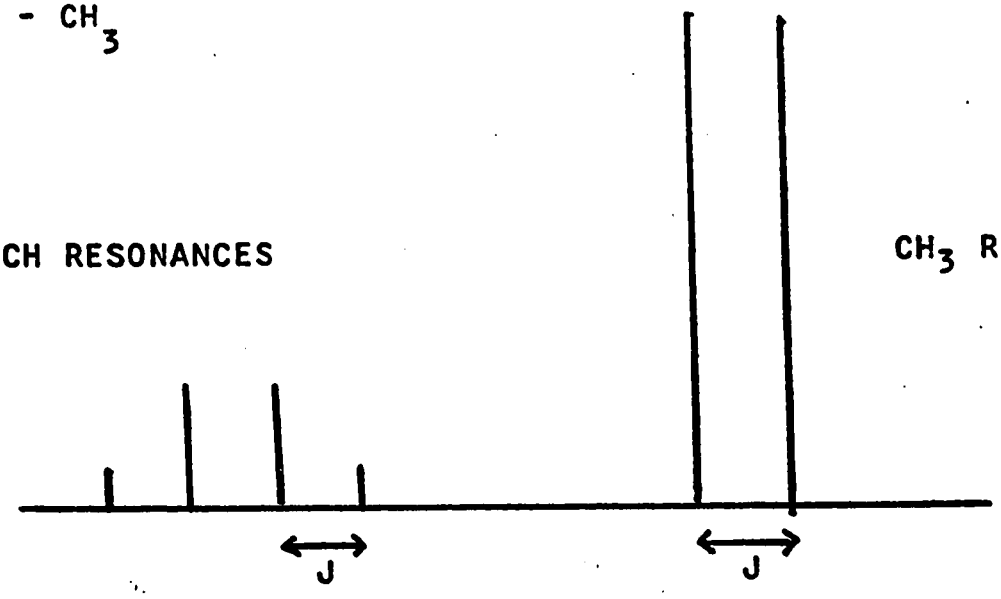

ENERGY LEVELS:

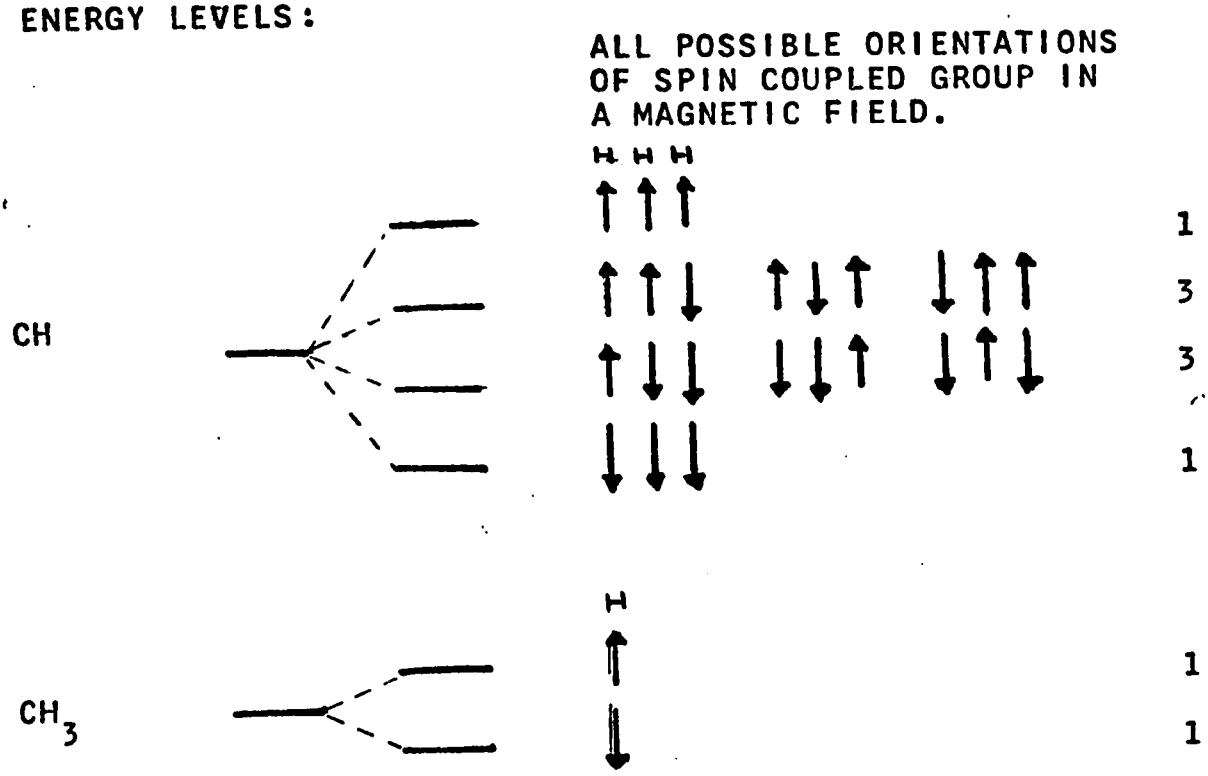

UNPERTURBED

PERTURBED BY SPIN-SPIN COUPLING

equal to (n+1), where n is the number of neighbouring protons. In the case of nuclei with spin other than 1/2 a more general formula is used. n nuclei with spin I split the resonances of other nuclei into (2nI + 1) lines. For protons the intensity of the lines in the multiplet follows a binomial expansion.

The spectrum of dibromoethane is a so-called 'first order' spectrum. A spectrum is considered 'first order' if the coupling constants are small when compared to the difference between the chemical shifts of the coupled nuclei. When coupling constants and chemical shift differences are of the same order of magnitude, the spectrum becomes so-called 'second-order' , Chemical shifts and coupling constants usually cannot be measured directly from the spectrum in these cases.

Methods of analysing spectra in order to find coupling constants and chemical shifts are outlined in the next chapter.

1.3 Note on ^{13}C NMR Spectroscopy.

^{13}C has a spin of 1/2 as does the proton. All the principles formulated to describe the resonance phenomenon in protons apply to ^{13}C. The magnetogyric ratio of ^{13}C is diffrent from that of protons, this is what keeps the spectra from overlapping. Protons in a magnetic field of 23,490 Gauss resonate at 100 MHz. ^{13}C in the same field resonates at 25.2 MHz. Modern spectrometers are built in such a way that one can observe either nucleus after a few changes in the spectrometer are made.

Chapter 7 deals with ^{13}C NMR spectroscopy of small peptides and oxytocin. Techniques particular to ^{13}C are described in that chapter.

1.4 References.

1. R.P. Feynman, R.B. Leighton and M. Sands, The Feynman Lectures on Physics, Addison-Wesley, Reading Mass., 1965, Vol II, Chapter 34.

2. J.A. Pople, W.G. Schneider and H.J. Bernstein, High Resolution Nuclear Magnetic Resonance, McGraw-Hill Book Co. Inc., N.Y., 1959

3. R.M. Lynden-Bell and R.K. Harris, Nuclear Magnetic Resonance Spectroscopy, Thomas Nelson and Sons Ltd., London, 1969

4. E.D. Becker, High Resolution NMR, Theory and Chemical Applications, Academic Press, N.Y. 1969

5. F.A. Bovey, Nuclear Magnetic Resonance Spectroscopy, Academic Press, N.Y., 1969

6. D.W. Mathieson, Nuclear Magnetic Resonance for Organic Chemists, Academic Press, London, 1967

7. A. Carrington, A.D. McLachlan, Introduction to Magnetic Resonance, Harper and Row, N.Y., 1967

8. A. Abragam, The Principles of Nuclear Magnetism, Oxford University Press, Amen House, London, 1961

9. T.C. Farrar and E.D. Becker, Pulse and Fourier Transform NMR, Introduction to Theory and Methods, Academic Press, N.Y., 1971.

10. J.W. Emsley, J. Feeney and L.H. Sutcliffe, High Resolution Nuclear Magnetic Resonance Spectroscopy, Pergamon Press Ltd, Oxford, 1965, Vol. I

11. M. Ohnishi and D.W. Urry, Biochem. Biophys. Res. Comm. 36 194 (1969)

12. M. Ohnishi and D.W. Urry, Biochem. Biophys. Res. Comm. 34 803 (1969)

13. D.W. Urry, M. Ohnishi and R.W. Walter, Proc. Natl. Acad. Sci. U.S. 66 111 (1970)

14. D.H. Von Dreele, A.1.Brewster, H.A. Scheraga, M.F. Ferger and V. du Vigneaud, Proc. Natl. Acad. Sci. U.S. 68 1028 (1971)

CHAPTER 2.

CHARACTERISTICS OF AB AND ABX SPECTRA.

CHAPTER 2.

CHARACTERISTICS OF AB AND ABX SPECTRA.

2.1 Definitions.

First order spectra occur only when the coupling between two nuclei is small compared to their difference in chemical shift. Coupling constants and chemical shifts can be measured directly from first order spectra. The coupling is the separation between the lines associated with a particular resonance and the chemical shift is the center of the multiplet.

In actual fact most spectra are second order. In these cases chemical shifts and coupling constants cannot be measured directly from the spectrum.

A certain amount of nomenclature is involved in the classification of spectra. Pople, Schneider and Bernstein (1) divide spectra as follows: the symbols A and B refer to two nonequivalent nuclei, of the same species, whose chemical shift difference is of the same order as the coupling between them, The symbols X and Y refer to a similar set of nuclei. The chemical shift difference between the AB nuclei and the XY nuclei is large. The AB and XY nuclei can be of the same species but this is not necessarily the case.

In an AMX spectrum, the chemical shift difference between the A, M and X nuclei is large when compared to the coupling between each pair.

Magnetically equivalent nuclei are represented by the same letter, a subscript is used to indicate the number of equivalent nuclei (eg A_2B_2). Magnetically equivalent nuclei all have the same chemical shift and all the nuclei in the set are coupled equally to any other single nucleus in the molecule.

Chemically equivalent nuclei, which are not also magnetically equivalent are indicated by repeating the same letter accompanied by a prime (eg AA'BB'). Chemically equivalent nuclei all have the same chemical shift but are not coupled equally to other nuclei in the molecule. Chemical equivalence can arise from molecular symmetry but it can also result from accidental coincidence of shielding effects.

2.2 Characteristics of AX and AB Spectra.

An AX spectrum consists of two lines if there is no coupling between the A and the X nuclei. If A and X are coupled four lines are observed, two A resonances and two X resonances. Doubling of lines occurs because the coupling changes the transition energies. A positive coupling implies that parallel spins (↑↑) are destabilized, therefore have more energy. Antiparallel spins (↓↑) will have less energy and be more stable.

This can be explained schematically. If we consider an AX system, there are four possible combinations of the spins of A and X. Spin +1/2 is designated by α, spin -1/2 is designated by β. The α spin is aligned parallel to the applied magnetic field and is of lower energy than the β spin which is antiparallel to the applied field. The four combinations of ↑ and ↓ spins are:

A X	Spin of A	Spin of B	Total spin (Fz)
$\alpha\,\alpha$	+1/2	+1/2	+1
$\alpha\,\beta$	+1/2	-1/2	0
$\beta\,\alpha$	-1/2	+1/2	0
$\beta\,\beta$	-1/2	-1/2	-1

Transitions occur only between states which will

yield an Fz difference of ± 1. This is shown in Figure 2.1

In the AX case where no coupling is present, transitions 4→2 and 3→1 have the same energy and therefore produce only one resonance line. The same applies to the X transitions 4→3 and 2→1.

When A and X are positively coupled the $\alpha\alpha$ and $\beta\beta$ states are destabilized and have higher energy. The $\alpha\beta$ and $\beta\alpha$ states have lower energies. The energy of the 3→1 transition is now different from that of the 4→2 transition therefore two A lines are observed. This is also the case for the X nucleus.

AB spectra consist of four lines but the intensities are different from the AX case. The intensity of a line reflects the probability of a particular transition. The energy levels of states 2 and 3 have changed; due to the proximity of the interacting energy levels of 2 and 3 each has taken some character of the other. This is dealt with in detail in most textbooks on NMR. (2,3).

A number of relationships have been determined which enable one to calculate the chemical shifts of the A and B nuclei from an observed spectrum. These are illustrated in Figure 2.2

Figure 2.1

Energy levels and transitions in AX and AB spectra with and without coupling.

ENERGY LEVELS AND TRANSITIONS BETWEEN ENERGY LEVELS.

STATE	AX	Fz
1	ββ	-1
2	βα	0
3	αβ	0
4	αα	+1

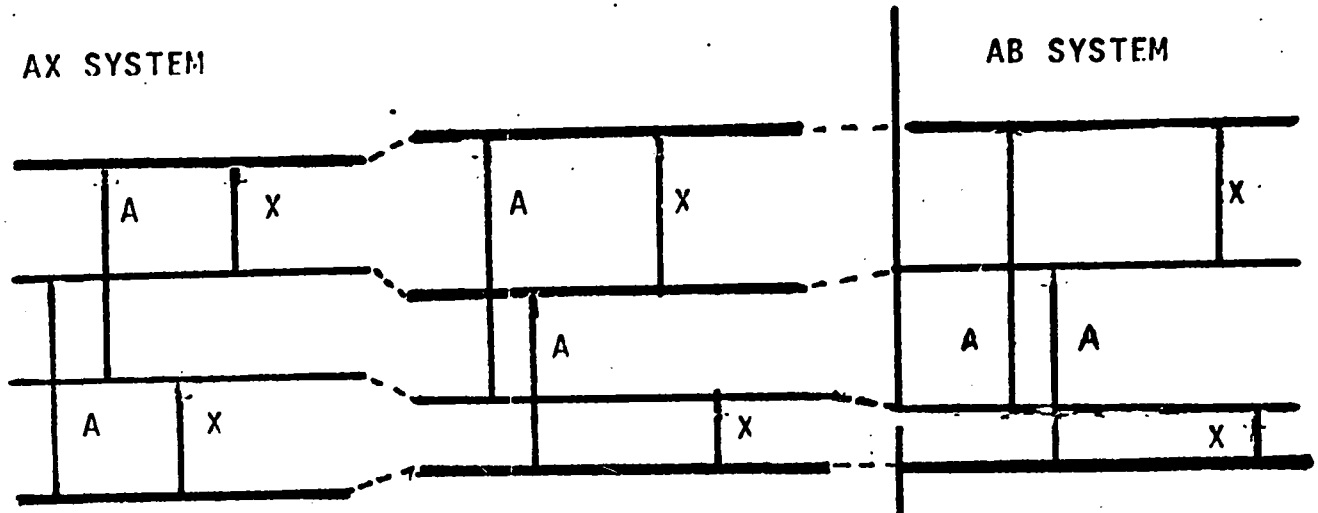

NO COUPLING | POSITIVE COUPLING | POSITIVE COUPLING

OBSERVEED SPECTRUM

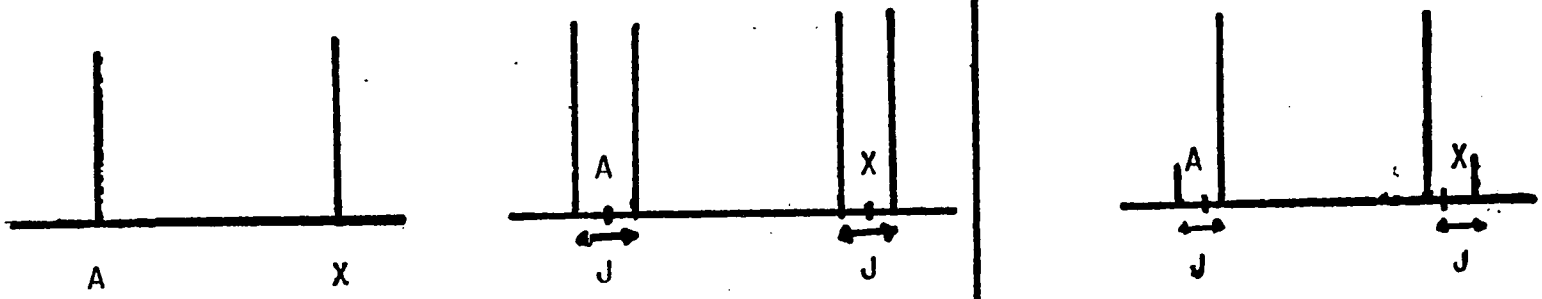

TRANSITION				
	4→2 3→1	4→3 2→1	3→1, 4→2	2→1, 4→3
			3→1, 4→2	2→1, 4→3

Figure 2.2

Characteristics of AB spectra.

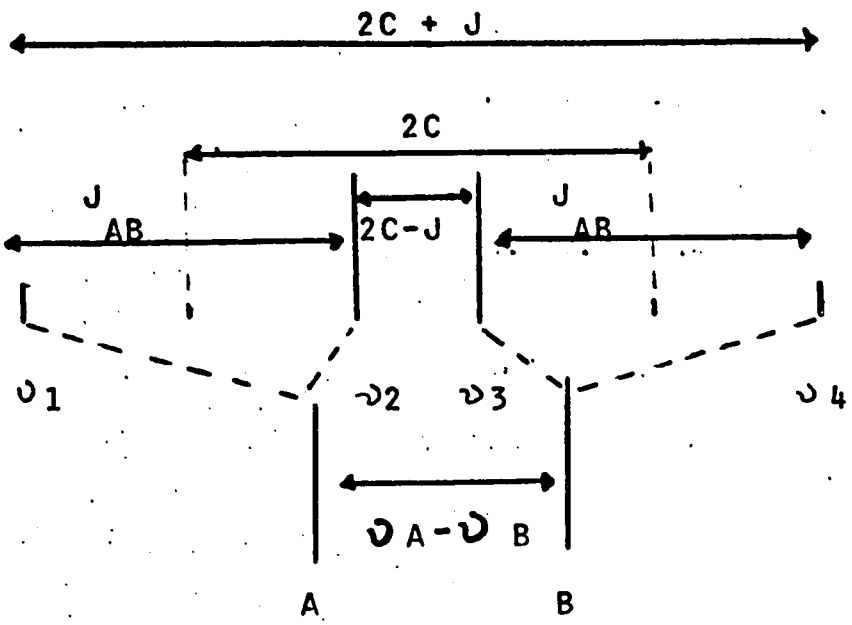

INTENSITY OF INNER LINES:

$$1 + \frac{J_{AB}}{\sqrt{J^2_{AB} + (\nu_A - \nu_B)^2}}$$

INTENSITY OF OUTER LINES:

$$1 - \frac{J_{AB}}{\sqrt{J^2_{AB} + (\nu_A - \nu_B)^2}}$$

DISTANCE BETWEEN CENTERS OF DOUBLETS:

$$2C = \left[(\nu_A - \nu_B)^2 + J^2_{AB}\right]^{1/2}$$

DISTANCE BETWEEN TWO OUTER LINES:

$$2C + J$$

DISTANCE BETWEEN TWO INNER LINES:

$$2C - J$$

SEPARATION OF TWO CHEMICAL SHIFTS:

$$\left[(\nu_1 - \nu_4)(\nu_2 - \nu_3)\right]^{1/2}$$

2.3 Characteristics of AMX and ABX Spectra.

2.3.1.Construction of Spectra.

Typical ABX spectra contain twelve to fourteen observable lines. In order to see the origin of most of these lines it is useful to simulate a spectrum. A first order approach yields twelve lines. This spectrum is shown in Figure 2.3. I have chosen

ν_A = 260 Hertz J_{AB} = 14.0 Hertz

ν_B = 270 Hertz J_{AX} = 8.0 Hertz

ν_X = 800 Hertz J_{BX} = 6.0 Hertz

ν = chemical shift

J = coupling constant

The procedure for building the spectrum is as follows:

1) The three chemical shifts are plotted to scale.

2) A and X lines are split symmetrically by the coupling J_{AX}. The two resulting lines in the A part are due to the two possible spin orientations of the X nucleus. ($\uparrow$ or $\downarrow$, i.e. with or against the applied magnetic field.) These two possible orientations are

indicated on the A lines. A positive coupling is indicated by placing ↑ on the high field line.

3) The process described in 2) is repeated on the B and the X lines using the BX coupling.

4) The AB coupling is used to split the A and B lines.

5) The result is a spectrum consisting of twelve lines. In actual fact this type of spectrum only arises in the AMX case.

A more accurate simulation can be achieved if the AB part of the spectrum is divided into two subspectra each of which consists of the lines which are due to the same spin orientation of the X nucleus.(either ↑ or ↓). This is shown in Figure 2.4.A 1^{o}

The correct spacings of the AB subspectra are c calculated using the following relationships:

Spacing of outer lines $\quad J_{AB} + \sqrt{J_{AB}^2 + (\nu_A - \nu_B)^2}$

Spacing of inner lines $\quad -J_{AB} + \sqrt{J_{AB}^2 + (\nu_A - \nu_B)^2}$

Intensity of inner lines

$$1 + \frac{J_{AB}}{\sqrt{J_{AB}^2 + (\nu_A - \nu_B)^2}}$$

Intensity of outer lines

$$1 - \frac{J_{AB}}{\sqrt{J_{AB}^2 + (\nu_A - \nu_B)^2}}$$

These are shown in Figure 2.4 2^0

Figure 2.4A illustrates the AB region. Figure 2.4B shows the X region of the same spectrum. The separation 2D is the difference between the first and third line of each AB subspectrum. In this case $2D^+$ refers to tha AB subspectrum with X ↑; $2D^-$ to the AB subspectrum with X ↓. These separations are important because combinations of D^+ and D^- show up in the X region as well.

2.3.2. Analysis of ABX Spectra.

To analyse observed spectra one simply applies, in reverse, the rules used for calculating spectra. However, certain ambiguities can arise which will be discussed in Chapter 4. To illustrate the methods of analysis of ABX spectra I will use the spectrum shown in Figure 2.5

First Order Analysis.

When using this method, it is assumed that the

Figure 2.3

Construction of a spectrum of three coupled nuclei using a first order approach.

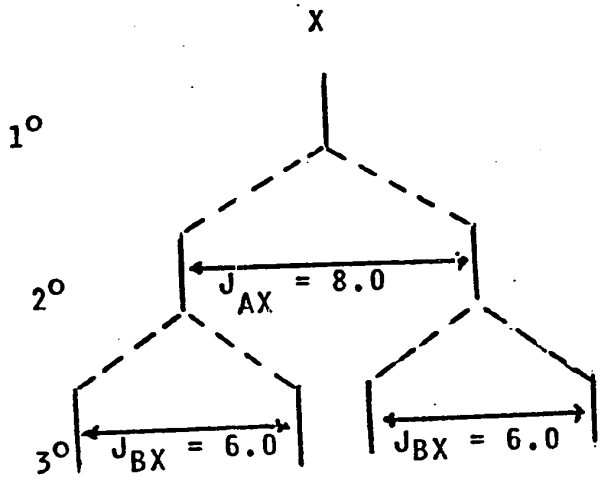

FIRST ORDER APPROACH TO CONSTRUCTION OF AN ABX TYPE SPECTRUM.

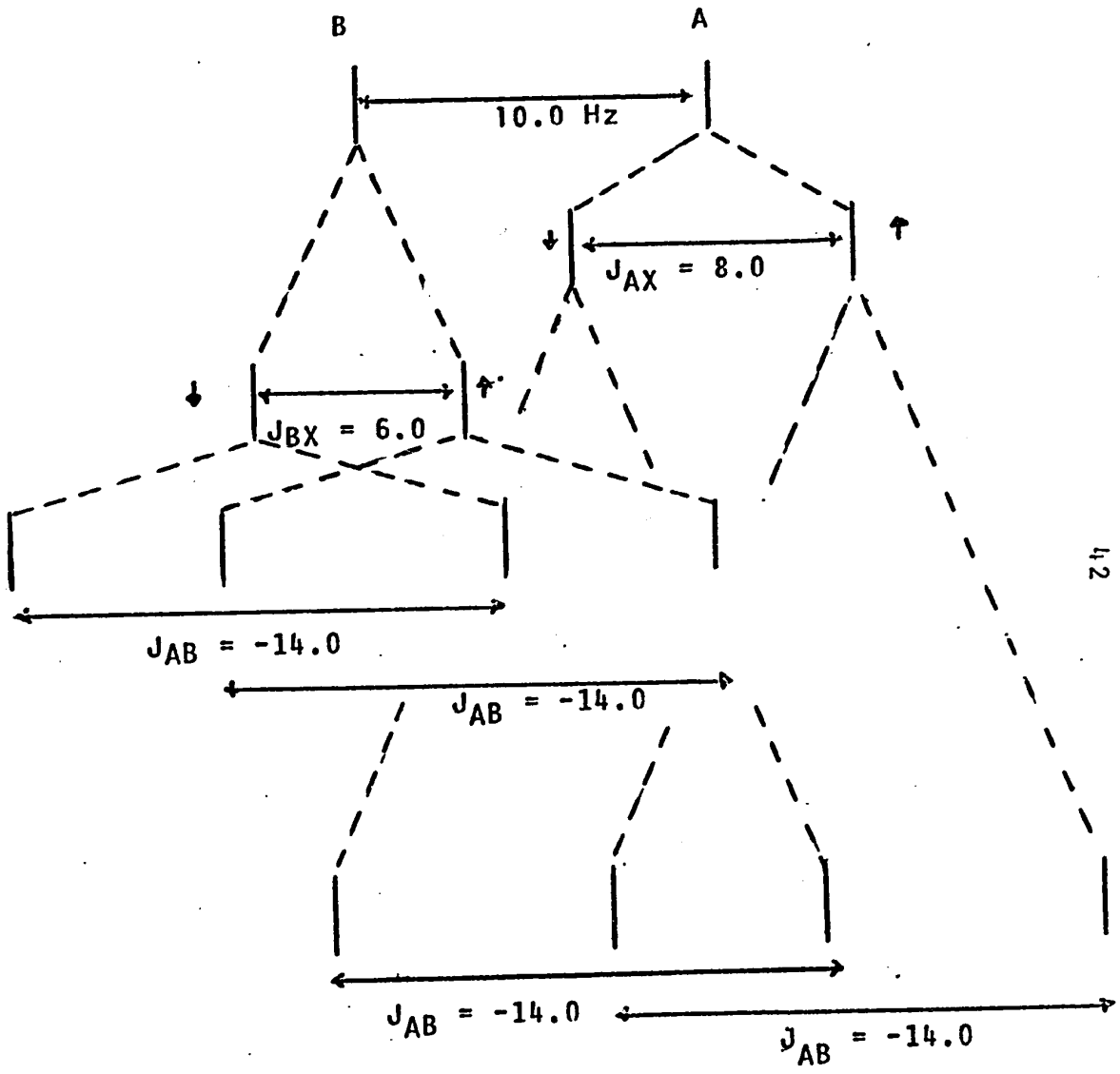

OBSERVED SPECTRUM: AMX TYPE SPECTRUM RATHER THAN TRUE ABX

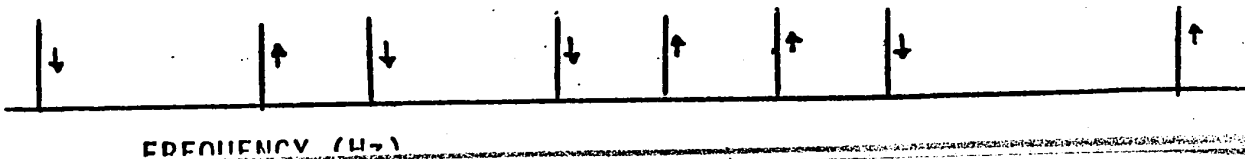

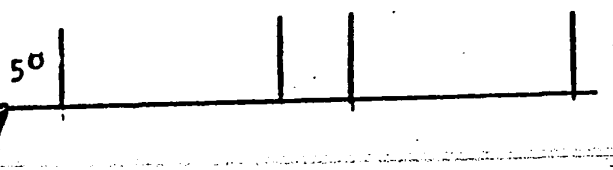

Figure 2.4A

AM region of an AMX spectrum

AB region of an ABX spectrum.

AMX SPECTRUM: AM REGION

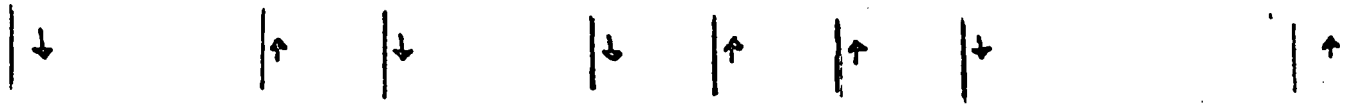

CONSTRUCTION OF ABX SPECTRUM: AB REGION

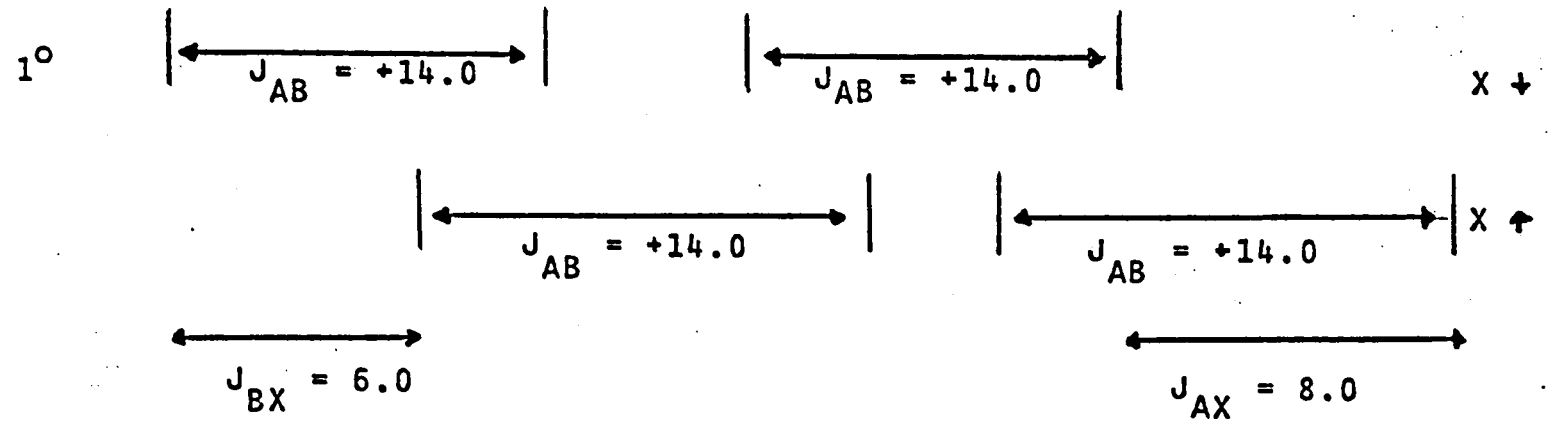

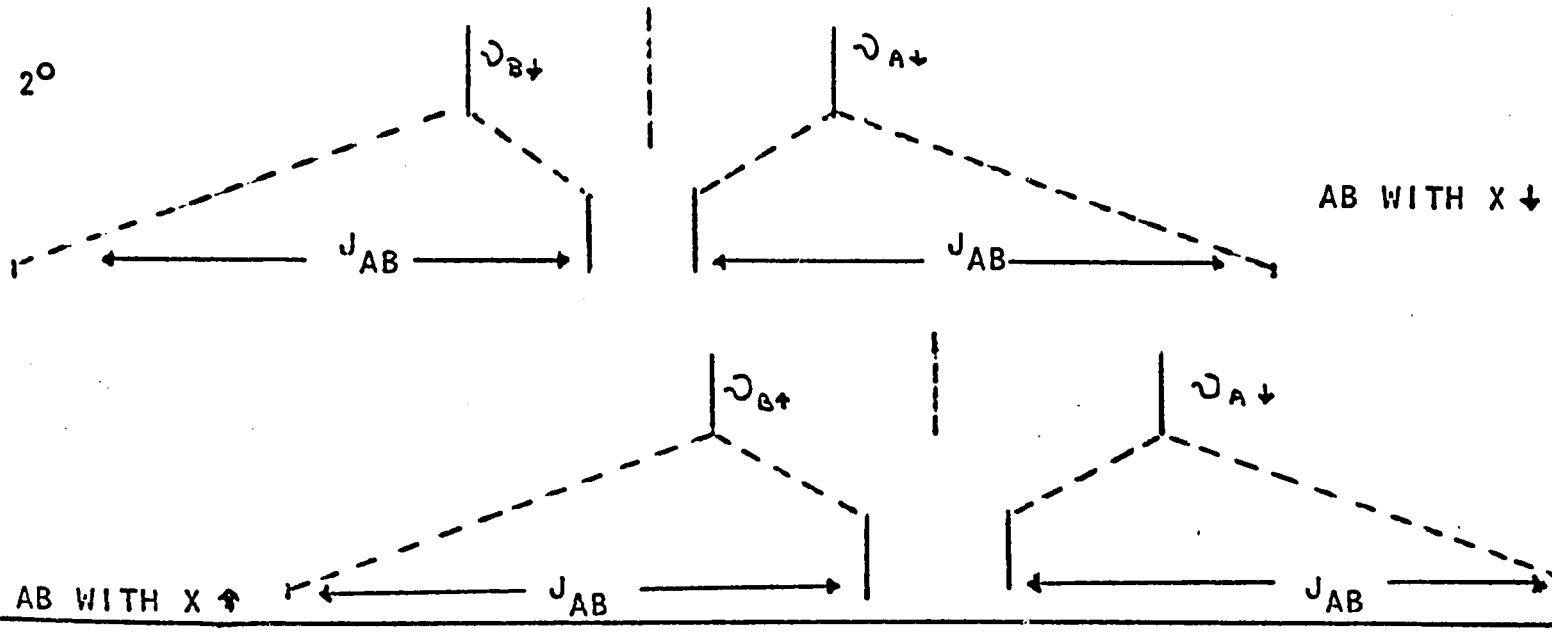

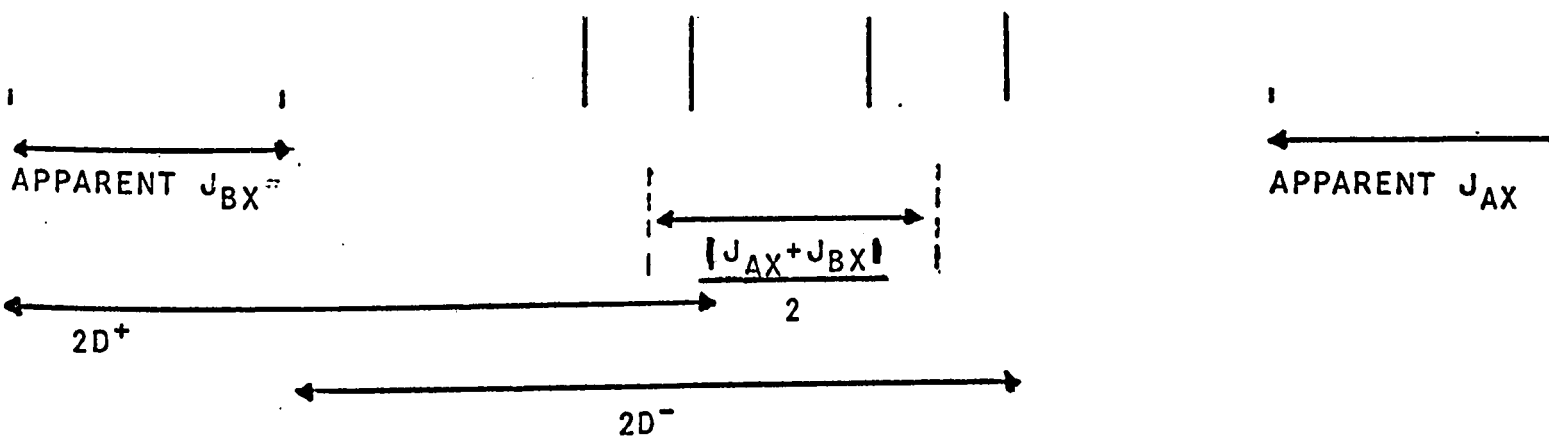

OBSERVED SPECTRUM: AB REGION.

Figure 2.4B

X region of an ABX spectrum.

OBSERVED SPECTRUM: X REGION.

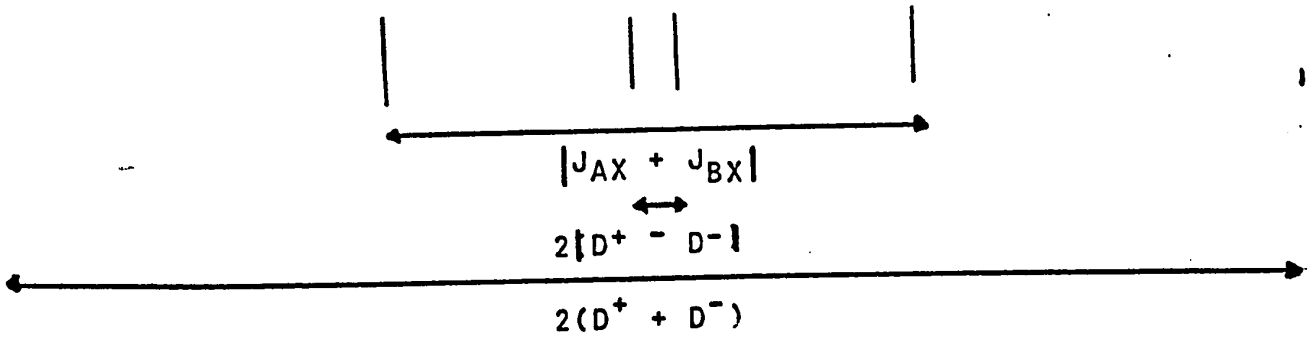

Figure 2.5

ABX spectrum analysed by the Construction Method.

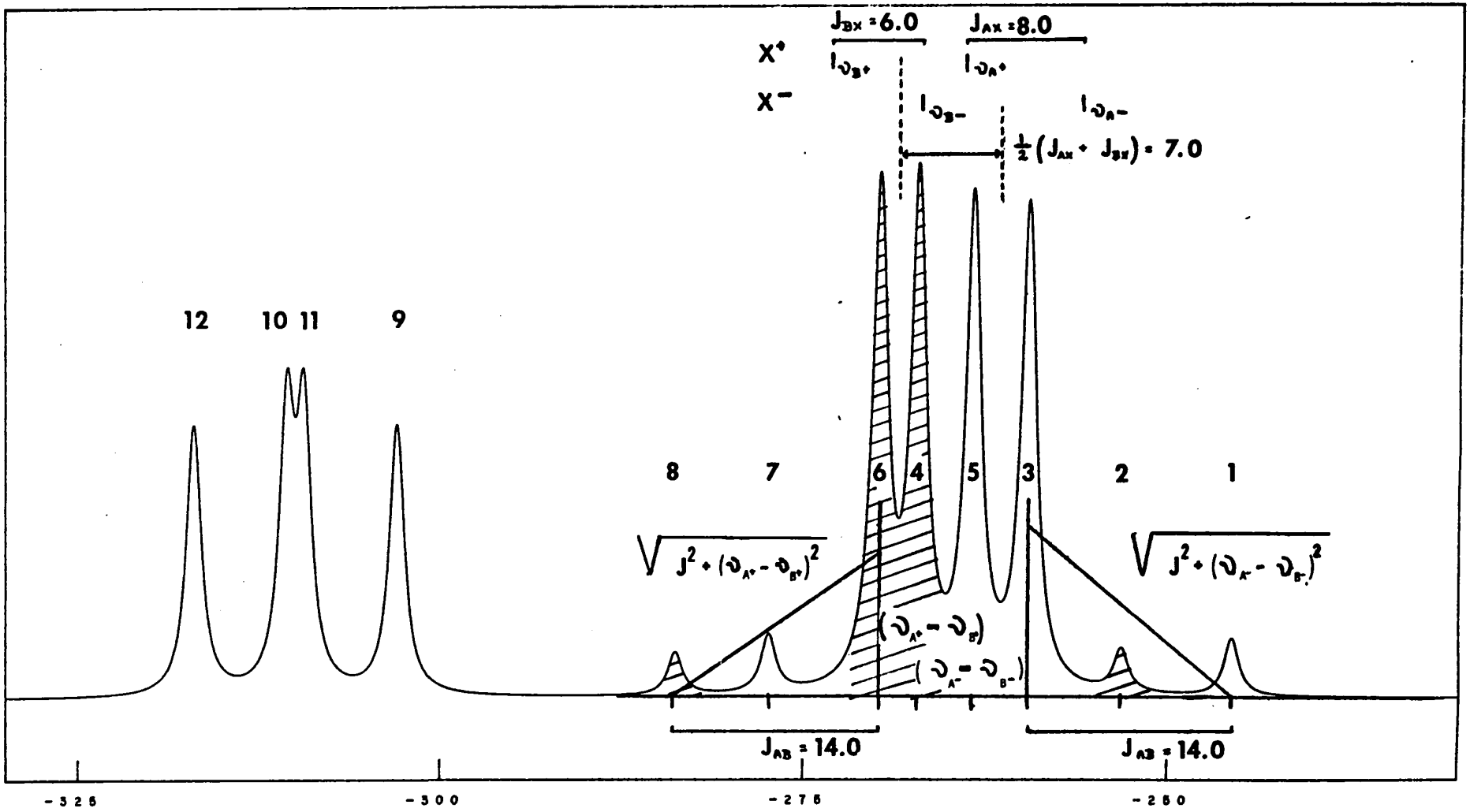
$J_{BX} = 6.0$
$J_{AX} = 8.0$
X^+
X^-
ν_{B+}
ν_{A+}
ν_{B-}
ν_{A-}
$\frac{1}{2}(J_{AX} + J_{BX}) = 7.0$
12
10 11
9
8
7
6
4
5
3
2
1
$\sqrt{J^2 + (\nu_{A+} - \nu_{B+})^2}$
$\sqrt{J^2 + (\nu_{A-} - \nu_{B-})^2}$
$(\nu_{A+} - \nu_{B-})$
$(\nu_{A-} - \nu_{B+})$
$J_{AB} = 14.0$
$J_{AB} = 14.0$
-325
-300
-275
-250

separation between the lines is a direct measure of the coupling. In Figure 2.5, J_{AX} = 6.4 Hz would be the separation between lines 5 and 6, 7 and 8, 9 and 10 or 11 and 12. J_{BX} = 7.6 Hz would be the separation between lines 1 and 2, 3 and 4, 9 and 11 or 10 and 12.

First order analysis has neglected the interaction (mixing) which occurs between spin states and the values of J_{AX} and J_{BX} can be highly inaccurate.

AB Subspectral Analysis.

By this method, the observed spectrum of the AB region is divided into two AB subspectra each of which is due to one possible orientation or value of the spin of the X nucleus. There are several possible ways to choose the components of each quartet. However, a number of features in the spectrum aid analysis,

AB quartets are symmetrical and when choosing the lines which make up each quartet, one must look for two inner lines of equal intensity and two outer lines of equal intensity. Differences in the intensity of each quartet will be more difficult to observe when the spectrum tends towards the ABC case. I have chosen lines 8,6,4,2 as one quartet and lines 7,5,3,1 as the other.

Having chosen the quartets, it is then possible

to determine the value of $|J_{AX}+J_{BX}|$. The separation between the center of the AB quartets is equal to 1/2 $|J_{AX}+J_{BX}|$ = 7.0 Hz. This can be verified in the X region.. In a six line X spectrum the separation between the two most intense lines is $|J_{AX}+J_{BX}|$. If the X region contains only four observable lines, as is the case with our spectrum, $|J_{AX}+J_{BX}|$ cannot be assigned because all four lines are of approximately equal intensity.

The correctness of the quartet assignment can also be verified by yet another measurement in the X spectrum. The separation between the first and third line of each quartet is $2D^+$ and $2D^-$. Although it is impossible to assign the correct D to a particular quartet, the difference $2|D^+-D^-|$ gives the separation between the difference lines. The separation between the the combination lines when they appear is $2|D^++D^-|$ These relationships are shown in Figure 2.4A and 2.4B.

After identifying the two quartets the next step is to calculate tha value of ν_A and ν_B for each quartet. The simplest way of determining these values is by the 'construction' method. It is less accurate than the algebraic method but it is quite useful as a starting point when followed by computer analysis.

The Construction Method:

One simply sets the distance between the first and third line of a quartet on a divider and uses this as a measure of the hypotenuse of the right angle triangle formed by the base and the second line. The height of the triangle is a measure of $\Delta = \nu_A - \nu_B$. The value of $\Delta/2$ is then measured off to each side of the center point of the quartet. This gives ν_A and ν_B for each spin orientation of X.

Having eliminated the AB coupling, we have four lines, two due to the splitting of A by X and two from the splitting of B by X. These lines must be paired in order to determine the chemical shift of A and the chemical shift of B, as well as J_{AX} and J_{BX}. Each pair must consist of a line due to the two possible orientations of the X spin. There are two ways of doing this. A large (wide) coupling of A and X or B and X would give an X part which consists of six widely spaced lines. A small (narrow) coupling gives an X part in which only four of the six lines appear.

In Figure 2.5 the coupling must therefore be a narrow one. J_{AX} is found to be 8.0 Hz, J_{BX} is 6.0 Hz.

Because of the very brief description of AB and

ABX spectra I have given here it is impossible to understand the details of spectral analysis and realize the ambiguities associated with the process. I have included in the Reference section a number of articles which deal with the subject of spectral analysis (4-11). Textbooks are cited in references 1,2 and 3.

2.4 References.

1. See reference 2 in CHAPTER 1.

2. See references 3,4,5,6,7 in CHAPTER 1.

3. J.D. Roberts, An Introduction to the Analysis of Spin-Spin Splitting in High Resolution Nuclear Magnetic Resonance Spectra, W.A. Benjamin Inc., N.Y., 1962

4. G. Slomp, Analysis of ABX Spectra in NMR Spectroscopy, Appl. Spectr. Rev. 2 263 (1969)

5. P.L. Corio and R.C. Hirst, Magnetic Resonance Spectra of Multispin Systems, J. Chem. Educ. 46 345 (1969)

6. E.W. Garbisch Jr., Analysis of Complex NMR Spectra for the Organic Chemist, I Second order approach with specific application to the two spin system, J. Chem. Educ. 45 311 (1968)

7. E.W. Garbisch Jr., II Three spin systems of ABC, ABX, ABK and AB_2 types, J. Chem. Educ. 45 402 (1968)

8. E.W. Garbisch Jr., III Four spin systems of the ABC_2, ABX_2, ABK_2, AA'BB' and AA'XX' types, J. Chem. Educ. 45 480 (1968)

9. P. Diehl and R.J. Chuck, The analysis of an ABXY N.M.R, spectrum using sub-spectral and direct methods, Mol. Phys. 13 417 (1967)

10. R.J. Abraham and H.J. Bernstein, Analysis of deceptively simple spectra, Can. J. Chem. 39 216 (1961)

11. S. Castellano and J.S. Waugh, Exact analysis of three spin spectra, J. Chem. Phys. 34 295 (1961)

CHAPTER 3.

COUPLINGS AND CONFORMATION.

CHAPTER 3.

COUPLINGS AND CONFORMATIONS.

3.1 Definitions.

Couplings can be either positive or negative. In previous chapters I mentioned only positive couplings. A positive coupling arises when antiparallel spins of coupled nuclei are stabilized, have lower energy, than parallel spins.

When antiparallel spins of coupled nuclei are associated with higher energy than parallel spins, the coupling is negative.

First order spectra do not yield information regarding signs of coupling constants. Complex spectra yield relative signs only. Relative signs may be determined by techniques such as double resonance.

Coupling constants for nuclei separated by n bonds are designated ^{n}J. ^{2}J defines geminal couplings. ^{3}J defines vicinal couplings.

The strength of couplings usually decreases as the number of bonds between coupled nuclei increases.

The term 'long range coupling' applies to couplings over four or more bonds.

3.2 Factors Influencing the Magnitude of Coupling Constants.

Geminal ^{1}H -^{1}H couplings can vary between -20 and +40 Hertz (1). A number of factors influence the values of observed couplings, I will mention only the major ones. The hybridization of the carbon atom causes the largest effects. Electronegative α substituents increase couplings while the same substituent in a β position decreases couplings. Hyperconjugation decreases couplings (2). The magnitude of this effect is orientation dependent.

Vicinal couplings are usually positive. Gauche couplings are found to be weaker than trans couplings. This implies that coupling occurs through the bonding electrons and not through space, otherwise gauche couplings would be the largest. The presence of electronegative atoms in α positions decrease the aliphatic vicinal couplings. The same substituents in β positions increase ^{3}J. Bond angles also affect couplings; as the H-C-C' and C-C'-H angles increase the couplings decrease. As the C-C' bond length increases ^{3}J decreases.

3.3 The Karplus Relationship.

A very useful relationship between dihedral angles (ϕ) of protons on adjacent sp^3 hybridized carbons and couplings has been derived by Karplus (3-4). The original relation is:

$$J = 8.5 \cos^2\phi - 0.28 \text{ Hz} \qquad 0^\circ \leq \phi \leq 90^\circ$$
$$J = 9.5 \cos^2\phi - 0.28 \text{ Hz} \qquad 90^\circ \leq \phi \leq 180^\circ$$

It must be made clear that these equations are useful in predicting trends only and should not be used for accurate angle measurements because the couplings are strongly influenced by substituents and molecular geometry.

A more general form of the Karplus relation is:

$$J = J^0 \cos^2\phi - C \qquad 0^\circ \leq \phi \leq 90^\circ$$
$$J = J^{180} \cos^2\phi - C \qquad 90^\circ \leq \phi \leq 180^\circ$$

where J^0, J^{180} and C are constants appropriate for the system studied (1).

In order to evaluate the error which may be involved in using the Karplus relation, it is common

practice to do calculations using both plausible extremes of J^0 and J^{180}. This is especially important when calculations of rotamer populations are attempted.

The Karplus relation is often used to estimate rotamer populations. For instance, in substituted ethanes, such as amphetamines, rotation about sp^3-hybridized bonds can occur. The rotational isomers usually differ in energy and the observed coupling is an average over unequal rotamer populations. α-methyl-β-phenylethylamine (Figure 3.1) gives rise to an ABX type spectrum for the CH and CH_2 resonances. Spectral analysis gives average values for the J_{AX} and J_{BX} couplings. If one assumes that 60^o staggered rotamers (Figure 3.1) represent positions of energy minima, the relative population in each conformation can be estimated.

$\bar{J}_{AX}$ is the time average of all the AX couplings in rotamers I II and III.

$$\bar{J}_{AX} = P_I J_t + P_{II} J_g + P_{III} J_g$$

$$\bar{J}_{BX} = P_I J_g + P_{II} J_t + P_{III} J_g$$

Figure 3.1

60^{o} staggered rotamers in amphetamine.

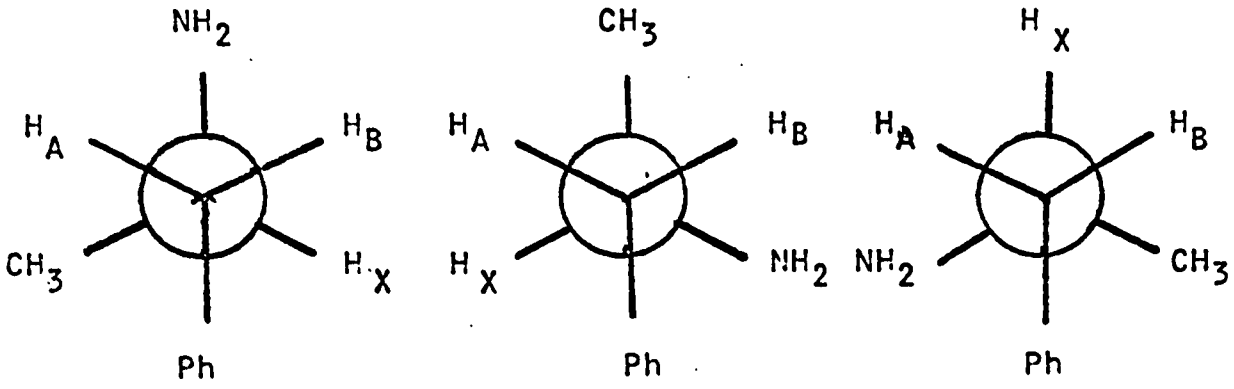

I II III

60° STAGGERED ROTAMERS IN AMPHETAMINE.

J_g is the gauche coupling

J_t is the trans coupling

P_I, P_{II} and P_{III} are the mole fractions of each rotamer which can be calculated if a third equation is added to the first two:

$$1 = P_I + P_{II} + P_{III}$$

A number of errors are inherent in these calculations. The main ones occur in estimating the values of J^0 and J^{180} and in the assumption that 60^0 staggered rotamers represent states of energy minima. Useful information can however be gained from such calculations if one takes these facts into account. Calculations using off-staggered rotamers are sometimes useful if repulsions can occur between substituents when 60° staggered are considered (5,6). This calculation indicated how the initial assumptions influence the conclusions.

Temperature studies should be of use because as the temperature is increased the population distribution in each rotamer would tend to be equalized. This is usually the case with 60° staggered rotamers.

4.4 Long Range Couplings.

Long range couplings are usually small and sometimes difficult to observe. They normally range between -2.5 and +2.5 Hz. The larger couplings are those transmitted through π bond systems. In allylic systems one can relate the magnitude of the coupling to the angle (θ) between the plane containing the olefinic proton and the C-H bond of the allylic carbon:

$$J_{\pi} = -3.41\cos^2\theta \quad (7)$$

J^4 is maximum when θ is 90^o, it is minimum when θ is 0^o or 180^o.

In allylic systems maximum couplings occur when the atoms between the coupled nuclei are planar and arranged along a 'W' path. As the number of planar deviations from the 'W' path increases (i.e. 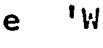 or ) J^4 decreases. When one bond is rotated out of the plane

$$J = J_o\cos^2\theta$$

When two bonds are rotated out of the plane

$$J = A\cos^2\theta + B\cos^2\phi - 0.8$$

θ and ϕ are the angles formed by the rotated bond and the plane.(8). A and B are constants.

Planar zig-zag paths favour couplings across five bonds. In unsaturated systems J^5 values range between 0.5 and 1.0 Hz. J^5 couplings decrease when systems are non-planar.

3.4 References

1. S. Sternhell, Quart. Rev. 23 236 (1969)
2. J.A. Pople and A.A. Bothner-By, J. Chem. Phys. 42 1339 (1965)
3. M. Karplus, J. Chem. Phys. 30 11 (1959)
4. M. Karplus, J. Amer. Chem. Soc. 85 2870 (1963)
5. H.S. Gutowsky, G.G. Belford and P.E. McMahon. J. Chem. Phys. 36 3353 (1962)
6. N. Sheppard and J.J. Turner, Proc. Roy. Soc. Ser. A 252 506 (1959)
7. G. P. Newsoroff and S. Sternhell, Tetrahed. Lett. 6117 (1968)
8. M. Barfield, J. Chem. Phys. 41 3825 (1964)

CHAPTER 4.

CONFORMATIONAL STUDIES ON AMPHETAMINES.

4.1 Introduction.

4.1.1 Possible Sites of Action.

4.1.2 Structure Activity Relationships.

4.2 NMR Studies.

4.2.1 Material.

4.2.2 Spectral Analysis.

4.2.3 Discussion of Spectra.

4.2.4 Possible Conformation of Amphetamine Rotamer Calculations.

4.3 Conclusion.

4.4 References.

CHAPTER 4.

CONFORMATIONAL STUDIES ON AMPHETAMINES.

4.1 Introduction.

Amphetamine (α methyl β phenethylamine) and amphetamine derivatives induce a number of physiological responses in the organism, such as tachyphylaxis, hyperthermia, anorexia,and are potent central nervous system stimulants. They are used clinically as appetite depressants, antidepressants and antifatigue drugs. Methoxylated amphetamines are hallucinogens (1,2). These derivatives, when administered in large doses even over short periods, can induce symptoms of paranoid psychosis (3).

The central stimulant effect of d-amphetamine is related to norepinephrine metabolism (4). Norepinephrine and dopamine are located in vesicles found in nerve terminals and are believed to be neurotransmitters. Norepinephrine is synthesized in brain cells from phenylalanine.(5). Most norepinephrine is bound intracellularly in vesicles but the mechanisn by which binding occurs is not known (4). Active transport

may be involved because exogenous norepinephrine is accumulated in nerve cells against a gradient; the process can be inhibited by metabolic inhibitors (7). Norepinephrine is released into the synaptic cleft by various stimuli and can either be taken up again by the membrane or degraded extraneuronally. Norepinephrine is degraded via two main enzymatic pathways: o-methylation and oxidative deamination (6). Catechol-o-methyl transferase is believed to act mainly extraneuronally while monoamine oxidase is found in brain cell mitochondria (4).

4.1.1 Possible Sites of Action of Amphetamines.

Drugs such as amphetamine can interfere with the action and metabolism of norepinephrine at several levels. They can interfere with synthesis by binding to enzymes, with storage by inhibiting uptake in vesicles or by displacement from vesicles of norepinephrine. After norepinephrine has been released into the synaptic cleft they can inhibit reuptake or degradation. Drugs can also produce direct effects at the postsynaptic membrane.

Amphetamine seems to affect mainly the uptake and release of norepinephrine although direct action on post-synaptic receptors is also possible.

Amphetamine causes an increase in release of tritium labeled norepineprhine from brain slices (8).This increase in norepinephrine release may be responsible for the stimulating activity of amphetamine.

The amount of catecholamine released by amphetamine is more pronounced after reserpine pretreatment which is known to deplete vesicular stores of norepinephrine. Amphetamine therefore releases norepinephrine preferentially from extragranular sites in nerve cells (9). The site of action of amphetamine may then be the cell membrane transport mechanism.

The release of norepinephrine by amphetamine could also be caused by an increase in norepinephrine synthesis. Amphetamine causes an increase in monoamine oxidase activity which increases the turnover of amphetamine and therefore probably causes an increase in the activity of tyrosine hydroxylase, the rate limiting enzyme in norepinephrine synthesis. α methyl tyrosine which inhibits tyrosine hydroxylase is found to have anti-amphetamine effects (21). Alternatively, amphetamine could inhibit binding of norepinephrine in vesicles and promote a more rapid enzymatic attack of free cytoplasmic norepinephrine.

Amphetamine inhibits uptake of norepinephrine by brain slices (22). The effect of norepinephrine released into the synaptic cleft would be potentiated because the norepinephrine would not be taken up again by the cell and metabolized as readily as normally.

It does not seem likely that amphetamine acts directly at the post-synaptic receptor because it cannot stimulate the central nervous system in the absence of norepinephrine (26).

It is possible that the effect of amphetamine is not direct but occurs via one of its metabolic products. The metabolism of amphetamine takes place mainly along two pathways: ring hydroxylation and deamination (22). In man, deamination is the main pathway. Psychosis could be caused in humans by para-hydroxyamphetamine which serves as a false neuro-transmitter (21). There is evidence which casts doubt on this interpretation. Amphetamine still releases norepinephrine after disulfiram treatment which prevents formation of the false neurotransmitter. Furthermore, the l-isomer of amphetamine produces no para-hydroxyamphetamine and still norepinephrine is released (23).

The hallucinogenic methoxylated amphetamines do not inhibit norepinephrine uptake by brain slices.

These derivatives may act directly on post-synaptic receptors (24).

4.1.3 Structure Activity Relationships.

Studies of structure-activity relationships have shown that certain structures are related to definite properties of the molecules (25). For instance, the α methyl group protects amphetamine from monoamine oxidase and also confers to the molecule a moderate amount of inhibitory activity. This α methyl group is responsible for preventing the reuptake of norepinephrine at the neuronal membrane.

Hydroxylating either the ring or the side chain decreases the inhibition of reuptake of norepinephrine. Polyalkoxylation of the ring increases psychotomimetic properties.

The β phenethylamine arrangement is necessary for norepinephrine release and blocking norepinephrine reuptake.

All the above mentioned physiological effects of amphetamine involve binding with some type of receptor whether it be an enzyme in a metabolic pathway or a membrane protein. In order to understand these interactions it is necessary to know the conformation

of amphetamine in solution.

Solid state studies showed the same conformation for noradrenaline.HCl (10), dopamine.HCl (11) and phenylethylamine (12). The phenyl ring is trans to the amino group and perpendicular to the plane formed by the ethylamine group. Whether this conformation persists in dilute aqueous solutions remains to be demonstrated.

NMR studies of (-)N,N-dimethyl-1,2-diphenyl-ethylamine (13) showed a 60% preference for the trans phenyl-phenyl rotamer. The trimethylsilyl ether of adrenaline and other hydroxyphenylalkylamines (14) have been shown, by NMR studies, to prefer the trans phenyl-amino rotamer.

4.2 NMR Studies.

4.2.1 Material.

The following molecules were studied (Figure 4.11)

amphetamine (α-methylphenethylamine)

amphetamine.HCl

methamphetamine.HCl (^{N}-methyl amphetamine)

methoxyphenamine.HCl (o-methoxy methamphetamine)

benzphetamine.HCl (N-benzyl-N,α-dimethyl phenethylamine)

All spectra were run in 0.1 M aqueous solutions except amphetamine (free base) which was a saturated solution. No concentration dependance of the NMR spectra was observed when concentrations were 0.1 M or less.

4.2.2 Spectral Analysis.

NMR spectra were taken on a Varian XL-100 spectrometer operating at 100 MHz and a probe temperature of 30°C.

The spectra of the phenyl regions were unanalysable AA'BB'C spectra. The CH and CH_2 protons gave rise to ABC spectra which could be analysed as ABX spectra before final computer analysis as ABC spectra.

Figures 4.1,4.2,4.3,4.4 and 4.5 show the CH and CH_2 resonances of the various amphetamines.

Preliminary analysis was first carried out by the Construction Method (15) described in CHAPTER 2. A complete analysis was done using the computer program LAOCOON II (16). The results are presented in Table 4.1 (27).

Comparison of the phenthylamines with substituted ethanes led to choosing AB quartets in which the AC and BC couplings are of the same sign and positive (17,18). The AB coupling was considered

Table 4.1

Chemical shifts (p.p.m.) and coupling constants (Hz) obtained by ABC analysis of spectra taken at 100MHz.

Compounds	H_A	H_B	H_C	CH_3	J_{AB}	J_{AC}	J_{BC}	J_{CH_3,H_C}
Amphetamine (I) [a]	2.58	2.70	3.12	1.05	-13.30	7.50	6.28	6.40
Amphetamine.HCl (II)[b]	3.26[c]	3.26[c]	3.95	1.61[d]	-13.8[c]	7.4[c]	6.9[c]	6.60
Methamphetamine.HCl (III)[e]	2.90	3.10	3,54	1.28	-13.72	8.08	6.25	6.50
Methoxyphenamine.HCl (IV)[e]	2.92	3.05	3.55	1.25	-13.75	7.19	6.00	6.40
Benzphetamine.HCl (V)[b]	3.24	3.51	4.03	1.63	-13.46	9.07	5.80	6.60

a. Measured relative to internal 0.5% DSS.

b. Measured relative to HMDS in a coaxial capillary tube.

c Obtained by extrapolation from DMSO-d_6:D_2O mixtures.

d. Obtained directly from spectra in D_2O.

e. Measured relative to internal TSP.

At 32°C the principal peaks of the internal references DSS and TSP are 0.36 and 0.33 p.p.m. downfield from external HMDS, respectively, as measured on an A60 NMR spectrometer.

Observed and simulated 100 MHz spectra of amphetamine and amphetamine derivatives in aqueous solutions.

Figure 4.1

Amphetamine (free base)

Figure 4.2

Methamphetamine.HCl

Figure 4.3

o-methoxymethamphetamine.HCl

Figure 4.4

Amphetamine.HCl

Figure 4.5

Benzphetamine.HCl

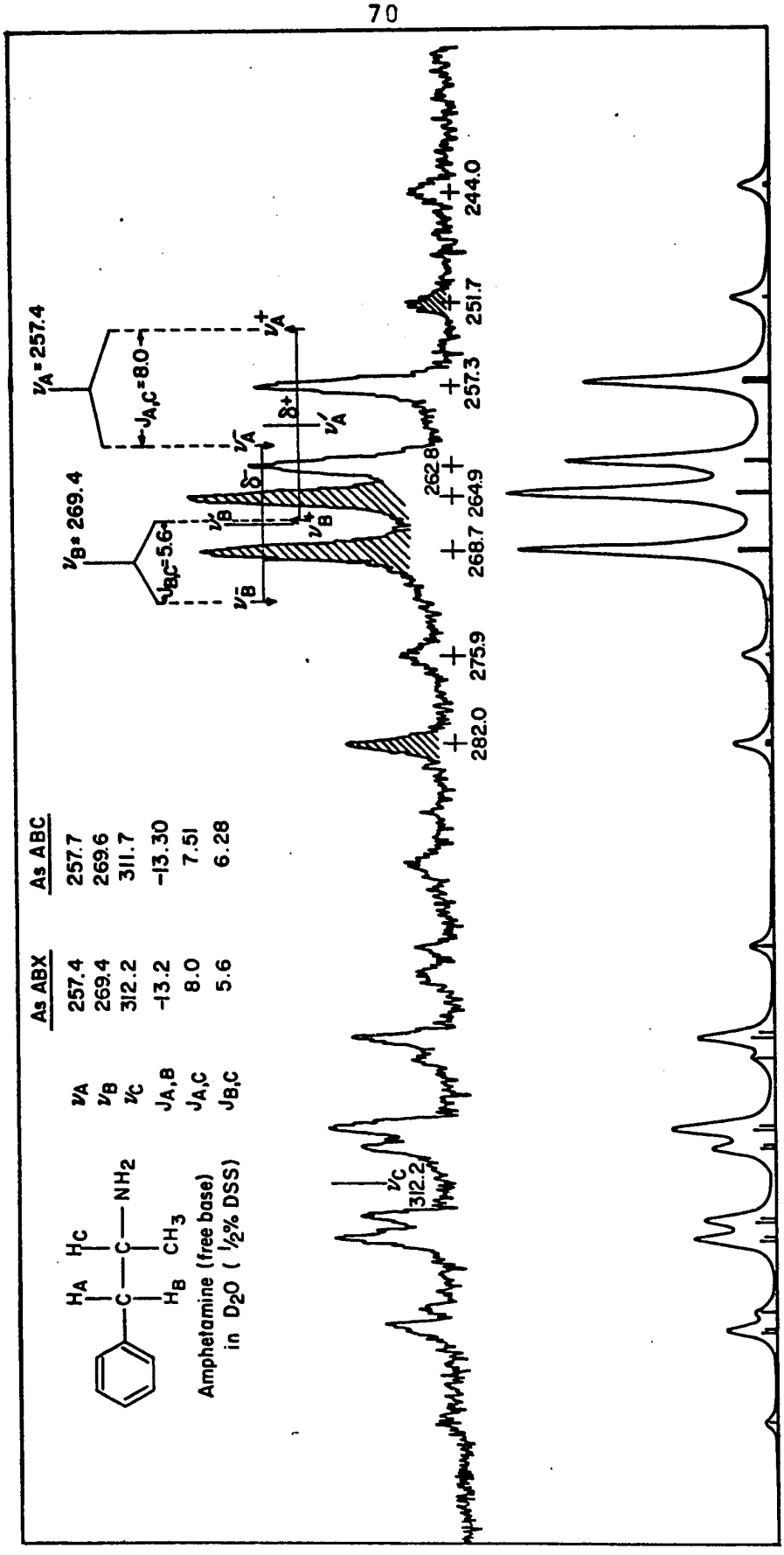
As ABX
As ABC
νA 257.4 257.7
νB 269.4 269.6
νC 312.2 311.7
JA,B -13.2 -13.30
JA,C 8.0 7.51
JB,C 5.6 6.28
Amphetamine (free base)
in D2O (½% DSS)
HA HC
HB CH3
NH2
νA = 257.4
JA,C = 8.0
νB = 269.4
JB,C = 5.6
νC 312.2
282.0 275.9
268.7 264.9
262.8
257.3 251.7
244.0

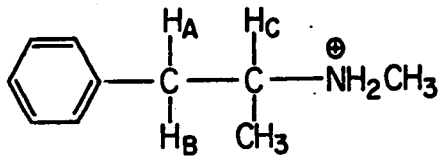

METHAMPHETAMINE • HCl

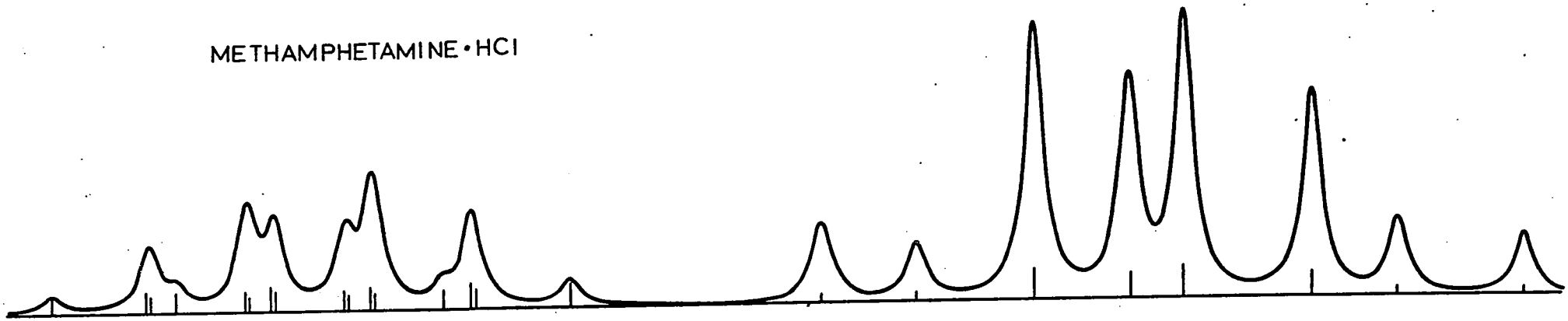

(P.P.M RELATIVE TO INTERNAL TSP)

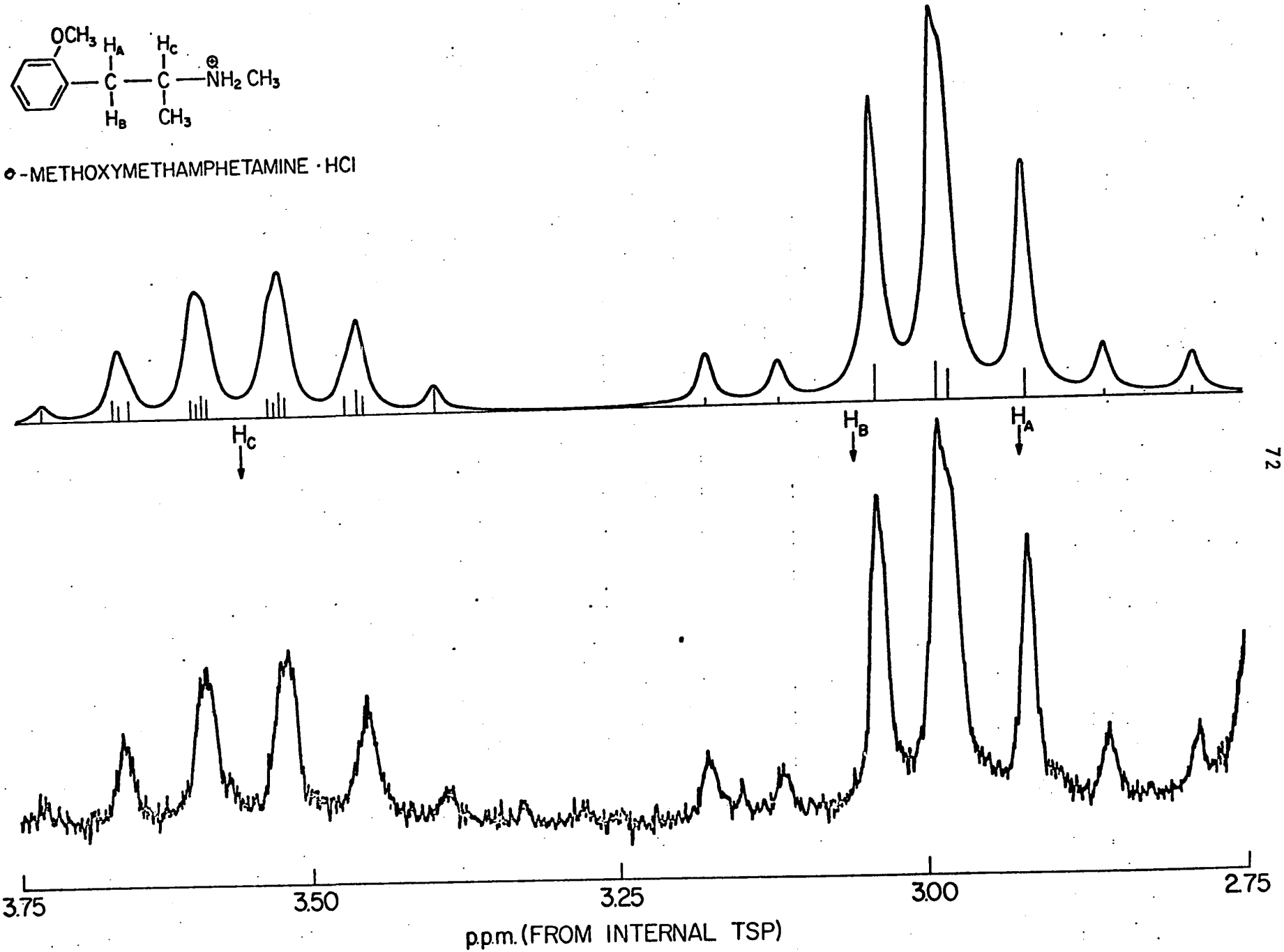
OCH3 HA HC
C C ⊕NH2 CH3
HB CH3
o-METHOXYMETHAMPHETAMINE · HCl
HC
HB
HA
3.75
3.50
3.25
3.00
2.75
p.p.m. (FROM INTERNAL TSP)

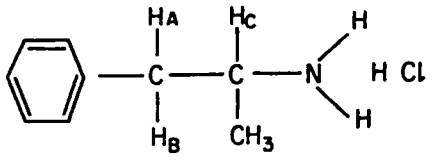

amphetamine · HCl

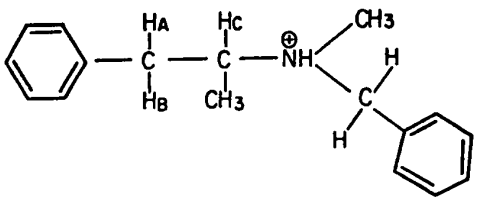

benzphetamine·HCl

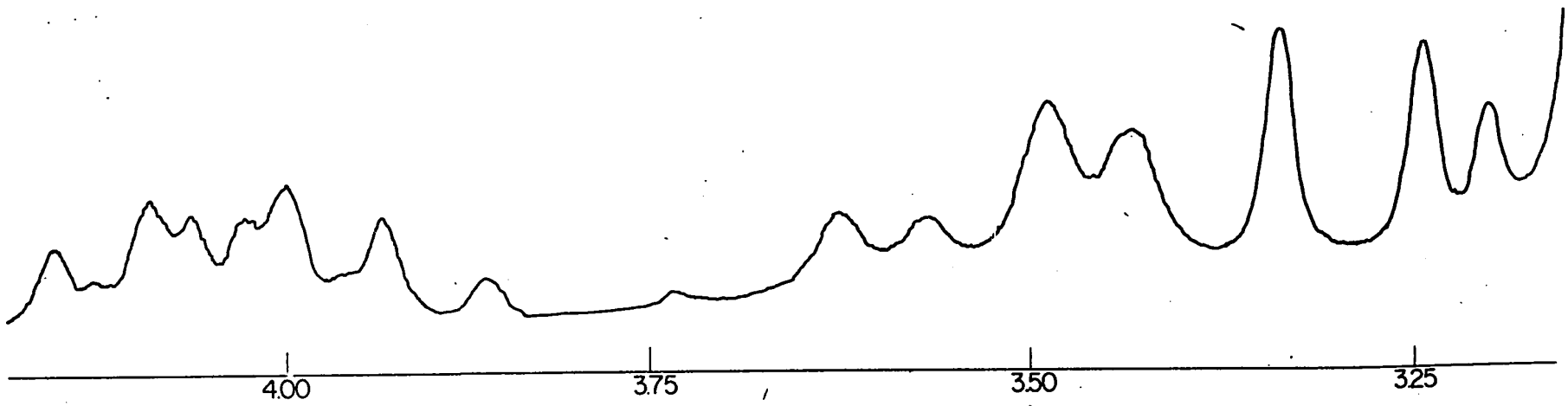

negative as is the case for most geminal couplings in methylene groups (19).

To illustrate the general method used in analysing amphetamime spectra I will use the spectrum shown in Figure 4.2

In actual fact the spectrum has some ABC character but an ABX analysis is carried out before final refinements are done with the computer analysis.

The AB region is divided into two AB subspectra each of which is due to a particular orientation of the X spin. AB spectra are symmetric, therefore lines 4,2,8 and 6 were chosen for one quartet and lines 3,1,7,and 5 for the other. The low field quartet was arbitrarily called ab_- and the high field quartet ab_+. The center of ab_- is at 302.4 Hz and ab_+ is centered at 295.2 Hz. The separation between the centers of the two quartets is $1/2|J_{AX}+J_{BX}| = 7.2$ Hz. This could be verified if the X region were available because in a six line X spectrum the separation between the most intense lines is $|J_{AX}+J_{BX}|$. In amphetamine spectra, the X region contains more lines than predicted in an ABX model due to coupling between the methine proton and the α-methyl group. This is a first order coupling and its value can be measured on the methyl resonances. J_{CH,CH_3} is

measured as 6.4 Hz.

Normally the correct choice of quartets can be made by examining the X region of the spectrum. If the quartets are chosen properly, the separation between the difference lines in the X region is $2|D^{+} - D^{-}|$. The values of D^{+} and D^{-} are the separations between the first and third lines of each quartet. In metamphetamine this check cannot be made, after elimination of the first order coupling in the X region there are only four lines of almost equal intensity.

Each ab subspectrum is analysed by the Construction Method in order to determine ν_A and ν_B for each orientation of the X nucleus.

In the ab_- subspectrum (Fig. 4.6), the distance between the first and third lines is measured and used as the hypotenuse of a right angle triangle formed by the base and the second line. The height of the triangle is the separation between ν_{A-} and ν_{B-}. ν_{A-} and ν_{B-} are equidistant from the center of the quartet.

The process is repeated for the ab_+ spectrum (Fig. 4.6) and this gives the values of ν_{A+} and ν_{B+}.

ν_{A+}, ν_{B+}, ν_{A-}, ν_{B-} are the lines which result from the splitting of A and B by the X nucleus. The four lines must be factored into two doublets, each doublet must be composed of one (+) line and one (-) line, for each orientation of X.

There are two ways of choosing the doublets (15) (Fig. 4.6). Large couplings would have opposite signs while small couplings would have like signs. This can be seen when one examines the orientations of the X spin. When both couplings have the X spin up (↑) on the high field line this means the couplings are of same sign. When one coupling has the spin orientation of X up (↑) on the high field line while the other has the the spin orientation of X down (↓) on the high field line, the couplings are of opposite signs. (See CHAPTER 1).

If the correct choice of couplings has been made, $J_{AX}+J_{BX}$ should be twice the separation between the centers of the quartets.

A narrow (small) coupling gives values of J_{AX} and J_{BX} of 8.4 Hz and 6.0 Hz. The sum of these values is twice the separation between the centers of the two quartets (7.2 Hz).

J_{AB} is the separation between the first and

Figure 4.6

Partly eclipsed AB subspectra in methamphetamine.HCl

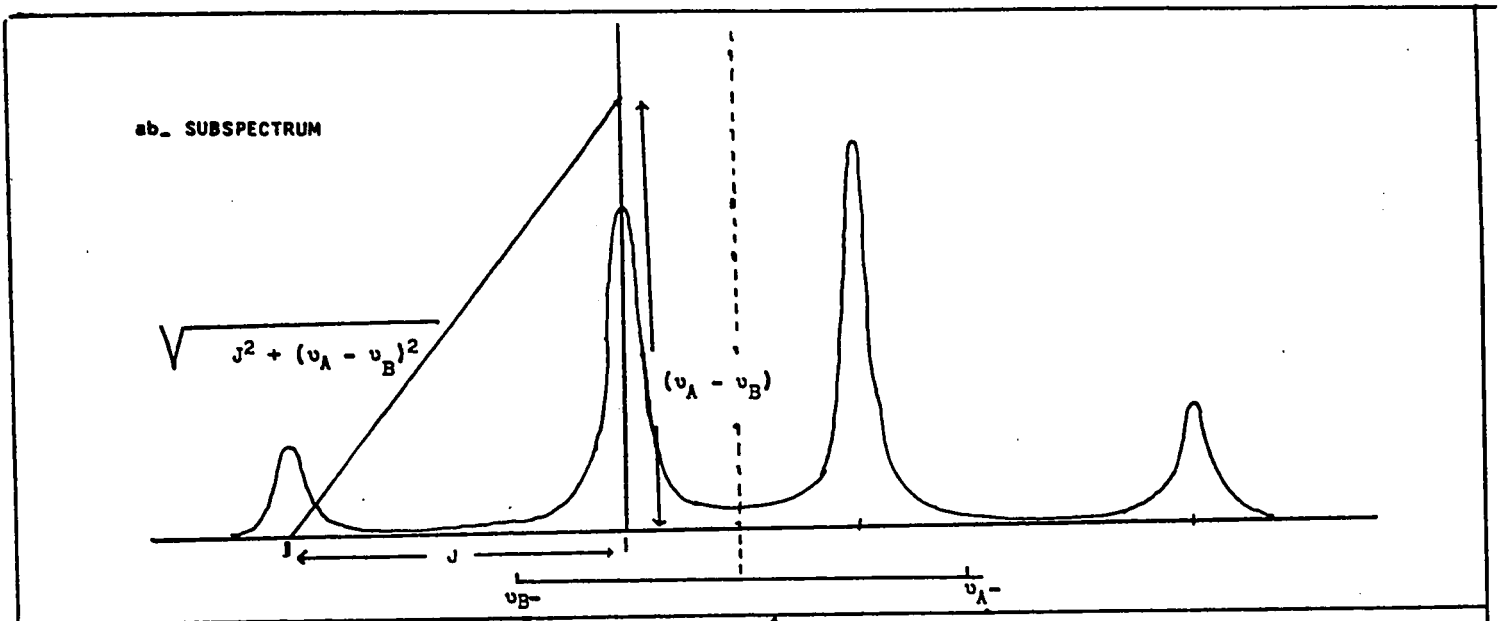

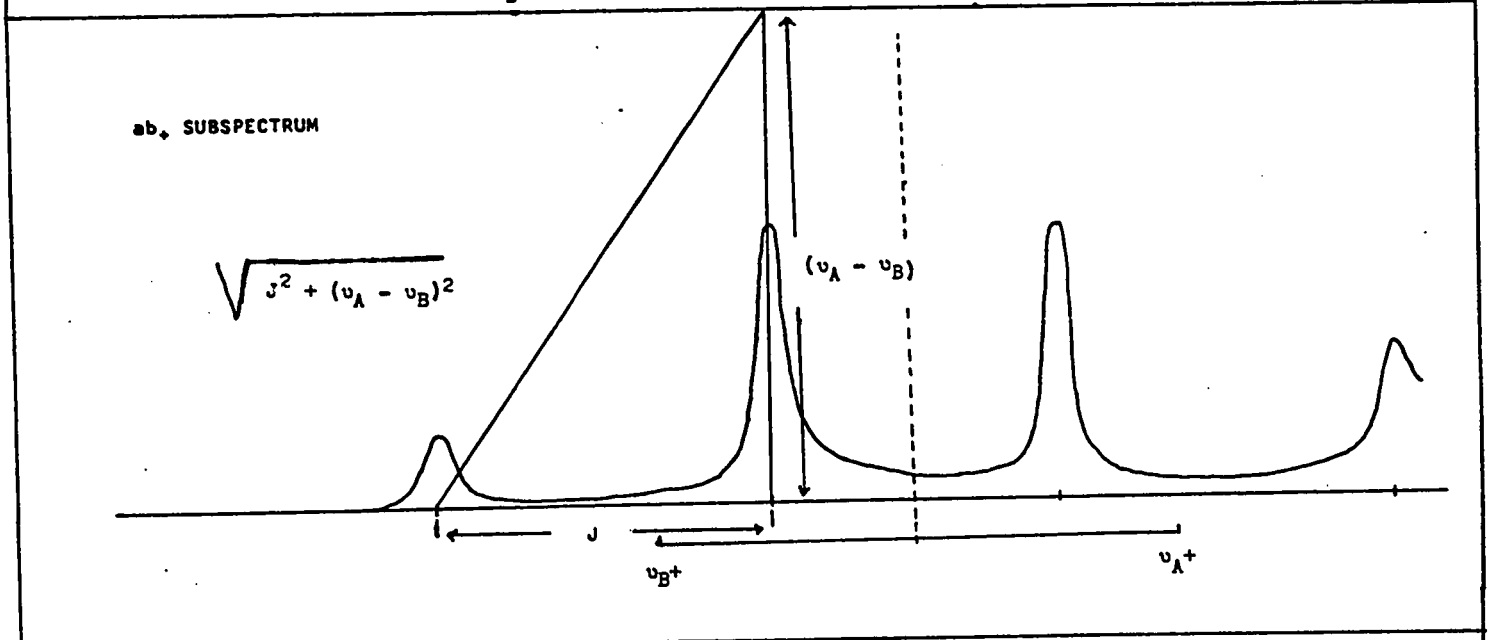

ROOTS OF ab SPECTRUM WHEN X = -1/2

ROOTS OF ab SPECTRUM WHEN X = + 1/2

NARROW COUPLING

LIKE SIGNS

$\upsilon_B = 308.8$

$J_{BX} = 6.0$

$\upsilon_A = 288.9$

$J_{AX} = 8.4$

WIDE COUPLING

UNLIKE SIGNS

$\upsilon_A = 298.2$

$J_{AX} = 27.0$

$\upsilon_B = 299.4$

$J_{BX} = -12.6$

Figure 4.7

Eclipsed AB subspectra in methamphetamine.HCl

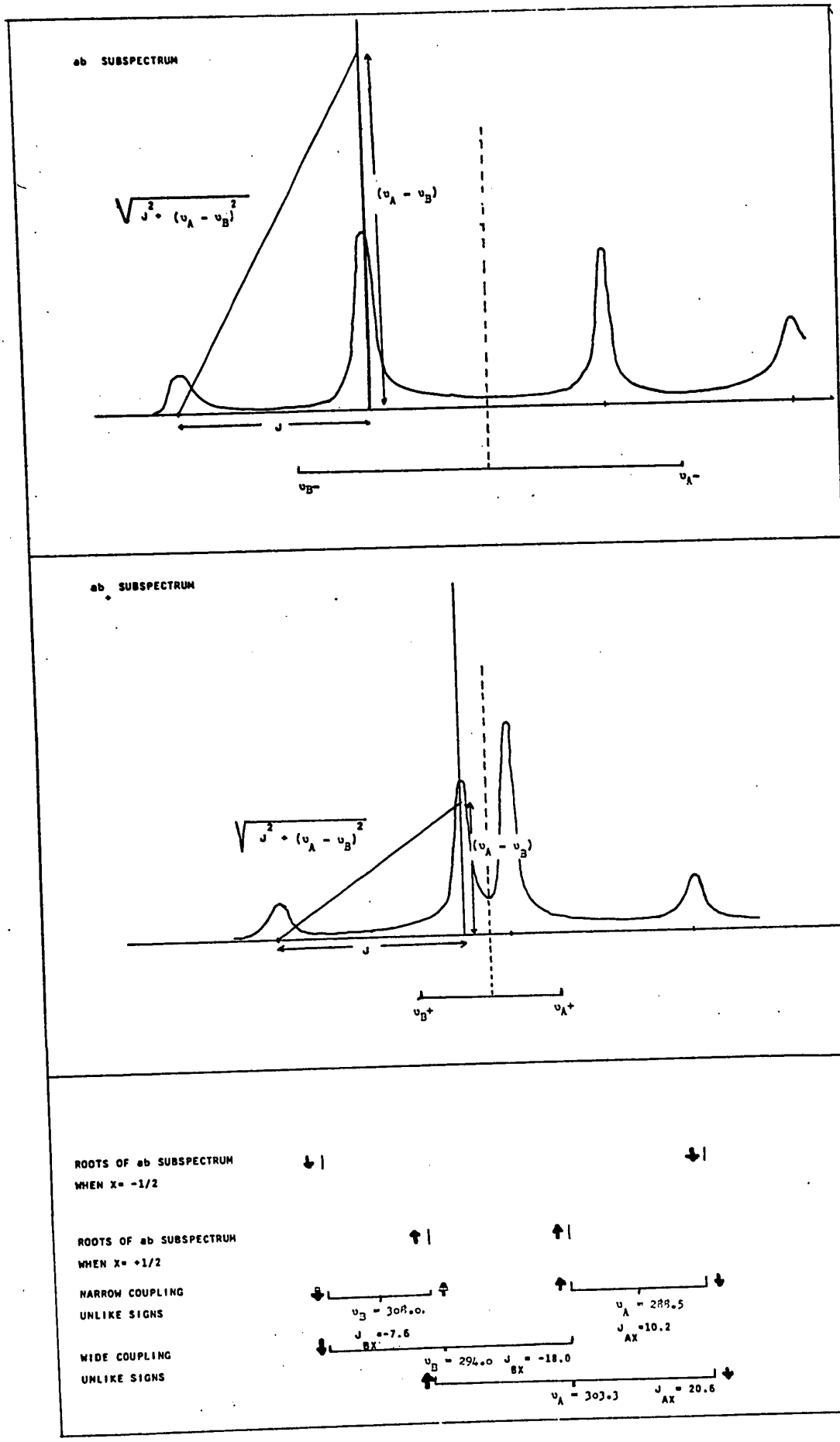
ab SUBSPECTRUM
$\sqrt{J^2 + (\upsilon_A - \upsilon_B)^2}$
$(\upsilon_A - \upsilon_B)$
J
υ_B-
υ_A-
ab SUBSPECTRUM
$\sqrt{J^2 + (\upsilon_A - \upsilon_B)^2}$
$(\upsilon_A - \upsilon_B)$
J
υ_B+
υ_A+
ROOTS OF ab SUBSPECTRUM
WHEN X= -1/2
ROOTS OF ab SUBSPECTRUM
WHEN X= +1/2
NARROW COUPLING
UNLIKE SIGNS
υ_B = 308.0
J_{BX} =7.6
υ_A = 288.5
J_{AX} =10.2
WIDE COUPLING
UNLIKE SIGNS
υ_B = 294.0 J_{BX} = -18.0
υ_A = 303.3 J_{AX} = 20.6

Figure 4.8

Simulated spectra of ABC region in methamphetamine.HCl using both choices of AB subspectra and both choices of coupling constants.

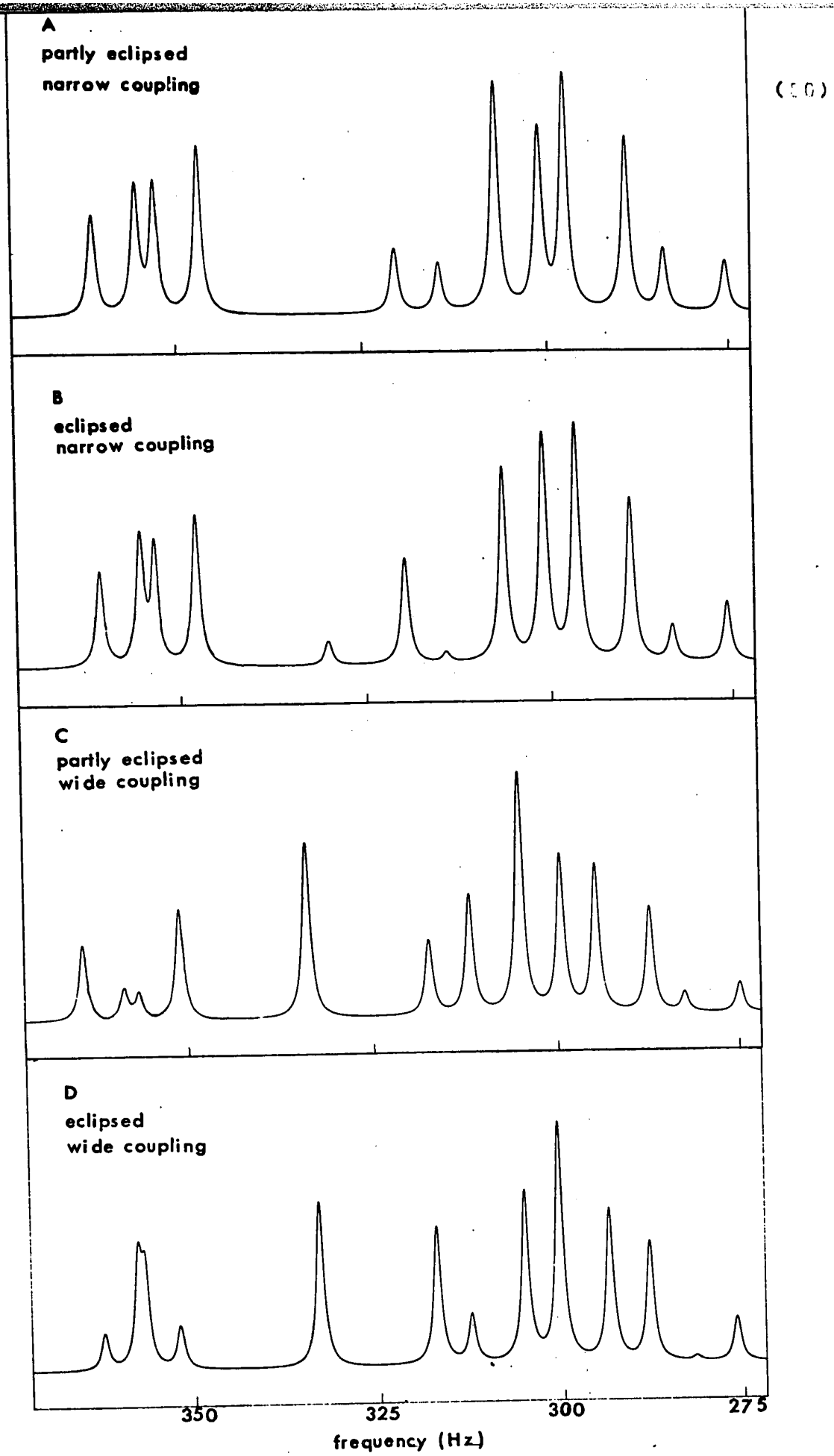
A
partly eclipsed
narrow coupling
B
eclipsed
narrow coupling
C
partly eclipsed
wide coupling
D
eclipsed
wide coupling
350
325
300
275
frequency (Hz)

second, third and fourth line of each quartet. The sign of this coupling cannot be determined from the spectrum.

In order to verify the analysis, calculations were repeated using both possible choices of quartets (Figures 4.6,4.7) Wide and narrow couplings were measured for each choice of quartets. The results of these calculations were used to simulate spectra and the intensities of the lines were compared with the observed spectrum (Fig. 4.8). The best fit was found for values of J_{BX} and J_{AX} of 6.0 Hz and 8.4 Hz.

4.2.3 Discussion of Spectra.

Amphetamine.HCl has a 'deceptively simple' spectrum (Fig. 4.4). A ''deceptively simple'' spectrum arises when J_{AX} and J_{BX} are about equal and J_{AB} is much larger than the difference in chemical shifts between A and B (15). Spectra at pD's of 10 and 2 were also deceptively simple (pD = pH + 0.4)(31). Studies were undertaken in mixtures of dimethyl sulfoxide-d_6 (DMSO) and D_2O in various proportions in order to remove the deceptively simple character. These spectra were analyzed, the results are presented in Table 2 and plotted in Figures 4.9 and 4.10.

Table 4.2

Chemical shifts (p.p.m.) and coupling constants (Hz) of amphetamine.HCl in mixed solvents of DMSO-d_6 and D_2O.

%D_2O	%DMSO-d_6	H_C	H_B	H_A	CH_3	J_{BC}	J_{AC}	$J_{CH_3,HC}$	J_{AB}
33	67	379.9	334.9	305.5	148.7	5.2	9.4	6.4	-13.4
40	60	381.1	333.2	307.4	150.1	5.3	9.3	6.6	-13.5
50	50	384.9	332.3	311.1	153.4	5.5	9.2	6.6	-13.5
60	40	387.9	330.5	315.0	155.4	5.6	8.6	6.6	-13.6
75	25	390.1	328.1	319.7	157.8	6.2	8.4	6.6	-13.7
80	20	391.3	328.4	319.1	158.2	6.2	8.2	6.6	-13.6
			Line positions[a]						
85	15	393.2	328.5,321.7,320.5		159.5	-	-	6.6	-
90	10	393.4	328.5,321.4,321.0		160.1	-	-	6.6	-
95	5	395.5	328.7	321.6	160.8	-	-	6.6	-
100	0	395.1	329.0	321.8	160.7	-	-	6.6	-

a. The line positions reported in the second part of the table are not the chemical shifts of the A and the B protons, an estimate of the chemical shifts can be obtained by extrapolation from the the values reported in the first section of this table (see text).

Figure 4.9

Proton chemical shifts of amphetamine.HCl as a function of solvent composition.

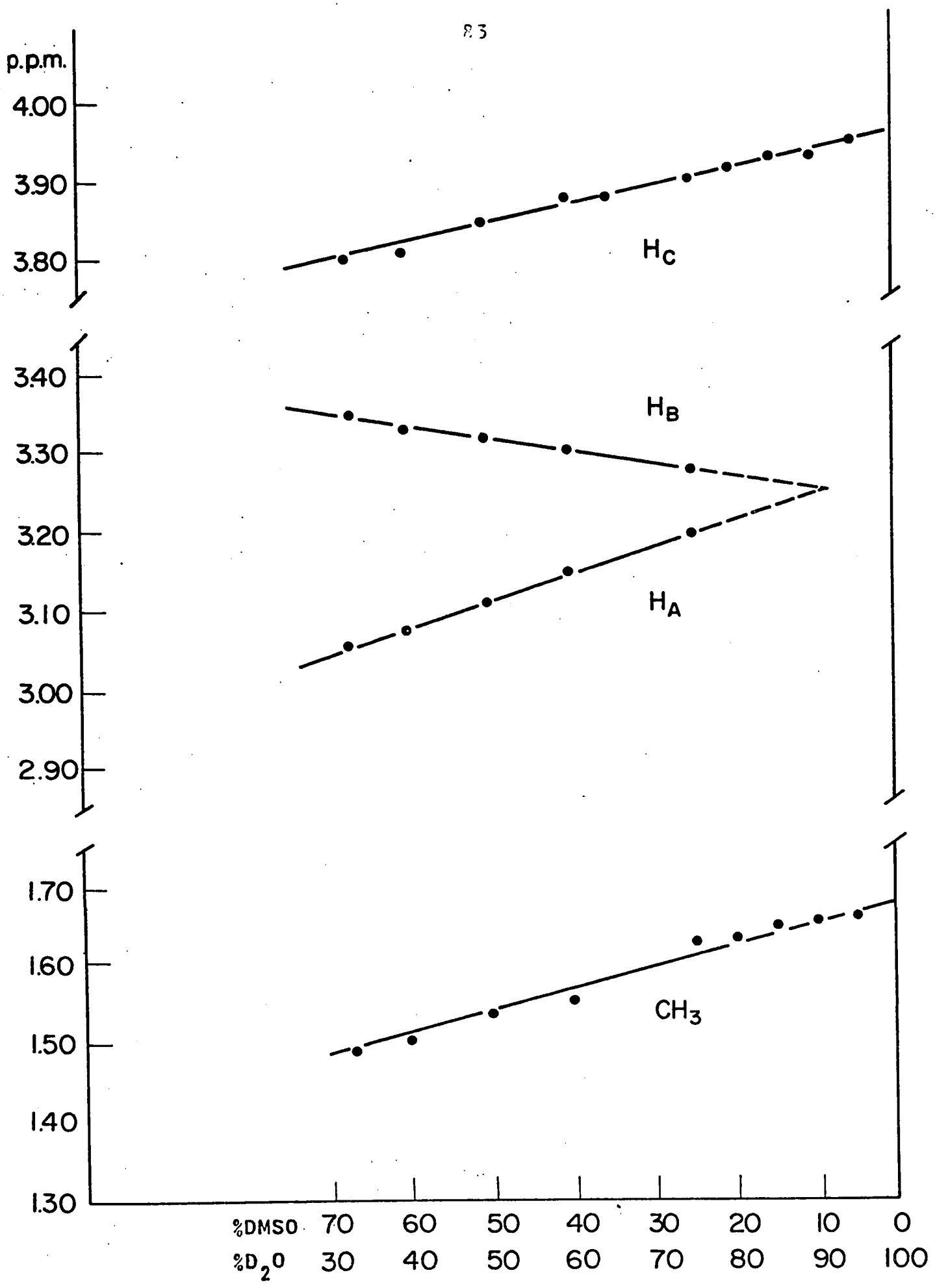
p.p.m.
4.00
3.90
3.80
H_C
3.40
3.30
3.20
3.10
3.00
2.90
H_B
H_A
1.70
1.60
1.50
1.40
1.30
CH_3
%DMSO 70 60 50 40 30 20 10 0
$\%D_2O$ 30 40 50 60 70 80 90 100

Figure 4.10

Coupling constants of amphetamine.HCl as a function of solvent composition.

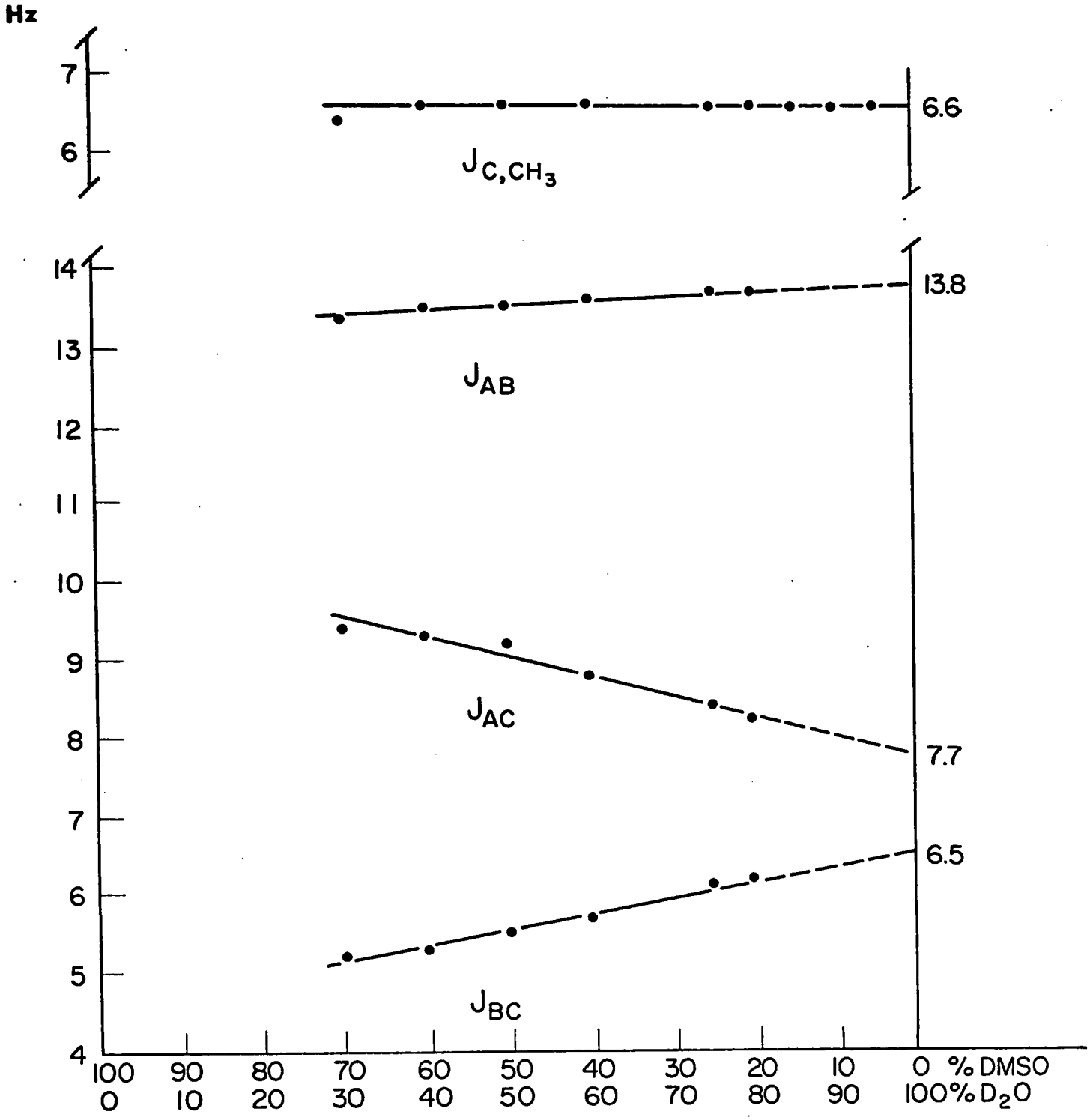
Hz
7
6
6.6
J_{C,CH_3}
14
13
12
11
10
9
8
7
6
5
4
13.8
J_{AB}
J_{AC}
7.7
6.5
J_{BC}
100 0
90 10
80 20
70 30
60 40
50 50
40 60
30 70
20 80
10 90
0 % DMSO
100% D_2O

Extrapolation of the values calculated for the mixed solvents to 100% D_2O gives an estimate of the values of J_{AC} and J_{BC}. J_{AC} is found to be $\simeq$ 7.7 Hz and J_{BC} $\simeq$ 6.5 Hz. This result is plausible because the separation between the two peaks is 7.2 Hz and is equal to $1/2|J_{AC}+J_{BC}|$.

The spectrum of benzphetamine (Fig.4.5) produces lines of different widths in the ABC part of the spectrum Lines belonging to the B resonance are twice as broad as the A or C lines. Among the amphetamines analyzed, benzphetamine is the only one in which such a phenomenon occurs. Broadening of the lines could be due to an unresolved coupling between the B nucleus and the α methyl group. However, spin decoupling experiments proved this was not the case. Irradiation of the α methyl group produced a decoupled spectrum of the C region but had no effect on the width of the B region. In the next section it will be shown that the benzphetamine molecule is the most hindered molecule as far as rotation about the ethane linkage is concerned. 99% of the time the B proton is <u>gauche</u> to the nitrogen atom whereas the A proton is <u>gauche</u> to the nitrogen only 65% of the time. Nitrogen has a quadrupole moment and this could be responsible for the observed line broadening.

4.2.4. Preferred Conformations of Amphetamines. Rotamer Calculations.

The values of the AC and BC couplings are average values because of rotation about the ethane linkage. Assuming that the observed values of the AC and BC couplings arise from an average over 60^{o} staggered rotamers (Figure 4.11), it is possible to calculate the relative populations of each rotamer using the following set of equations

$$\bar{J}_{AC} = P_{I}J_{t} + P_{II}J_{g} + P_{III}J_{g}$$

$$\bar{J}_{BC} = P_{I}J_{g} + P_{II}J_{t} + P_{III}J_{g}$$

$$1 = P_{I} + P_{II} + P_{III}$$

where Pi is the mole fraction of each rotamer, J_g and J_t are the values of the gauche and trans couplings respectively.

Values of 2.0 Hz and 13.0 Hz for J_g and J_t were used. These are average values of vicinal couplings and apply to systems containing not more than one strongly electronegative substituent (20). The results of these calculations indicate a preference for the trans phenyl-amino rotamer. In

Figure 4.11

Rotamer populations of amphetamine and amphetamine derivatives in aqueous solutions.

ROTAMER POPULATIONS IN D_2O

Amphetamine (free base)

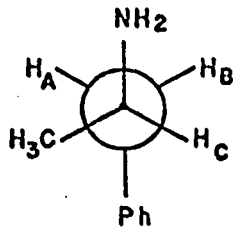

Ia 50%

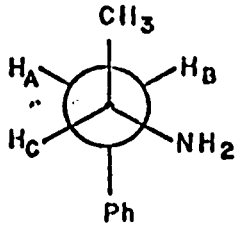

Ib 39%

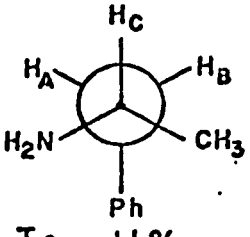

Ic 11%

Amphetamine·HCl

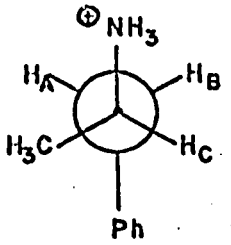

IIa

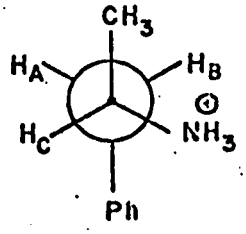

IIb

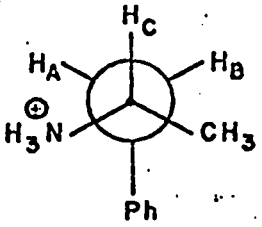

IIc

Methamphetamine·HCl

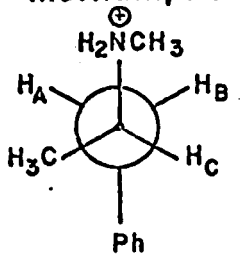

IIIa 55%

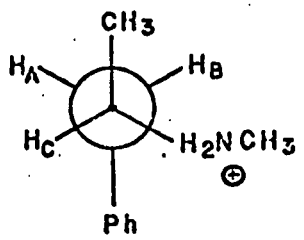

IIIb 39%

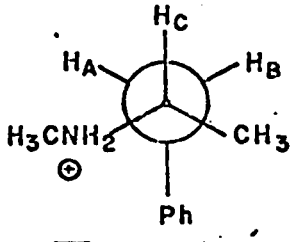

IIIc 6%

o-Methoxymethamphetamine·HCl

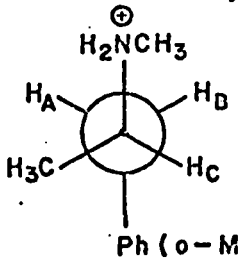

IVa 47%

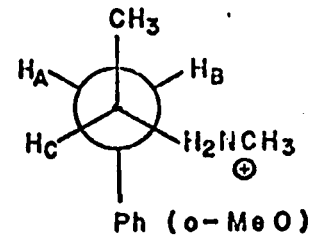

IVb 36%

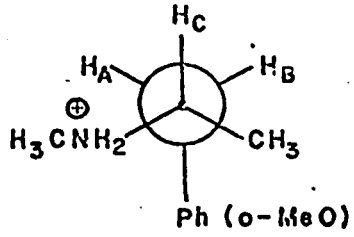

IVc 17%

Benzphetamine·HCl

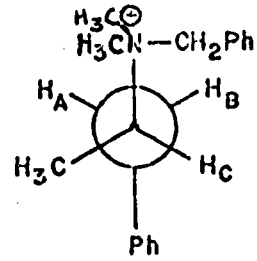

Va 64%

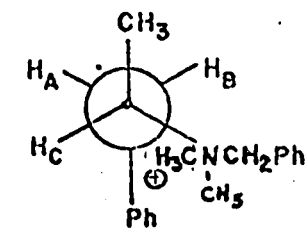

Vb 35%

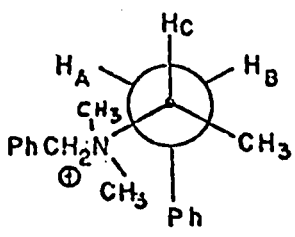

Vc 1%

order to estimate the possible errors in these calculations extreme values of J_g = 1.5 and 2.5 Hz and J_t = 10.0 and 15.0 Hz were used. These calculations also indicate preference for the trans phenyl-amino rotamer.

A general trend in rotamer populations can be seen. As the substituents on the the nitrogen atom get bulkier there is less free rotation about the ethane linkage. This is understandable, the bulky groups are more staggered in the trans phenyl-amino conformation and this rotamer becomes increasingly populated as the size of the substituents increase from amphetamine through to benzphetamine.

This work was done in collaboration with Drs G. Neville and B.J. Blackburn and has been published (27).

4.3 Conclusion.

It has been proposed (28) that the mechanism for the stimulating activity of amphetamine in the central nervous system (CNS) is similar to that which occurs in the peripheral nervous system. Amphetamines are believed to act by releasing naturally occurring amines such as norepinephrine. This implies some type of interaction with receptors. The fact that amphetamine and amphetamine derivatives increase the release of norepinephrine from brain slices (8) and inhibit the reuptake of norepinephrine (9) could imply that amphetamine binds preferentially to an element in the transport system. If norepinephrine concentration in the vesicles or the cell cytoplasm itself is maintained by an active transport mechanism, amphetamines could bind irreversibly to a transport 'protein' . The membrane could be naturally leaky to norepinephrine and norepinephrine would be maintained in the vesicles by an active uptake mechanism. This mechanism would be inhibited by amphetamine, the norepinephrine would leak out of the vesicles and not be taken up again. Amphetamine, due to the presence of an α-CH_3 group, is a monoamine oxidase inhibitor.

therefore the norepinephrine which escapes from the storage granules would not be metabolized by monoamine oxidase and would be in a physiologically active state for long periods of time. The norepinephrine would cross the cell membrane and interact at postsynaptic receptors.

The fact that amphetamine does not produce direct stimulation of the CNS (26) implies that the structure and conformation of amphetamine does not mimic a norepinephrine molecule at the post-synaptic receptor. This could be due to a lack of hydroxyl or methoxy groups on the phenyl ring. It has been proposed that the hallucinogenic amphetamines may act directly on the post-synaptic membrane receptor (24).

Amphetamine and methoxylated amphetamines probably act in diffrent manners. Only the methoxylated amphetamines are hallucinogenic (1,2). Snyder and Richelson (29) proposed a conformation for 2,4,5 trimethoxy amphetamine in which a hydrogen bond exists between the oxygen of the methoxy group at C-2 of the phenyl ring and a hydrogen from the amino group thus giving rise to a six membered ring mimicking the C ring of LSD. The phenyl ring of amphetamine would mimic the A ring of LSD. The NH of 3,4,5 trimethoxyamphetamine could

hydrogen bond to the π electrons at C-2 and C-6 of the phenyl ring thus giving rise to a five membered ring similar to the B ring of LSD. Mescaline, 3,4,5 trimethoxyphenylethylamine , could form the A and B rings of LSD.

The hydrogen bonded structures involve conformations in which the free rotation normally possible about an ethane linkage is considerably hindered or not present. In these structures the phenyl and amino groups are in a more gauche than trans conformation.

Our studies have demonstrated that the trans phenylamino rotamers are preferred in amphetamine and amphetamine derivatives. However, only one methoxylated compound was studied. In future experiments, Snyder's and Richelson's hypothesis could be more directly tested. This would simply involve a study of amphetamine and hallucinogenic derivatives in non-aqueous solvents in which hydrogen bonds can form and be observed. This type of experiment is subject to the criticism that the preferred conformation in a non-aqueous solvent is not necessarily the same as that in aqueous solution. This series of studies would however indicate if there is any difference in hydrogen bonding properties between various non-hallucinogenic amphetamines and the hallucinogenic methoxyamphetamines.

Chothia and Pauling (30) have proposed a model for the conformation of 2,4,5-trimethoxyamphetamine in which the phenyl and amino groups are trans to each

other. This model is stereochemically less hindered than that of Snyder and Richelson but it does not account for the lack of hallucinogenic activity of amphetamine derivatives which are not trimethoxylated.

In amphetamines hallucinogenic activity appears to be related to ring methoxylation at specific sites and although the preferred conformation about the ethane linkage is probably involved, it does not account for hallucinogenic activity by itself.

Having found the preferred conformation for amphetamine and amphetamine derivatives in solution it should be possible to relate structure and activity in these compounds. If the preferred conformation of trimethoxyamphetamines in solution is also the conformation in which these compounds interact with receptors, the model proposed by Snyder and Richelson would be less likely to interact at post-synaptic norepinephrine receptors than that of Chothia and Pauling. This is based on the observation that the trimethylsilyl ether of adrenaline and other hydroxyphenylalkylamines in solution (14) show a preference for the <u>trans</u> phenyl-amino rotamer.

4.4 References.

1. J.R. Smithies, V.S. Johnston,R.J. Bradley F. Benington, R.D. Morin and L. Clark, Nature 216 128 (1967)

2. J.M. Braton, J.R. Smythies,R.D. Morin and L.C. Clark, Nature 220 800 (1968).

3. B.M. Angrist, J.W. Schweitzer, A.J. Friedhoff and S. Gershon, Nature 225 615 (1970)

4. J. Glowinski and R.D. Baldessarini, Pharm. Rev. 18 #1 1201 (1966)

5. G.H. Bell, J.N. Davidson and H. Scarborough, Textbook of Physiology and Biochemistry 6th ed., The Williams and Wilkins Co. Baltimore, 1965

6. P. B. Molinoff and J.B. Axelrod, Ann. Rev. Biochem. 40 465 (1971)

7. A. Carlsson, Pharm. Rev. 18 #1 541 (1966)

8. K.Y. Ng, T.N. Chase and I.J. Kopin, Nature 228 468 (1970)

9. A. Carlsson, International Symposium on Amphetamines and Related Compounds, E. Costa and S. Garattini eds. Raven Press, N.Y., 1970 p.289

10. D. Carlstrom and R. Bergin, Acta Cryst. 23 313 (1967).

11. R. Bergin and D. Carlstrom, Acta Cryst. B24 1506 (1968)

12. G. Tsoucaris, Acta Cryst. 14 909 (1961)

13. T. Sasaki, K. Kanematsu, Y. Tsuzuki and K. Tanaka, J. Med. Chem. 9 847 (1966)

14. J.E. Forrest, R.A. Heacock and T.P. Forrest, J. Pharm. Pharmac. 22 517 (1970)

15. G. Slomp, Appl. Spectrosc. Rev. 2 263 (1969)

16. S. Castellano and A.A. Bothner-By, J. Chem. Phys. 41 3868 (1964)

17. R.R. Fraser, R.U. Lemieux and J.D. Stevens, J. Amer. Chem. Soc. 83 3901 (1961)

18. L.M. Jackman and S. Sternhell, Applications of Nuclear Magnetic Resonance Spectroscopy in Organic Chemistry 2nd ed. Pergamon Press, Oxford, 1969 p. 286

19. A.A. Bothner-By, Adv. Mag. Res. 1 196 (1965)

20. S. Sternhell, Quart. Rev. (London) 23 247 (1969)

21. A.J. Mandell and M. Morgan, Nature 227 75 (1970)

22. J. Axelrod, International Symposium on Amphetamine and Related Compounds, E. Costa and S. Garattini eds., Raven Press, N.Y., 1970 p. 207

23. B.B. Brodie, A.K. Cho and G.L. Gessa, International Symposium on Amphetamine and Related Compounds, E. Costa and S. Garattini eds. Raven Press, N.Y., 1970 p.217

24. F.D. Hendley and S.H. Snyder, Nature 229 264 (1971)

25. J.H. Biel, International Symposium on Amphetamine and Related Compounds, E. Costa and S. Garattini eds., Raven Press, N.Y., 1970 p. 3

26. E. Muscholl, Pharm. Rev. 18 #1 551 (1966)

27. G. Neville, R. Deslauriers, B.J. Blackburn and I.C.P. Smith, J. Med. Chem. 14 717 (1971)

28. L. Stein, Fed. Proc., Fed. Amer. Soc. Exptl. Biol. 23 836 (1964)

29. S.H. Snyder and E. Richelson, Proc. Natl. Acad. Sci. U.S.A. 60 206 (1968)

30. C. Chothia and P. Pauling, Proc. Natl. Acad. Sci. U.S.A. 63 1063 (1969)

31. P.K. Glascoe and F.A. Long, J. Phys. Chem. 64 188 (1960)

CHAPTER 5

NMR STUDIES OF RARE NUCLEOSIDES FOUND IN TRANSFER RNA.

5.1 Introduction.

5.2 Conformation of a Rare Nucleoside in Aqueous Solution

- 5.2.1 Dihydrouridine.
- 5.2.2 Comparison with Uridine and β-pseudouridine.

5.3 Conformation of β-pseudouridine at Basic pD.

- 5.3.1 Conformational Analysis
- 5.3.2 Comparison with α-pseudouridine and β-cyanuric acid riboside.

5.4 Conformation of Rare Nucleosides in Dimethyl Sulfoxide and in Water.

- 5.4.1 Conformational Analysis
- 5.4.2 Measurement of OH Couplings in Dimethyl Sulfoxide.

5.5 Conclusion

5.6 References

CHAPTER 5.

NMR STUDIES OF RARE NUCLEOSIDES FOUND IN TRANSFER RNA.

5.1 Introduction.

A number of sequences of transfer RNA molecules have appeared in the literature (1 - 15). Transfer RNA differs from messenger RNA and ribosomal RNA by the presence of a number of modified nucleosides. The main modifications are methylation at various positions of the bases and O-methylation at the 2' position of the ribose ring. A third group of bases undergoes transformation which fall into neither of the above categories. This last group comprises pseudouridine (ψ), dihydrouridine ($\mathcal{D}$), inosine (I), thiouridine (U*), isopentenyl adenosine (IpA) (16), N-(purin-6-yl carbamoyl) threonine (17),6-(4-hydroxy-3-methyl-2-butenyl-amino)9-β-D ribofuranosyl purine (18).

Transfer RNA is synthesized using only the common bases guanine, adenine, uracil and cytosine.

Modifications occur after termination of synthesis, by a group of specific enzymes(19,20).

Rare nucleosides occur mainly in the looped regions of the cloverleaf model of transfer RNA. One of the loops has been called the dihydroU loop because it contains most of the dihydrouridine found in the transfer RNA molecules. Pseudouridine always occurs in the TψC sequence of the loop adjacent to the 3' end, and occasionally in the anticodon region in place of uridine.

This leads one to question the role of the rare nucleosides in transfer RNA. The rare bases could have binding properties which differ from those of the common bases (21). This would influence the overall configuration of the transfer RNA molecule (22 - 24). The conformation of the molecule may affect such processes as codon-anticodon binding (25,26), acetylation (27,28), or ribosome binding (29) and could provide a sensitive control mechanism for protein synthesis.

NMR has already been applied to the study of uridine (30) and pseudouridine (31,32)(Fig.5.1) in aqueous solution. Continuing this series of in investigations I have analysed the conformation

Figure 5.1

Molecular structures of uridine (U), dihydro-uridine (D), β-cyanuric acid riboside (β-CAR) and β-pseudouridine (β-ψ).

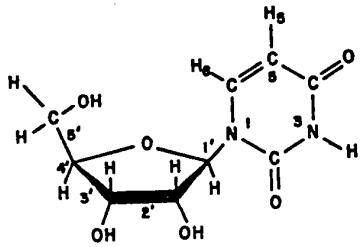

U

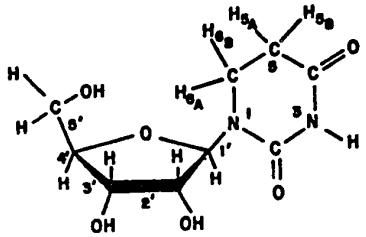

D

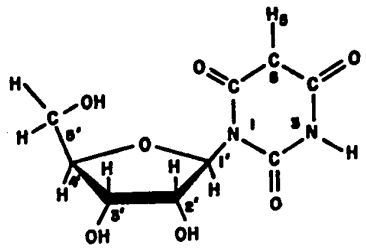

β-CAR

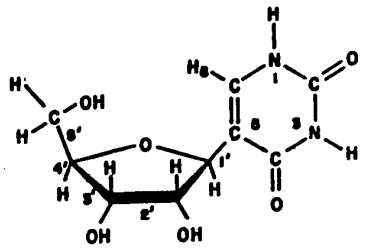

β-ψ

(001)

of dihydrouridine.

5.2 Conformation of a Rare Nucleoside in Aqueous Solution.

5.2.1 Conformational Analysis of Dihydrouridine.

Dihydrouridine was purchased from Cyclo Chemicals and used without further purification. No impurities were observed in the NMR spectrum demonstrating that they were present to less than 5% of the total solute. 0.1 M solutions were prepared in D_2O and triply lyophilized in order to minimize the resonances from HDO. The solutions were run at pD 6.8 (pD = pH + 0.4)(33). Spectra were run on Varian XL-100 and HR-220 spectrometers (Canadian 220 MHz Center, Ontario Research Foundation, Sheridan Park, Ontario), at temperatures of 23°C, 60°C and 80°C.

No spectral changes occurred when samples were rerun at 23°C, after having been run at higher temperatures.

Spectral assignments were made by reference to the data available for uridine (U)(30), pseudouridine (Ψ)(31,32) and dihydrouracil (36).

Spectral analysis was first carried out by a first order and an ABX approximation, data gained

in this manner were then refined by computer analysis using a modified version of LAOCOON II (34).

Results and Discussion.

The observed and simulated spectra are shown in Figure 5.2 . The chemical shifts and coupling constants obtained from the spectra are in Table 5.1. Analysis of the base conformation was carried out by Dr. R.D. Lapper (35). The two 5 and two 6 protons give rise to an ABXY spectrum. The spectrum however proved to be 'deceptively simple' even at 220 MHz. The data indicate that the dihydrouracil base in the nucleoside is in a conformation similar to that of the free base (36). It appears that the dihydrouracil ring interconverts between various puckered conformation with an average torsional angle of 30°. The dihydrouracil ring is not as rigid as the rings in uridine and pseudouridine. The mobile base conformation may influence the hydrogen bonding properties of dihydrouridine in transfer RNA.

FIGURE 5.2

Observed and simulated 220 MHz spectra of dihydrouridine.

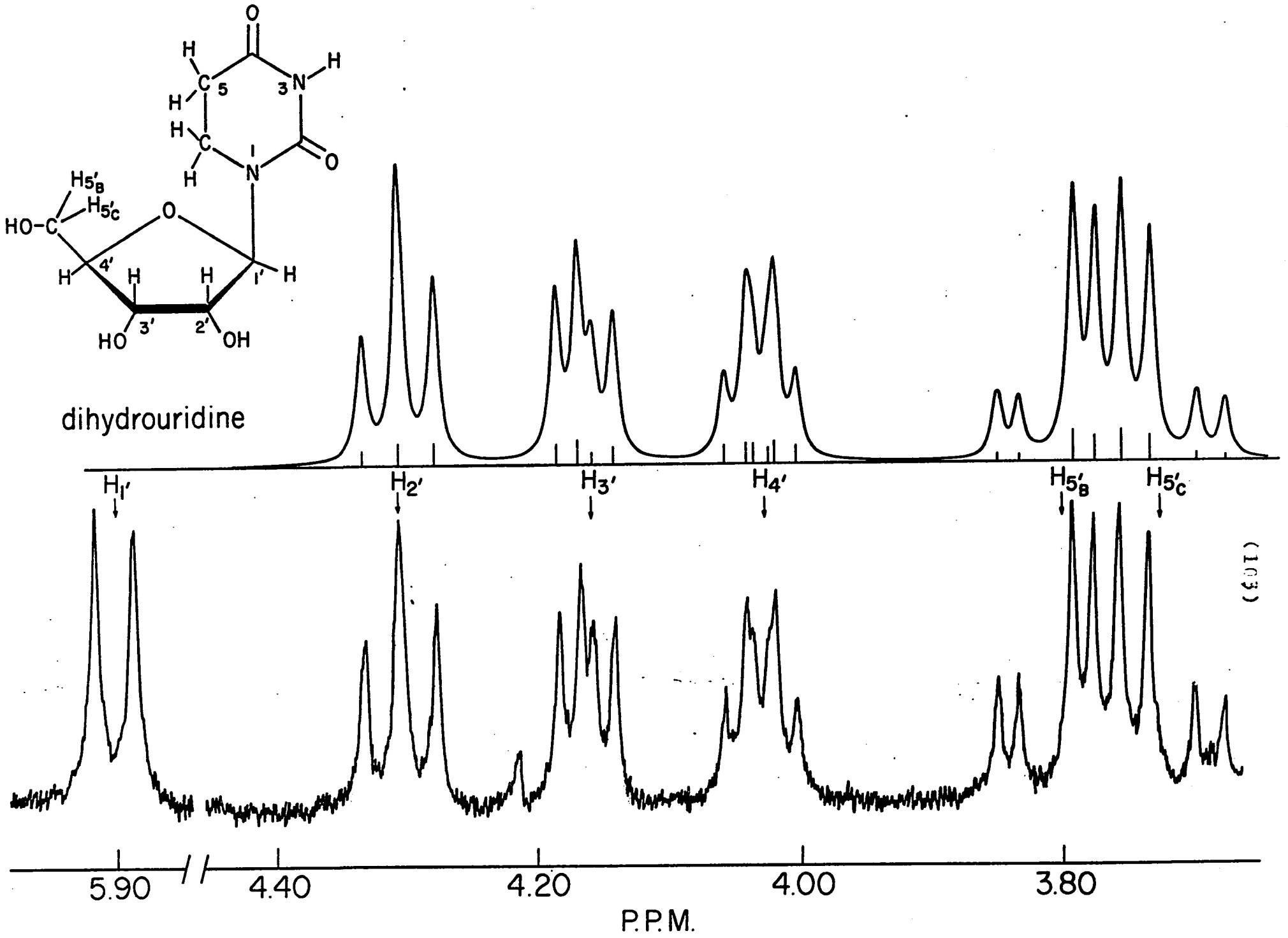
dihydrouridine
H1'
H2'
H3'
H4'
H5'B
H5'C
5.90
4.40
4.20
4.00
3.80
P.P.M.

Table 5.1

Chemical shifts and coupling constants of dihydrouridine.

Table 1. Chemical Shifts and Coupling Constants of Dihydrouridine[1]

Chemical Shifts[2] (ppm)			Coupling Constant (Hz)		
	23°	60°		23°	60°
$H_{1'}$	5.864	5.829	$J_{1'2'}$	6.0	6.1
$H_{2'}$	4.303	4.298	$J_{2'3'}$	6.0	5.9
$H_{3'}$	4.164	4.160	$J_{3'4'}$	3.6	4.2
$H_{4'}$	4.030	4.024	$J_{4'5'B}$	3.6	3.9
$H_{5'B}$	3.804	3.813	$J_{4'5'C}$	4.8	5.2
$H_{5'C}$	3.727	3.735	$J_{5'B5'C}$	-12.6	-12.4
H_{5A}[3]	2.75	2.78	J_{5A5B}[4]	-	-
H_{5B}	2.75	2.78	J_{5A6A}	7.1	6.2
H_{6A}	3.59	3.60	J_{5A6B}	6.5	6.8
H_{6B}	3.53	3.55	J_{5B6A}	6.6	6.8
			J_{5B6B}	7.0	7.3
			J_{6A6B}	-12.9	-12.9

1. The estimated accuracy of the chemical shifts and coupling constants is 0.005 ppm and 0.2 Hz, respectively.
2. Measured in D_2O, pD 6.8, versus internal sodium-3-trimethylsilylpropionate-2,2,3,3-d_4 (TSP).
3. These are approximate values only, with estimated errors in the chemical shifts and coupling constants of 0.01 ppm and 1 Hz, respectively.
4. Not accurately determinable.

Conformation of the Ribose Ring.

The Karplus relation is often used in relating observed coupling constants to ribose ring conformations (31,32,37,38,39). A number of possible conformations exist for five-membered rings. Smith and Jardetzky (37) calculated coupling constants and dihedral angles for twenty conformations of ribose and deoxyribose nucleosides. Figure 5.3 illustrates four ring structures which can be found in nucleic acids. The dihedral angles and coupling constants associated with these structures are given in Table 5.2 (38). These were calculated using Dreiding models. Four atoms were kept in a plane and either the 2' or the 3' carbon was buckled out of the plane. The model was projected onto a surface and the relevant dihedral angles measured. Results were reproducible within 5°. (38).

The J_o values chosen were those suggested by Abraham et al (40) for several carbohydrate ring systems

$$J_o = 9.27 \text{ Hz} \qquad 0^\circ \leq \phi \leq 90^\circ$$

$$J_o = 10.36 \text{ Hz} \qquad 90^\circ \leq \phi \leq 180^\circ$$

Figure 5.3

Four possible ring puckered conformations of dihydrouridine.

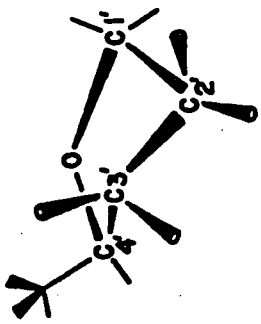

$C_{2'}$-exo

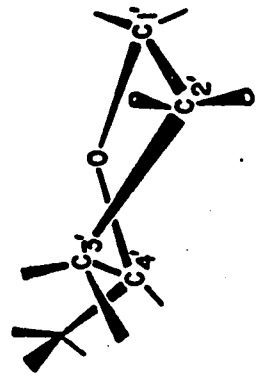

$C_{3'}$-endo

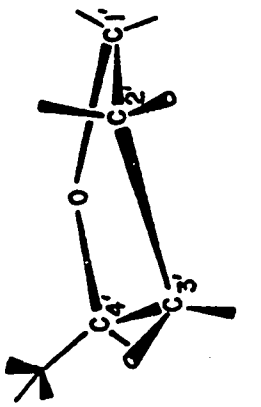

$C_{3'}$-exo

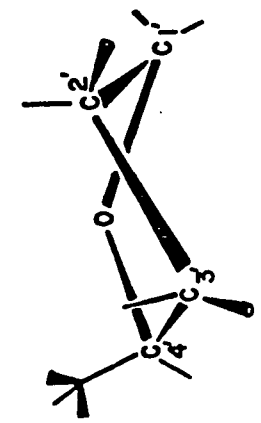

$C_{2'}$-endo

Table 5.2

Expected angles and coupling constants for diffrent ribofuranose ring conformations.

Table 2. Expected Angles and Coupling Constants for Different Ribofuranose Ring Conformations[1]

Ribose conformation[2]	$\phi_{1'2'}$ degrees	$J_{1'2'}$ Hz	$\phi_{2'3'}$ degrees	$J_{2'3'}$ Hz	$\phi_{3'4'}$ degrees	$J_{3'4'}$ Hz
C_2, endo	155	8.3	35	5.9	101	0
C_2, exo	83	0	35	5.9	143	6.2
C_3, endo	97	0	32	6.4	159	8.5
C_3, exo	140	5.8	28	7.0	95	0
Observed 23°C		6.3		6.0		3.6
60°C		6.1		5.8		4.2

1. From reference (38).
2. These angles were calculated for four atoms of the ribofuranose ring defining a plane.

These values of J_o were the same as those used in earlier studies on υ and β-ψ.

Table 5.2 shows that for a C_2'endo conformation $J_{1'2'}$ is large, $J_{2'3'}$ is intermediate and $J_{3'4'}$ is small. The reverse holds true for a C_3'endo conformation. A rapid time-average with equal populations in each conformation would give an average coupling of 5 Hz for $J_{1'2'}$, $J_{2'3'}$ and $J_{3'4'}$. This has been observed in pseudouridine (31).

The data in Table 5.2 indicate that the ribose ring of dihydrouridine in aqueous solution is not in any of the classical ring conformations. It does not fit any of the twenty conformations calculated by Smith and Jardetzky either (37).

This indicates that dihydrouridine, like β— pseudouridine, is interconverting rapidly between various ring conformations. The equilibrium is shifted towards the C_2'endo and C_3'exo conformational equilibrium. Raising the temperature to 60° did not change the ring conformation.

X-ray studies of crystals of dihydrouridine (41) have shown that the ribose conformation in

the solid state is C_2,endo. This shows that caution must be exerted when using data gained from solid state studies to construct models of biologically active molecules. I do not imply by this that the conformation of a molecule in aqueous solution is the same as that found in biological systems. However, the conformation of a molecule in a crystal may be greatly influenced by intermolecular interactions and packing effects.which are minimized in dilute aqueous solutions. One cannot either ignore the fact that a nucleoside in a tightly coiled polynucleotide may be influenced by its neighbours and may not be in a hydrophilic environment at all. Recently, NMR data for polyuridylic acid (50) has been interpreted (38) as showing that the ribose rings are in rapid conformational equilibrium between various puckered forms, as is the case with uridine (30).

Conformation about the C_4'-C_5' Exocyclic Bond.

The H_4'$_A$, H_5'$_B$, H_5'$_C$ protons give rise to an ABC spin system. Chemical shifts and coupling constants were first estimated on the basis of an ABX analysis and further refined using LAOCOON II. The results are in Table 5.1.

The observed vicinal couplings are average values arising from rapid rotation of $H_{5'C}$ and $H_{5'B}$ about the $C_{4'}-C_{5'}$ bond. The difference between $J_{4'A5'B}$ and $J_{4'A5'C}$ exists because the populations of each rotamer are diffrent (Fig.5.4). $J_{4'A5'B}$ and $J_{4'A5'C}$ would have the same value only if all rotamers were equally populated. The populations were estimated using the equations given in CHAPTER 3 Section 3 with

$$J_o = 9.27 \text{ Hz} \qquad 0^o \leq \phi \leq 90^o$$
$$J_o = 10.36 \text{ Hz} \qquad 90^o \leq \phi \leq 180^o$$
$$\text{and} \quad J_o = 12.00 \text{ Hz} \qquad 90^o \leq \phi \leq 180^o$$

Two values of J_0 were used for the 90^o to 180^o angles in order to estimate the population variations with variation of J_o.

The results of calculations for 60^o staggered rotamers (Fig. 5.4) at 23^oC amd 60^oC are in Table 5.3. At 23^oC the gauche-gauche rotamer is favoured. At 60^oC the preference for the gauche-gauche rotamer is less, as expected. These conclusions are not dependent on the choice of J_o value in the limits I have used or on the assignment of the $H_{5'}$ resonances. Calculations were done using both possible assignments

Figure 5.4

Possible 60° staggered rotamers of the exocyclic hydroxymethyl group about the $C_{4'} - C_{5'}$ bond in dihydrouridine.

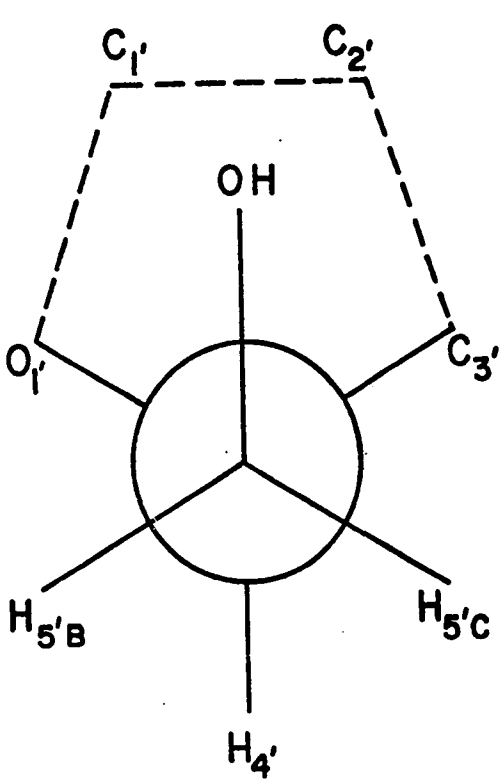

I

(GAUCHE-GAUCHE)

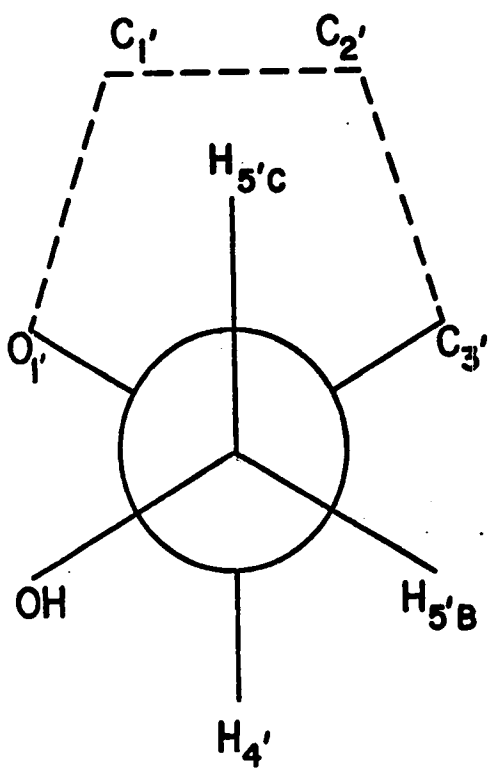

II

(GAUCHE-TRANS)

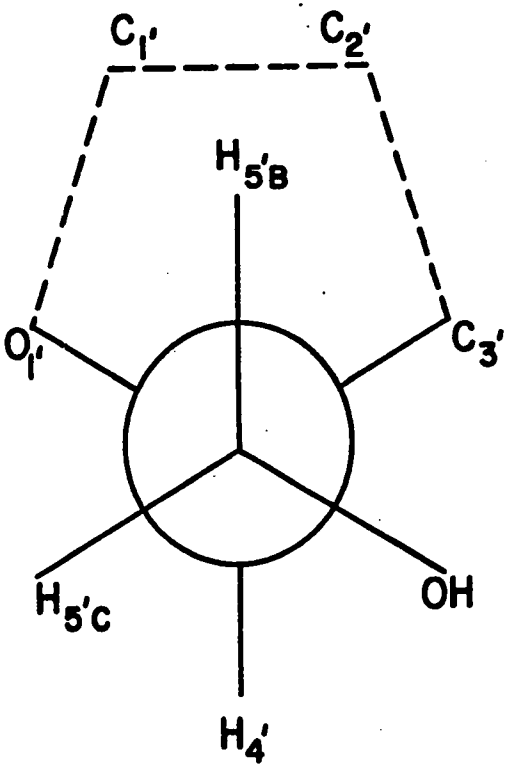

III

(TRANS-GAUCHE)

Table 5.3

Rotamer populations of 60° staggered and rotamers with 15° oxygen-oxygen repulsions.

	60° STAGGERED ROTAMERS					15° OFF-STAGGERED ROTAMERS			
	23°C	60°C	23°C	60°C		23°C	60°C	23°C	60°C
J_{AB}	3.6	3.9	4,8	5.2		3.6	3.9	4.8	5.2
J_{AC}	4.8	5.2	3.6	3.9		4.8	5.2	3.6	3.9
$J_{o(90-180)}$	10.36	10.36	10.36	10.36		10.36	10.36	10.36	10.36
P_1	.45	.38	.45	.38		.26	.13	.26	.13
P_{11}	.35	.39	.20	.23		.38	.48	.25	.33
P_{111}	.20	.23	.35	.39		.36	.39	.49	.54
J_{AB}	3.6	3.9	4.8	5.2		3.6	3.9	4.8	5.2
J_{AC}	4.8	5.2	3.6	3.9		4.8	5.2	3.6	3.9
$J_{o(90-180)}$	12.00	12.00	12.00	12.00		12.00	12.00	12.00	12.00
P_1	.54	.48	.54	.48		.43	.33	.43	.33
P_{11}	.29	.33	.17	.19		226	.33	.15	.21
P_{111}	.17	.19	.29	.33		.31	.33	.42	.46

$J_{o\ (0-90)}$ = 9.27 in all cases.

of the H_5, resonances because it is impossible to make an absolute assignment from the observed spectrum.

Calculations were carried out for rotamers with 15° oxygen-oxygen repulsions (Table 5.3). In this case the preferred rotamers are gauche-trans and trans-gauche. At 60°C however, these rotamers are even more populated. This is physically unrealistic because an increase in temperature ought to increase the rate of rotation and should tend to equalize the populations in each rotamer.

X-ray data (41) indicate that crystals of dihydrouridine are made up of asymmetric units each containing two molecules. In one molecule of the unit cell the hydroxymethyl group is 100% in the gauche-trans conformation (rotamer III). In the other molecule, the exocyclic hydroxymethyl group is 88% trans-gauche (rotamer II) and 12% gauche-gauche (rotamer I). This result does not necessarily prove the invalidity of Karplus relation for systems such as dihydrouridine. It possibly indicates that data gained from the solid state are not necessarily applicable to aqueous solutions, as indicated previously. In crystals, the close packing of

molecules may allow a large number of intermolecular interactions to occur. These interactions may in turn influence the conformation of groups which, potentially, are freely rotating.

Sugar-Base Torsion Angle.

Most of the pyrimidine nucleosides studied in the solid state occur in the anti conformation as defined by Donohue and Trueblood (42)(Fig. 5.5). When a pyrimidine nucleoside exists in a syn conformation, the C_2 keto group lies over the ribose ring. Magnetic anisotropy of the keto group (relative to a hydrogen substituent) is expected to cause downfield shifts of the $H_{2'}$ and $H_{3'}$ resonances and will also produce upfield shifts of the $H_{4'}$ and $H_{5'}$ resonances (43).

β-cyanuric acid riboside, a nucleoside analogue containing three keto groups must exist in a syn conformation. This molecule has already been analyzed by NMR (43).

The chemical shifts of the ribose protons of β-cyanuric acid riboside (β-CAR) are presented in Table 5.4 along with data for uridine (U), β-pseudouridine (β-ψ) and dihydrouridine (D).

Figure 5.5

<u>Syn</u> and <u>anti</u> conformations in pyrimidine nucleosides.

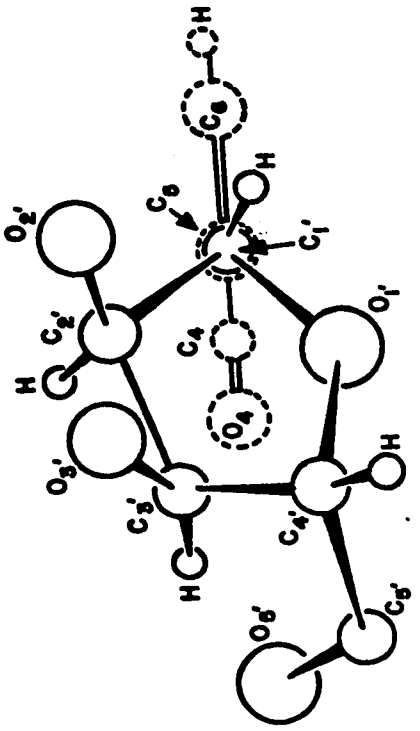

β-ψ SYN

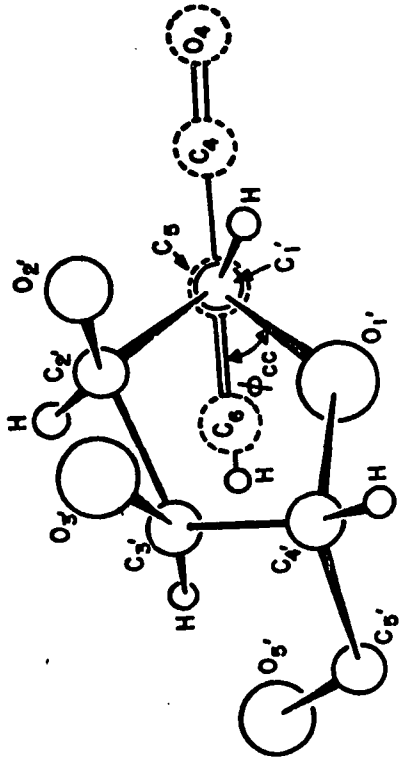

β-ψ ANTI

Table 5.4

Chemical shifts and coupling constants of dihydrouridine and related nucleosides.

Table Chemical Shifts and Coupling Constants of Dihydrouridine and Related Nucleosides

Chemical Shift (ppm)	D [1]	β-CAR [2]	U [3]	β-ψ [4]
$H_{1'}$	5.864	6.100	5.901	5.674
$H_{2'}$	4.303	4.680	4.341	4.279
$H_{3'}$	4.164	4.364	4.222	4.141
$H_{4'}$	4.030	3.952	4.128	4.009
$H_{5'B}$	3.804	3.848	3.907	3.804
$H_{5'C}$	3.727	3.718	3.803	3.726
Coupling Constant (Hz)				
$J_{1'2'}$	6.3	3.9	4.4	5.0
$J_{2'3'}$	6.0	6.4	5.3	5.0
$J_{3'4'}$	3.6	6.6	5.5	5.2
$J_{4'5'B}$	3.6	3.2	3.0	3.2
$J_{4'5'C}$	4.8	6.2	4.4	4.6
$J_{5'B5'C}$	-12.6	-12.8	-12.7	-12.7

1. 220 MHz data
2. 100 MHz, reference 43
3. 220 MHz data, reference 30
4. 100 MHz data, reference 31

This Table shows that the $H_{2'}$ and $H_{3'}$ resonances in dihydrouridine are at higher field and that the $H_{4'}$ resonance is at lower field than the corresponding resonances for the same protons in β-cyanuric acid riboside. The results imply that dihydrouridine occurs in the anti conformation, as do uridine and ψ-pseudouridine.

X-ray data (41) indicate that in crystals of dihydrouridine the base is in the anti conformation, The sugar-base torsion angle was measured to be 65.5° and 57.1° for the two molecules in the asymmetric unit.

Conclusion.

Analysis of proton magnetic resanance spectra of dihydrouridine yielded the following conformational information:

1) the ribose ring interconverts rapidly between various puckered conformations, a slight preference exists for the $C_{2'}$-endo and $C_{3'}$-exo conformational equilibrium.

2) the exocyclic hydroxymethyl group rotates about the $C_{4'}$-$C_{5'}$ bond and shows a preference for the gauche-gauche rotamer.

3) the dihydrouracil base is in the anti conformation with respect to the ribose ring.

4) the dihydrouracil base is non-rigid in contrast to uridine and pseudouridine.

The role of dihydrouridine in transfer RNA may be related to the base mobility and hydrogen-bonding properties which are diffrent from those of the more common nucleoside uridine.

This problem is suited to study by NMR and will be discussed fater in this CHAPTER.

5.3 Conformation of β pseudouridine at Basic pD.

5.3.1 Conformational Analysis.

The H_1 proton in β-pseudouridine (Fig. 5.6) dissociates four times more readily from the nitrogen in position 1 than does the H_1 proton in α-pseudouridine (Fig. 5.7).

The pK_{N1} in α-pseudouridine is 9.5, the same as the pK_{N3}. In β-pseudouridine the pK_{N1} is 9.2 and the pK_{N3} is 9.7. Chambers (44) suggested that the reason for the difference was that the 1-anion is stabilized by a hydrogen bond. This is shown in Figure 5.8. Two conditions are required for formation of the hydrogen bond.1) The exocyclic hydroxymethyl group should be gauche-gauche. In this way the hydroxyl residue will lie over the the ribose ring. 2) The base must be in a syn conformation. The oxygen in position 4 will then lie above the ribose ring.

In order to verify the proposed structure I have studied three molecules : β-pseudouridine (β-ψ), α-pseudouridine (α-ψ), which cannot form the proposed hydrogen bond, and β-cyanuric acid riboside (β-CAR, Fig.5.9) which serves

Figure 5.6

Observed and simulates 220 MHz spectra of α-pseudouridine at pD = 11.1

Figure 5.7

Observed and simulated 100 MHz spectra of β-pseudouridine at pD = 10.6

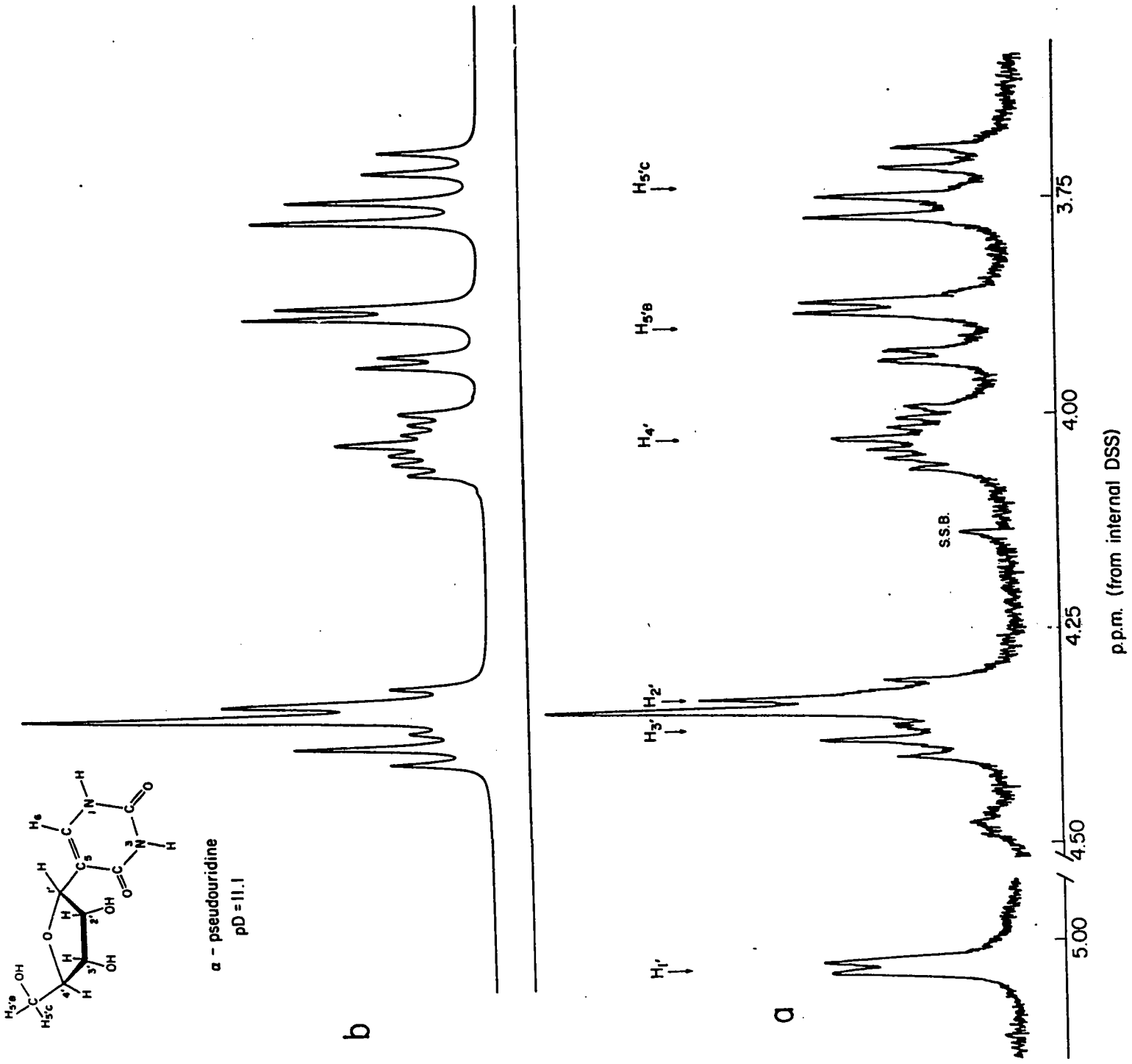
b
α - pseudouridine
pD = 11.1
a
H1'
H3'
H2'
H4'
H5'B
H5'C
S.S.B.
5.00
4.50
4.25
4.00
3.75
p.p.m. (from internal DSS)

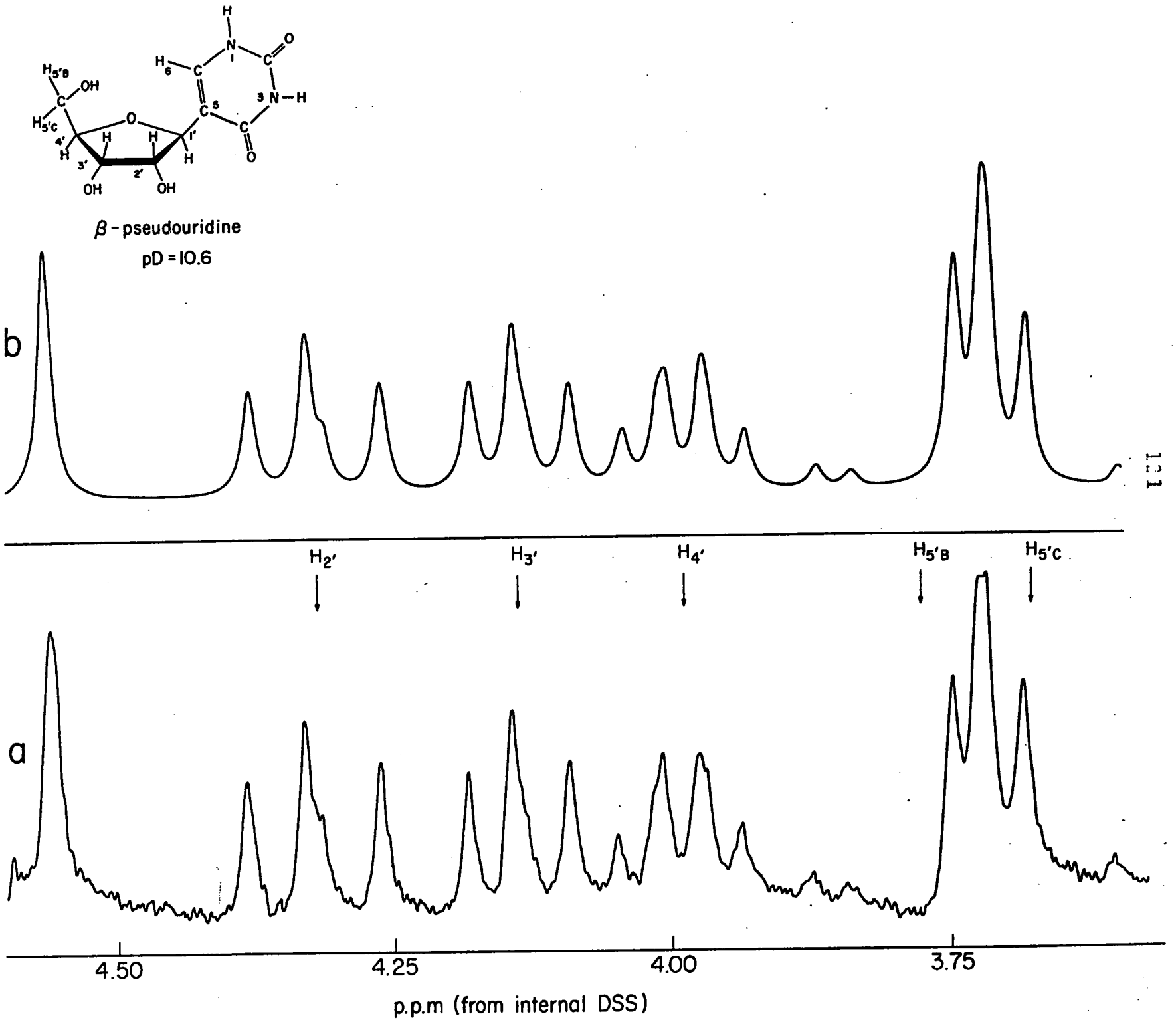
β - pseudouridine
pD = 10.6
b
a
H2'
H3'
H4'
H5'B
H5'C
4.50
4.25
4.00
3.75
p.p.m (from internal DSS)

Figure 5.8

Proposed hydrogen bond formed in β-pseudouridine solutions above pH 9.1

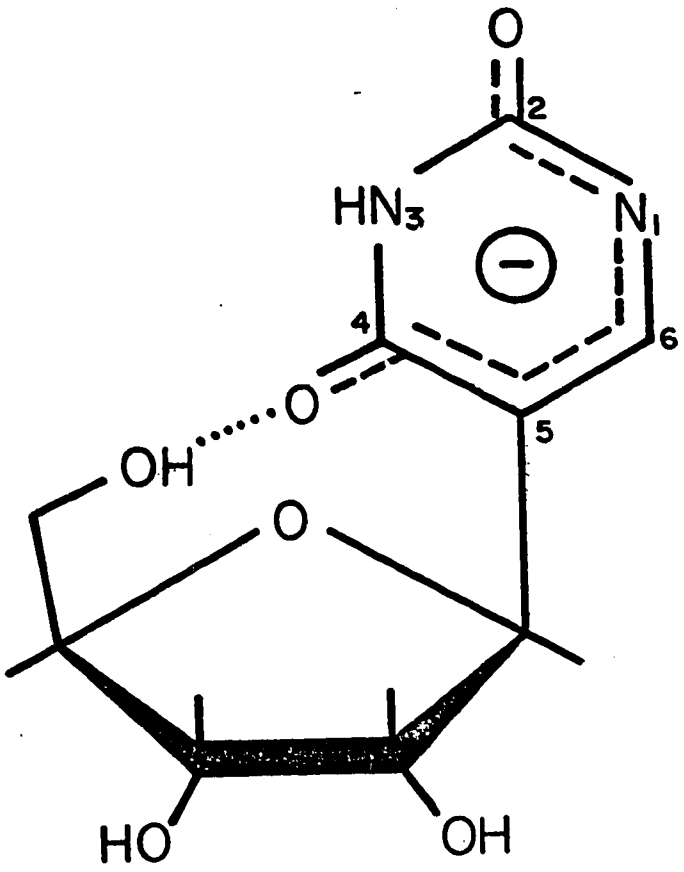
O
2
HN3
N1
4
6
O
5
OH
O
HO
OH

Figure 5.9

Observed and simulated 220 MHz spectra of

β- cyanuric acid riboside at pD = 11.2

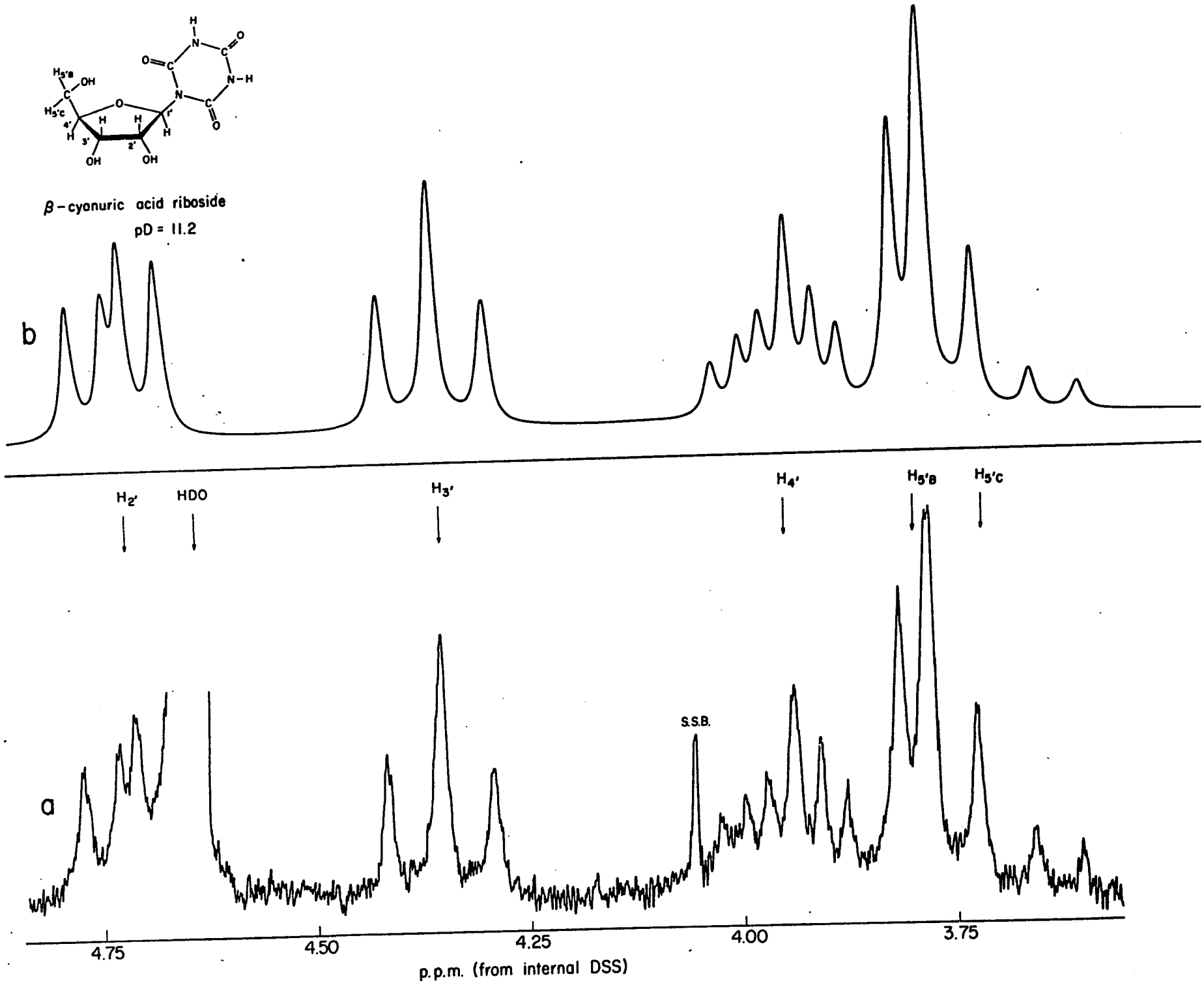
β-cyanuric acid riboside
pD = 11.2
b
a
H2'
HDO
H3'
H4'
H5'B
H5'C
S.S.B.
4.75
4.50
4.25
4.00
3.75
p.p.m. (from internal DSS)

Table 5.5

Chemical shifts of β-pseudouridine, α-pseudouridine and β-cyanuric acid riboside in aqueous solutions at various pD's.

pD	1.1	2.5	6.7[1]	9.7	10.6	1.1	2.4	6.7[2]	10.0	11.1	1.1	4.7	8.0[3]	11.0
$H_{1'}$	N.O.	N.O.	4.67	4.61	4.61	4.99	4.99	4.99	5.00	5.00	6.06	6.07	6.10	6.16
$H_{2'}$	4.28	4.28	4.28	4.33	4.33	4.35	4.35	4.36	4.30	4.27	4.71	4.71	4.71	4.73
$H_{3'}$	4.13	4.13	4.14	4.15	4.15	4.33	4.33	4.33	4.34	4.31	4.36	4.36	4.36	4.36
$H_{4'}$	4.00	4.00	4.01	4.01	4.00	4.00	4.00	4.00	4.00	3.98	3.95	3.95	3.95	3.96
$H_{5'B}$	3.83	3.83	3.84	3.78	3.78	3.87	3.87	3.88	3.87	3.85	3.85	3.85	3.85	3.85
$H_{5'C}$	3.72	3.72	3.73	3.69	3.69	3.70	3.70	3.71	3.71	3.70	3.71	3.71	3.72	3.73
H_6	7.65	7.65	7.66	7.67	7.68	7.57	7.55	7.56	7.64	7.63	-	-	-	-
	beta pseudouridine					alpha pseudouridine					beta cyanuric acid riboside			

1) REFERENCE 31
2) REFERENCE 32
3) REFERENCE 43

N.O.:NOT OBSERVED, RESONANCE OBSCURED BY LARGE HDO PEAK.

CHEMICAL SHIFTS ARE REPORTED IN P.P.M. FROM INTERNAL DSS (3-trimethylsilyl-propane sulfonic acid).

as a model nucleoside in the syn conformation.

β-pseudouridine (90% anomeric purity) and α- pseudouridine (100% anomeric purity) were purchased from Calbiochem. β-cyanuric acid riboside, a gift from Dr. R.K. Robins was prepared by the method of Winkley and Robins (45). Sample pD's were adjusted using dilute solutions of NaOH and then triply lyophilized. pD's were measured before the first lyophilization and again after the spectra were recorded. Reported pD's (Table 5.5) are those measured after experiment. 0.1 M solutions were run at 100 MHz and 220 MHz on the spectrometers mentioned in CHAPTER 5 Section 5.2.1.

Starting parameters for the complete analysis were gained from first order and ABX analysis. Final refinements were done using a modified version of the computer program LAOCOON III (51). Spectra were simulated using chemical shifts and coupling constants which satisfied both the observed 100 MHz and 220 MHz spectra. Only one set of spectra for each compound is presented

Table 5.6

Coupling constants in β-pseudouridine, α-pseudouridine and β-cyanuric acid riboside in aqueous solutions at various pD's.

	beta pseudouridine						alpha pseudouridine						beta cyanuric acid riboside			
pD	1.1	2.5	6.7[3]	9.7	10.6	9.7	1.1	2.4	6.7[4]	10.0	11.1	10.0	1.1	4.7	8.0[5]	11.0
TEMP.	30[1]	30[1]	30[2]	30[2]	30[1]	60[2]	30[1]	30[1]	30[1]	30[2]	30[1]	60[2]	30[1]	30[1]	30[1]	30[1]
$J_{1'2'}$	5.2	5.0	6.8		6.5		3.3	3.3	3.3		3.0		3.9	3.9	4.2	
$J_{2'3'}$	5.2	5.0	5.3		5.5		4.2	4.2	4.2		4.4		6.4	6.4	6.3	
$J_{3'4'}$	5.2	5.2	4.0		4.4		7.9	7.9	8.2		8.0		6.6	6.6	6.2	
$J_{4'5'B}$	3.2	3.2	3.2		3.2		2.4	2.4	2.6		2.9		3.2	3.2	3.1	
$J_{4'5'C}$	4.6	4.6	4.1		4.4		5.7	5.7	5.1		5.4		6.2	6.2	5.6	
$J_{5'B5'C}$	-12.7	-12.7	-12.3		-12.4		-12.4	-12.7	-12.4		-12.4		-12.3	-12.8	-12.4	
$J_{1'6}$	0.7	0.8	0.5		N.O.		1.0	1.1	0.9		N.O.		-	-	-	

(12C)

1) 100 MHz SPECTRUM.
2) 220 MHz SPECTRUM.
3) REFERENCE 31.
4) REFERENCE 32.
5) REFERENCE 43.

N.O. : NOT OBSERVABLE.

for brevity. Chemical shifts are reported in parts per million (p.p.m.) from internal DSS (sodium,2,2-dimethyl-2-silapentane-5-sulfonate)

Results and Discussion.

The chemical shifts of acidic and basic solutions of α-pseudouridine, β-pseudouridine and β-cyanuric acid riboside were assigned by comparison with spectra run at neutral pD (Table 5.5). Coupling constants are presented in Table 5.6.

Ribose Conformation.

Table 5.7 contains the values of observed couplings in neutral and basic solutions for α-pseudouridine, β-pseudouridine, and β-cyanuric acid riboside. These are compared to values calculated for a number of ribose ring conformations.

β-pseudouridine at neutral pD interconverts rapidly between various ring puckered conformations (31). The same phenomenon occurs at acidic pD. At basic pD's, above the pK for singly ionized species (44), the ribose ring tends towards a C_2,<u>endo</u> - C_3,<u>exo</u> conformational equilibrium as judged from the coupling constants of 6.8, 5.3

Table 5.7

Expected angles and coupling constants for various ribofuranose ring conformations. Observed coupling constants for β-pseudouridine, α-pseudouridine and β-cyanuric acid riboside in neutral and basic solutions.

RIBOSE CONFORMATION [1]	$\phi_{1'2'}$ degrees	$J_{1'2'}$ Hertz	$\phi_{2'3'}$ degrees	$J_{2'3'}$ Hertz	$\phi_{3'4'}$ degrees	$J_{3'4'}$ Hertz
$C_{2'}$ endo	155	8.3	35	5.9	101	0
$C_{2'}$ exo	83	0	35	5.9	143	6.2
$C_{3'}$ endo	97	0	32	6.8	159	8.5
$C_{3'}$ exo	140	5.8	28	7.0	95	0
β - ψ						
BASIC pD		6,8		5.3		4.0
NEUTRAL pD [2]		5.0		5.0		5.2
α - ψ						
BASIC pD		3.3		4.2		8.2
NEUTRAL pD [3]		3.3		4.2		7.9
β - CAR						
BASIC pD		4.2		6.3		6.2
NEUTRAL pD		3.9		6.4		6.6

1) REFERENCE 38
2) REFERENCE 31
3) REFERENCE 32

and 4.0 Hz for $J_{1',2'}$, $J_{2',3'}$ and $J_{3',4'}$ respectively.

α-pseudouridine, at all pD's studied, tends towards the C_3,<u>endo</u>-C_2,<u>exo</u> equilibrium. The conformation of the ribose ring in β-cyanuric acid riboside shows very little pD dependance. It does not reside in any of the conformations calculated in Table 5.7, and must interconvert rapidly between various puckered forms.

None of the molecules undergo large conformational changes when going from 30°C to 60 or 70°C.

Conformation about the Exocyclic $C_{4'}$-$C_{5'}$ Bond.

Rotamer populations were calculated in the manner described for dihydrouridine (Section 5.2.1) Results of these calculations are shown in Table 5.8 for β-pseudouridine, Table 5.9 for α-pseudouridine and Table 5.10 for β-cyanuric acid riboside.

Calculations show that β-pseudouridine prefers the <u>gauche</u>-<u>gauche</u> rotamer at all PD's. This rotamer represents 0.5 to 0.7 of the total population.

α- pseudouridine at neutral (32) and acidic pD's prefers the <u>gauche</u>-<u>gauche</u> rotamer. This also

Rotamer populations of nucleosides in basic aqueous solutions.

Table 5.8

β- pseudouridine

Table 5.9

α- pseudouridine

Table 5.10

β- cyanuric acid riboside.

pD = 10.6	beta pseudouridine							
TEMPERATURE	30°C				60°C			
J_o (0° - 90°)	9.27		9.27		9.27		9.27	
J_o (90° - 180°)	10.36		12.00		10.36		12.00	
$\bar{J}_{AB}$	4.1	3.2	4.1	3.2	4,4	3.2	4.4	3.2
$\bar{J}_{AC}$	3.1	4.1	3.2	4.1	3.2	4.4	3.2	4.4
60° STAGGERED ROTAMERS								
P_1	.60	.60	.67	.67	.57	.57	.64	.64
P_{11}	.15	.25	.12	.21	.14	.29	.12	.24
P_{111}	.25	.15	.21	.12	.29	.14	.24	.12
15° OFF-STAGGERED ROTAMERS								
P_1	.48	.48	.60	.60	.42	.42	.56	.56
P_{11}	.11	.20	.05	.13	.13	.26	.06	.17
P_{111}	.41	.32	.35	.27	.45	.32	.38	.27

pD = 11.1	alpha pseudouridine							
TEMPERATURE	30°C				60°C			
J_o (0 - 90) J_o (90 - 180)	9.27 10.36		9.27 12.00		9.27 10.36		9.27 12.00	
$\bar{J}_{AB}$ $\bar{J}_{BC}$	5.1 2.6	2.6 5.1	5.1 2.6	2.6 5.1	5.4 2.9	2.9 5.4	5.4 2.9	2.9 5.4
60° STAGGERED ROTAMERS								
P_1	.54	.54	.61	.61	.47	.47	.56	.56
P_{11}	.08	.38	.07	.32	.11	.42	.09	.35
P_{111}	.38	.08	.32	.07	.42	.11	.35	.09
15° OFF-STAGGERED ROTAMERS								
P_1	.39	.39	.53	.53	.28	.28	.45	.45
P_{11}	.08	.36	.02	.25	.16	.44	.07	.31
P_{111}	.53	.25	.45	.22	.56	.28	.48	.24

pD = 11.0	beta cyanuric acid riboside			
TEMPERATURE	30°C			
J_o (0° - 90°)	9.27		9.27	
J_o (90° - 180°)	10.36		12.00	
$\bar{J}_{AB}$	5.6	3.1	5.6	3.1
$\bar{J}_{AC}$	3.1	5.6	3.1	5.6
60° STAGGERED ROTAMERS				
P_1	.42	.42	.52	.52
P_{11}	.14	.44	.11	.37
P_{111}	.44	.14	.37	.11
15° OFF-STAGGERED ROTAMERS				
P_1	.20	.20	.38	.39
P_{11}	.22	.49	.12	.35
P_{111}	.58	.31	.50	.26

applies to basic solutions although the preference is less marked than in β-pseudouridine. β-cyanuric acid riboside shows no preference for any particular rotamer; the gauche-gauche rotamer varies between 0.2 and 0.5 of the mole fraction at basic pD.

Suger-Base Torsion Angle.

Comparison of the chemical shift data for the ribose protons in β-cyanuric acid riboside and β-pseudouridine implies that β-pseudouridine exists in the anti conformation at basic pD, as well as at neutral and acidic pDs, thus rendering implausible a hydrogen bond between the C_4 oxygen of the base and the hydroxyl group on the exocyclic C_5'.

Little change has been observed in the $J_{1'6}$ coupling in acidic and basic solutions of α-pseudouridine and β-pseudouridine. $J_{1'6}$ in α-pseudouridine is |1.0| Hz ± 0.1 Hz in all spectra examined.

β- pseudouridine in neutral solutions has a $J_{1'6}$ of |0.8| ± 0.1 Hz. Under alkaline conditions the coupling is |0.5| ± 0.1 Hz. This may reflect a small change in the sugar-base torsion angle but I feel numerical estimates are unwarranted owing

to the error in measurement of the coupling constants.

Conclusion.

Changes in the pD of solutions of α-pseudouridine and β-cyanuric acid riboside do not produce any change in the average conformation of the ribose ring. β-pseudouridine, in basic solution, tends more toward the C_2'-endo-C_3'-exo equilibrium. α-pseudouridine, at all pD's , tends toward the C_3'-endo-C_2'-exo conformational equilibrium. β-cyanuric acid riboside at all pD's interconverts between various ring puckered forms.

Among the molecules studied β-pseudouridine shows the strongest preference for the gauche-gauche rotamer about the exocyclic C_4'-C_5' bond. This places the 5' hydroxyl in an appropriate position for the postulated hydrogen bond between this hydroxyl and the C_4 oxygen of the base. The results presented above indicate however that the C_4 oxygen is not available for hydrogen bonding because the base is in the anti conformation.

The role of α-pseudouridine in transfer RNA has not been elucidated yet, but the presence of an extra hydrogen on N1 has been proposed as a potential source of extra hydrogen bonds (32). These could be used to link the different regions of the transfer RNA molecule.

Fissekis and Creegan (60), using synthetic hydroxyalkylpyrimidines, have studied the hydrogen-bonding properties of these molecules in relation to Chambers model for β-pseudouridine at pH 11. In neutral solution 5-hydroxyalkylpyrimidines such as 5-hydroxymethyluracil, 5-hydroxyethyluracil and 5-cydroxycyclopentyluracil have two potential hydrogen-bonding regions, the C-4 carbonyl and the C-5,C-6 double bond. The double bond is the weaker of the two. Dimethylated derivatives of the above mentioned compounds had to be made in order to increase their solubility. The infra red spectrum showed concentration independent peaks in the OH-stretching region. This is indicative of hydrogen-bonding (intramolecular). The 5-hydroxyethylated and 5-hydroxycyclopentyluracil derivatives gave evidence for hydrogen-bonding to a strong base, the C-4 carbonyl. 5-hydroxymethyluracil indicated only a weak hydrogen bond. This weak bond could be attributed to either a weak bond to the C-4 carbonyl or one to the C-5, C-6 double bond. From the geometry of the OH···O=C bond the authors expected a strong hydrogen bond but only a weak one was observed. This could mean that the hydrogen bond is to the C-5,C-6 double bond. This work was done on model compounds in carbon tetrachloride but the authors expressed the opinion that a similar situation could occur in β-pseudouridine in basic solution.

Although our spectra cannot provide direct evidence for such a hydrogen bond in β-pseudouridine at pH 11, indirect evidence does support this bonding scheme. The exocyclic hydroxymethyl group and the orientation of the base are appropriate for hydrogen-bonding to the π electron system of the C-5,C-6 double bond. This could explain the slight change in the ribose ring conformation which is not observed in α-pseudouridine or β- cyanuric acid riboside at basic pH.

5.4 Conformation of Rare Nucleosides in Dimethyl Sulfoxide and in Water.

5.4.1 Conformational Analysis.

In the course of magnetic resonance studies on nucleic acids and nucleosides it has sometimes been necessary to use non-aqueous solvents in order to observe exchangeable protons such as those found in the hydroxyl groups of the ribose rings or the amines of the bases.

The relevance of data gained in this manner can be questioned when it is used as evidence to support conformational data from aqueous solutions. I have analysed the spectra of uridine and the nucleosides containing rare bases, β pseudouridine and dihydrouridine in deuterated dimethyl sulfoxide. These conformational data arethen compared with data gained from aqueous solutions (30,31,35) in order to measure the changes induced by the solvent. The orientation of the hydroxyl groups relative to the ribose ring is determined.

Material and Methods.

Crystalline uridine was purchased from Sigma Chemical Company. Other nucleosides are from the same sources as previously mentioned. Deuterated dimethyl

sulfoxide was purchased from Merck, Sharp and Dohme of Canada and stored over molecular sieve (Linde 3A) in order to remove traces of water.

Spectra were recorded at 100 MHz and 220 MHz. 0.1 M solutions were prepared in the following manner. Two samples of each nucleoside were weighed out, one was dissolved in D_2O, lyophilized and then redissolved in DMSO-d_6 to exchange the protons of the hydroxyl groups and gain a clearer spectrum of the ribose ring protons. The other sample was dissolved in DMSO, lyophilized and redissolved in DMSO-d_6, to remove adsorbed water molecules from the compound. All manipulations were carried out in the dry box in an atmosphere of dry nitrogen,

Assignment of the hydroxyl protons was done by successively decoupling the 2',3' and 5' ribose ring protons using conventional double irradiation techniques (These are described in references 2 to 6 in CHAPTER 1).

In the case of 100 MHz spectra, the chemical shifts of the 2' and 3' protons are close together. This gives rise to a complex multiplet approximately 20 Hz in width. To decouple and assign the hydroxyl

resonances the decoupler frequency was set at the high field side of the multiplet and successively displaced towards low field.

Spectra of the hydroxyl region were recorded at each decoupler frequency. As the decoupler frequency was changed the collapse and reappearance of each doublet could be seen. When the decoupler was set at the low field side of the multiplet, for instance, decoupling of the H_1, occurred along with that of one of the doublets thereby assigning the H_2, resonances. The sharp hydroxyl lines belonged to the OH_2, while the broad line which had, at lower decoupler frequency, been narrow could be assigned to OH_3,.

A first approximation of coupling constants and chemical shifts was gained from first order and ABX analysis. Complete analysis was carried out using the computer program Hydra (46). All chemical shifts are reported relative to TMS (tetramethylsilane).

Results and Discussion.

Results of the analysis of the three molecules studied are presented in Table 5.11 and Table 5.12.

Hydroxyl Group Conformation.

The hydroxyl protons give rise to first order

Table 5.11

Chemical shifts of uridine, β-pseudouridine and dihydrouridine in D_2O and DMSO-d_6.

Table 5.12

Coupling constants in uridine, β-pseudouridine and dihydrouridine in D_2O and DMSO-d_6.

	URIDINE		BETA-PSEUDOURIDINE		DIHYDROURIDINE	
	D_2O[1]	DMSO	D_2O[2]	DMSO	D_2O[3]	DMSO
∂1'	5.901	5.790	4.674	4.471	5.864	5.682
∂2'	4.341	4.028	4.279	3.925	4.303	3.949
∂3'	4.222	3.969	4.141	3.877	4.164	3.857
∂4'	4.128	3.850	4.009	3.706	4.303	3.678
∂5'B	3.907	3.625	3.840	3.601	3.804	3.501
∂5'C	3.803	3.556	3.726	3.450	3.727	3.442
∂5A	5.887	5.640			2.75	2.5
∂5B					2.75	
∂6A	7.862	7.880	7.660	7.546	3.59	3.3
∂6B					3.53	
∂OH2'		5.312		4.855		5.016
∂OH3'		5.012		4.655		4.880
∂OH5'		5.038		4.743		4.760

1) REFERENCE 30
2) REFERENCE 31
3) REFERENCE 35

	URIDINE		BETA-PSEUDOURIDINE		DIHYDROURIDINE	
	D_2O	DMSO	D_2O	DMSO	D_2O	DMSO
$J_{1'2'}$	4.4	5.1	5.0	4.5	6.3	6.0
$J_{2'3'}$	5.3	4.8	5.0	4.5	6.0	5.3
$J_{3'4'}$	5.5	4.3	5.2	5.3	3.6	3.7
$J_{4'5'B}$	3,0	2.8	3.2	3.0	3.6	3.8
$J_{4'5'C}$	4.4	3.0	4.6	3.5	4.8	4.0
$J_{5'B5'C}$	-12.7	-12.3	-12.7	-11.9	-12.6	-12.1
$J_{OH2'H2'}$		5.0		4.8		5.4
$J_{OH3'H3'}$		4.0		5.3		4.4
$J_{OH5'H5'}$		4.0		4.8, 6.2		5.4
J_{5A6A}		8.0			7.1	
J_{5A6B}					6,5	
J_{5B6A}					6.6	
J_{6A6B}					7.0	
J_{5A5B}					-12.7	

spectra. The OH_2' and OH_3' protons are all doublets. The OH_5' proton spectrum is a triplet in uridine and dihydrouridine implying similar values of the OH_5'-H_5'$_B$ and OH_5'-H_5'$_C$ coupling constants. In uridine an average coupling of 4.0 Hz is seen and in dihydrouridine the coupling is 5.4 Hz. In β-pseudouridine the OH_5' region is a quartet. The OH_5'-H_5' couplings are found to be 4.8 and 6.2 Hz, assignment of the couplings to particular hydrogens was not possible.

H-C-O-H coupling constants are known to depend on the dihedral angle formed between the vicinal protons. A 'Karplus' type relationship has been derived to account for the variation of coupling constants with stereochemistry (47) where

$$J_{HCOH'} = 10.4\cos^2\phi - 1.5\cos\phi + 0.2$$

ϕ is the dihedral angle formed between the H-C-O and C-O-H' fragments.

This relation has already been applied to the study of common nucleosides in mixtures of dimethyl sulfoxide and benzene (48). For a freely rotating hydroxyl group an average coupling ($\bar{J}$) of 5.4 Hz

Table 5.13

Calculated rotamer populations about C-O bonds. Observed couplings of hydroxyl protons in uridine, β-pseudouridine and dihydrouridine are reported in Hz.

	BETA-PSEUDOURIDINE				DIHYDROURIDINE				URIDINE			
	OBSERVED COUPLING	P_t	P_g	P_g	OBSERVED COUPLING	P_t	P_g	P_g	OBSERVED COUPLING	P_t	P_g	P_g
$J_{OH2'H2'}$	4.8 Hz	.27	.37	.37	5.4 Hz	.33	.33	.33	5.0 Hz	.29	.35	.35
$J_{OH3'H3'}$	5,3	.32	.34	.34	4.4	.23	.38	.38	4.0	.19	.40	.40
$J_{OH5'H5'}$	4.8 6.2	.32	.41	.27	5.4	.33	.33	.33	4.0	.19	.40	.40

P_g Population of gauche rotamer

P_t Population of trans rotamer. (See text for details)

would be observed. This arises from the weighted average of two gauche (J_g) and one trans (J_t) coupling.

$$J_{obs} = PIJ_g + PIIJ_g + PIIIJ_t$$

$$1 = PI + PII + PIII$$

where J_g, using equation a), is 2.1Hz and J_t is 12.1 Hz. P_i is the population of each rotamer. PI, PII and PIII are equal to 0.33 in a freely rotating system.

Rotamer calculations for the H_2'-OH_2' and H_3'-OH_3' couplings were done using the following equations

$$J_{obs} = 2.1\ P_g + 12.1\ P_t$$

$$1 = P_g + P_t$$

There are two gauche couplings and the preceeding set of equations measures only the total gauche population. Table 5.13 shows two gauche populations these values were arrived at by dividing the gauche population by two. This is not necessarily the true distribution of the gauche rotamers but was done in order to emphasize the fact that there are two gauche populations and only only trans population.

Table 5.13 shows that the 2' and 3' hydroxyl groups in pseudouridine are freely rotating,

the 5' hydroxyl group shows a preference for one of the gauche rotamers. In dihydrouridine, the 2' and 5' hydroxyl protons are freely rotating while the 3' hydroxyl disfavours the trans orientation. In uridine, both the 3' and 5' hydroxyls favour the gauche rotamer. The data given above indicate that in the three nucleosides studied, the 2' hydroxyls are freely rotating. In no case is the trans rotamer favoured in the 3' or 5' hydroxyl group. When a preference is manifest a slight preference for the gauche rotamer exists. In a further series of experiments I would like to measure the effect of the proximity of a ribose ring on the free rotation of the 2' hydroxyl group by studying a dinucleoside monophosphate. This involves a difficult series of experiments on a high field NMR instrument, which is not at present readily available.

Ribose Ring Conformation.

The chemical shifts and coupling constants of the ribose ring protons are given in Tables 5.11 and 5.12. The data indicate that there are no large changes in ribose ring conformation when changing solvent from D_2O to DMSO. The largest changes occur in the couplings of uridine. In D_2O, the largest coupling is $J_{3'4'}$

(5.5 Hz). In DMSO, the largest one is $J_{1',2'}$ (5.1 Hz). This implies that although the ribose ring is still interconverting rapidly between various puckered forms, in DMSO the preferred conformation is slightly different from that in D_2O.

Conformation About the Exocyclic $C_{4'}$-$C_{5'}$ Bond.

In DMSO the geminal (5'B5'C) couplings are smaller than in D_2O. The same applies to the vicinal couplings (4'A5'B and 4'A5'C). The latter indicates a change in the rotamer population about the exocyclic $C_{4'}$-$C_{5'}$ bond. The relative populations of each rotamer (Table 5.14) were estimated in the manner described for dihydrouridine (Section 5.1.1). The preferred rotamer in all cases is gauche-gauche. These molecules in aqueous solution also prefer the gauche-gauche rotamer (30,31,35). The preference is even greater in DMSO however. There is a 20% increase in the gauche-gauche rotamer in DMSO, a 16% increase for β-pseudouridine and a 7% increase for dihydrouridine. This last figure is however just on the reliability limit of the method.

Chemical Shift Changes.

In DMSO, the proton resonances shift upfield. The $H_{2'}$, $H_{3'}$, $H_{4'A}$, $H_{5'B}$ and $H_{5'C}$ resonances shift

Table 5.14

Limits for relative populations of 60° staggered rotamers around the exocyclic $C_{4'}$-$C_{5'}$ bond in uridine, dihydrouridine and β-pseudouridine in DMSO solutions.

	URIDINE		BETA-PSEUDOURIDINE		DIHYDROURIDINE	
J_o (0 - 90)	9.27	9.27	9.27	9.27	9.27	9.27
J_o (90 - 180)	10.36	12.00	10.36	12.00	10.36	12.00
$J_{4'5'B}$	2.786	2.786	2.978	2.978	3.790	3.790
$J_{4'5'C}$	2.970	2.970	3.494	3.494	4.028	4.028
P_I	.79	.82	.70	.75	.53	.61
P_{II}	.12	.10	.18	.15	..25	.21
P_{III}	.09	.08	.12	.10	.22	.18

upfield by 24 to 35 Hz. This does not appear to be caused by any change in the sugar-base torsion angle. Such changes are usually measured by preferential shifts in the resonances of the ribose ring protons (43). The 1',2' and 3' protons should be deshielded and the 4' 5'B and 5'C resonances should be shielded if there is a change from anti to syn of the base. I have not observed any such changes, all proton resonances have shifted upfield by about the same number of Hertz. The $H_{1'}$ resonances are shifted upfield by 11 to 20 Hz only, the origin of this is probably a simple solvent effect.

The chemical shift changes induced in the base proton resonances by DMSO are less uniform than the shifts induced in the ribose protons. In uridine the H_5 resonance is shifted upfield by 25 Hz but the H_6 resonance is shifted downfield by 2 Hz. In β-pseudo-uridine, the H_6 resonance is shifted upfield by 11 Hz. In dihydrouridine, where the H_{5A}, H_{5B}, H_{6A} and H_{6B} resonances give rise to deceptively simple spectra, the resonances appear to be shifted upfield by 25 to 30 Hz. These changes are specific solvent effects on the base. Such effects have been postulated to explain other NMR data on uridine and related oligo-

nucleotides (49).

Conclusion.

Analysis of spectra of uridine, dihydrouridine and β-pseudouridine in DMSO have not shown any large conformational changes in the ribose ring when compared with spectra taken in D_2O. The conformation about the exocyclic C_4'-C_5' bond shows an increased preference for the gauche-gauche rotamer,(which is also preferred in aqueous solution). The sugar ring hydroxyl proton resonances have been assigned and the couplings were measured. My conclusions, in general, agree with those of Davies and Danyluk (48).for the common nucleosides. These data should be useful for construction of models for the conformation of large polynucleotides such as transfer RNA. No changes in the sugar-base torsion angle were detected .

The model deduced for the conformation of dihydrouridine has been published (35).

The data discounting the hydrogen bond in β- pseudouridine are in press (52)

5.5 Conclusion to chapter 5.

No general theory has yet been formulated regarding the role of the rare nucleosides in transfer RNA. A number of functions for the rare nucleosides are possible. The non-hydrogen bonded, looped, regions of the transfer RNA molecule could confer specificity of interaction between transfer RNA and the aminoacyl synthetases. Rare nucleosides near the anticodon could modify the codon-anticodon recognition pattern. The looped regions possibly form hydrogen bonds to one another and are responsible for the three dimensional structure of transfer RNA.

Numerous experiments have been devised in order to test these hypotheses but the data are often difficult to interpret. The reason for this lies in the fact that chemical modification of a base may also have caused changes in the overall geometry of the molecule. The observed effect may not necessarily be due to the modified base but may be caused by a change in molecular geometry. In spite of this, many such studies are slowly helping to elucidate the role of rare nucleosides.

Dudock *et al* (6) have found that in yeast $tRNA^{Phe}$ the synthetase recognition site is in the region

adjacent to the dihydrouridine loop. Intactness of the single stranded region is not required for specific transfer RNA charging by the synthetase enzyme (53).

Rare nucleosides are sometimes found in the anticodon region of transfer RNA. 2-thioU (S) is in the anticodon of yeast $tRNA^{Glu}$, SpUpCp. This anticodon recognizes the triplet GAA and not GAG. Yoshida et al (25) have proposed that the 2-thioU is specific for the recognition of GAA.

Rare nucleosides adjacent to the anticodon are quite common. The fluorescent 'Y' base is adjacent to the anticodon in yeast $tRNA^{Phe}$. Removal of this base causes the anticodon to respond better to UUC than to UUU (26). N^6 (Δ^2-isopentenyl) adenosine (16) is next to the 3' end of the anticodon in a $tRNA^{Ser}$. Selective iodonation of this base does not result in a loss of aminoacylation. It does however decrease binding to ribosomes by two thirds. This could be due to steric hindrance on the stacking of the triplet in the anticodon loop. Deletion of N^6 (Δ^2-isopentenyl) adenosine from the anticodon prevents the tRNA from carrying out its transfer function.

The lack of certain rare bases does not affect

aminoacylation or protein synthesis. Johnson et al (54) have isolated a ribothymidine deficient $tRNA^{Ile}$ from Kid. Kid $tRNA^{Ile}$ contains only one ribothymidine in the GT C sequence. This tRNA and remethylated $tRNA^{Ile}$ can be aminoacylated by homologous and heterologous amino-acyl - tRNA synthetase from E. coli. This implies that ribothymidine is not required for recognition of transfer RNA by aminoacyl - tRNA synthetase. Polyisoleucine can form in a cell free E. coli amino acid incorporating system mediated by $tRNA^{Ile}$. This implies that ribothymidine deficient $tRNA^{Ile}$ can function in protein synthesis and therefore is bound by ribosomes. However, kinetic parameters may be altered in ribothymidine deficient $tRNA^{Ile}$. This $tRNA^{Ile}$ also lacks thioU and yet acylation proceeds to near maximum value.

Hay et al (29) have studied the effect of hypermethylation on the functional characteristics of transfer RNA. Hypermethylation of E. coli $tRNA^{Phe}$ does not alter the binding of this tRNA to ribosomes. The ability to participate in polyphenylalanine synthesis decreases as the degree of hypermethylation increases. Hypermethylation affects amino acid recognition. Polylysine synthesis is more highly affected by hypermethylation than is polyphenylalanine synthesis. Polyproline synthesis is inhibited by a 7% increase in methylation.

The change of U to 4-thioU occurs in 40% of $tRNA^{Gly}$ from S. aureus and S. epidermidis. This transfer RNA does not participate in protein synthesis but it does participate in peptidoglycan synthesis (15). It has been proposed that the lack of participation in protein synthesis allows this transfer RNA to be available for the important function of cell wall synthesis.

These data seem to indicate that one cannot assign one particular function to the rare nucleosides in transfer RNA. The role of rare nucleosides in transfer RNA could be compared to the role of certain amino acids in enzymes. For instance, histidine residues are commonly found at the active site of many enzymes. The properties of this amino acid make it ideally suited for acid-base catalysis around pH 7, the physiological pH. However, all histidine residues are not found at the active site and many play only a structural role compatible with the geometric, electronic and hydrophobic properties of the amino acid.

NMR studies on uridine and uridine derivatives have shown that the ribose rings are not in a fixed conformation but interconvert rapidly between various

conformers. The bases are in the anti conformation. The protons of the exocyclic hydroxymethyl group generally prefer the gauche-gauche rotamer with respect to the 4' proton. Conformationally uridine, β- pseudouridine and dihydrouridine are not very different.

Differences between these nucleosides could reside in their hydrogen bonding properties. These properties can be examined by NMR techniques. The solvents involved are usually dimethyl sulfoxide (56,59), chloroform (57), mixtures of dimethyl sulfoxide and carbon tetrachloride (58), dimethyl sulfoxide and acetonitrile (58) or dimethyl sulfoxide and dimethyl formamide (56).

Infra red studies using 1-cyclohexyl derivatives of pyrimidines and 9-ethyl derivatives of purines in deuterochloroform have revealed that uracil binds three times more strongly to adenine than does dihydrouracil.(55). 4-thiouracil binds almost as strongly as does uracil to adenine. Thymine binds 30% more strongly to adenine than does uracil.

The binding properties of polyuridylic acid (polyU) and polydihydrouridylic acid (polyD) to polyadenylic acid (polyA) in D_2O have also been studied by infra red spectroscopy. It has been shown that the

binding capacity to polyA decreases as the ratio of U to D (U/D) decreases in a polymer.

These data may imply that dihydrouridine forms a less stable base pair in polynucleotides than does uridine. In transfer RNA, dihydrouridine could form weak bonds which are readily modified by environmental conditions. No such data are yet available for β-pseudouridine.

Methylation of bases decreases their hydrogen bonding properties (55). It has been suggested that the methyl groups are important in the genesis and stability of the final conformation of transfer RNA (19).

C-2' and C-3' o-methylated nucleosides could have decreased conformational freedom in the ribose ring. This could easily be investigated by NMR spectroscopy.

It has been found that 3' and 2' O-substitution of transfer RNA protects it from attack by CCA pyrophosphorylase. (19).

5.6 References.

1. M.B. Shapiro, C.R. Merrill. D.F. Bradley and J.E. Mosimann, Science 150 918 (1965)

2. R.W. Holley, J. Apgar, G.A. Everett. J.T. Madison, M. Marquisee, S.H. Merrill, J.R. Preswick and A. Zamir, Science 147 1462 (1965)

3. U.L. Rajbandary, A. Stuart, R.D. Faulkner, S.H. Chang H.G. Khorana, Proc. Natl. Acad. Sci. U.S.A. 57 751 (1967)

4. B.G. Barnell anf F. Sanger, FEBS Lett. 3 275 (1969)

5. M. Yaniv and B.G. Barnell, Nature 222 278 (1969)

6. B.S. Dudock, G. Katz, E.K. Taylor and R.W. Holley, Proc. Nat. Acad. Sci. U.S.A. 62 941 (1969)

7. J.T. Madison, G.A. Everett and H. Kung, Science 163 531 (1966)

8. S. Takamura, T. Mizutani and M. Miyazaki, J. Biochem. 63 277 (1968)

9. G.R. Philips, Nature 223 374 (1969)

10. S. Takemura, M. Murakami and M. Miyazaki, J. Biochem. 65 489 (1969)

11. M. Staehelin, H. Rogg, B.C. Baguley, T. Ginsburg and W. Wehrli, Nature 219 1363 (1968)

12. A.A. Baev, T.V. Venkstern, A.D. Mizabekov, A.I. Krutilina, L. Li and V.D. Aksel'rod, Molek. Biol. 1 754 (1967)

13. S. Cory, K.A. Marcker, S.K. Dube and B.F.C. Clark, Nature 220 1039 (1968)

14. S.K. Dube, K.A. Marcker, B.F.C. Clark and S. Cory, Nature 218 232 (1968)

15. T.S. Stewart, R.J. Roberts and J.L. Stroninger, Nature 230 36 (1971)

16. R.H. Hall, Prog. Nucl. Ac. Res. and Mol. Biol. 10 57 (1970)

17. M.P. Schweizer Biochem. 8 3283 (1969)

18. S.M. Hecht Science 160 1272 (1969)

19. D.H. Gauss, F. von der Haar, A. Maelicke and F. Cramer, Ann. Rev. Biochem. 40 1045 (1971)

20. D.B. Mowshowitz, J. Mol. Biol. 50 143 (1970)

21. P. Cerutti, H.T. Miles and J. Frazier, Biochem. Biophys. Res. Comm. 22 466 (1966)

22. H.G. Zachau, Angew. Chem. Internat. Edit. 8 711 (1969)

23. M. Levitt, Nature 224 759 (1969)

24. H.G. Zachau, D. Duttig, H. Feldmann, F. Melchers and W. Karau, Cold Spring Harbor Symp. Quant. Biol. 31 417 (1966)

25. M. Yoshida, K. Takeishi and T. Ukita, Biochem. Biophys. Res. Comm. 39 852 (1970)

26. K. Ghosh and H.P. Ghosh, Biochem. Biophys. Res. Comm. 40 135 (1970)

27. M.A.Q. Siddiqui and J. Ofengand, J. Biol. Chem. 245 4409 (1970)

28. R.T. Walker and U.L. RajBhandary, Biochem. Biophys. Res. Comm. 38 907 (1970)

29. J. Hay, D.J. Pillinger and E. Borek, Biochem. J. 119 587 (1970)

30. B.J. Blackburn, A.A. Grey, I.C.P. Smith and F.E. Hruska, Can. J. Chem. 48 2866 (1970)

31. F.E. Hruska, A.A. Grey and I.C.P. Smith, J. Amer. Chem. Soc. 92 4088 (1970)

32. A.A. Grey, F.E. Hruska and I.C.P. Smith, J. Amer. Chem. Soc. 93 1765 (1971)

33. P.K. Glascoe and F.A. Long, J. Phys. Chem. 64 188 (1960)

34. S. Castellano and A.A. Bothner-By, J. Chem. Phys. 41 3868 (1964)

35. R. Deslauriers, R.D. Lapper and I.C.P. Smith, Can. J. Biochem. 49 1279 (1971)

36. M. Chabre, D. Gagnaire and C. Nofre, Bull. Soc. Chim. Fr. 108 (1966)

37. M. Smith and C.D. Jardetzky, J. Mol. Spectrosc. 28 70 (1968)

38. T. Schleich, B.J. Blackburn, R.D. Lapper and I.C.P. Smith, Biochem. 11 137 (1972)

39. S.I. Chan and J.H. Nelson, J. Amer. Chem. Soc. 91 2843 (1968)

40. R.J. Abraham, L.D. Hall, L. Hough and K.A. McLaughlan, J. Chem. Soc. 3699 (1962)

41. M. Sundaralingam, S.T. Rao and J. Abola, Science 172 725 (1971)

42. J. Donohue and K.N. Trueblood, J. Mol. Biol. 2 363 (1960)

43. H. Dugas, B.J. Blackburn, R.K. Robins, R. Deslauriers and I.C.P. Smith, J. Amer. Chem. Soc. 93 3468 (1971)

44. R.W. Chambers, Prog. Nucl. Acid Res. Mol. Biol. 5 349 (1966)

45. M.W. Winkley and R.K. Robins, J. Org. Shem. 35 491 (1970)

46. R.D. Lapper, private communication.

47. R.R. Fraser, M. Kaufman, P. Morand and G. Govil Can. J. Chem. 47 403 (1969)

48. D.B. Davis and S.S. Danyluk, Can. J. Chem. 48 3112 (1970)

49. I.C.P. Smith, B.J. Blackburn and T. Yamane, Can. J. Chem. 47 513 (1969)

50. G.P. Kreishman and S.I. Chan, Biopolym. 10 159 (1971)

51. D.L.F. Detar, Computer Programs for Chemistry, W.A. Benjamin Inc., N.Y., 1968

52. R. Deslauriers and I.C.P. Smith, Can. J. Biochem. in press.

53. J. Schmidt and B.R. Reid, Biochim. Biophys. Acta 213 539 (1970)

54. L. Johnson, H. Hayashi and D. Söll, Biochem. 9 2823 (1970)

55. Y. Kyogoku, R.C. Lord and A. Rich, Proc. Natl. Acad. Sci. U.S.A. 57 250 (1967)

56. R.R. Shoup, H.T. Miles and E.D. Becker, Biochem. Biophys. Res. Comm. 23 194 (1966)

57. L. Katz and S. Penman, J. Mol. Biol. 15 220 (1966)

58. F.K. Schweighardt, C. Moll and N.C. Li, J. Mag. Res. 2 35 (1970)

59. R.A. Newmark and C.R. Cantor, J. Amer. Chem. Soc. 90 5010 (1968)

60. J.D. Fissekis and B.M. Creegan, J. Org. Chem. 32 3595 (1967)

CHAPTER 6.

NMR STUDIES OF NEUROHYPOPHYSEAL HORMONES: OXYTOCIN AND LYSINE VASOPRESSIN.

6.1 Historical Introduction.

When extracts of posterior pituitaries are administered to animals and humans a number of physiological changes occur. The effects produced include lowering of blood pressure, antidiuresis and uterine contractions.

Pituitary extracts had already been put to use clinically at the turn of the century. In 1917, Abel and Pincoff (1) detected albumoses and peptoses in all therapeutically used preparations of the posterior pituitary lobe of the hypophysis cerebri. They believed the posterior pituitary extracts were a mixture of active and inactive fractions; the albumoses accounted for all the physical characteristics attributed to the active fractions. The albumoses were removed from the pituitary extracts and found to be devoid of physiological activity.

Extracts of the posterior pituitary lobe

could be separated into several fractions with varying activities. Some fractions acted mainly on the uterus, others on blood pressure and others still acted on both. By 1925, three theories had been proposed: 1) a single hormone was responsible for all the observed effects 2) two hormones were present, one acting mainly on the uterus, the other acting mainly on blood pressure 3) the posterior pituitary contained many hormones which could be responsible for the observed physiological effects.

Isolation of Oxytocin and Vasopressin.

In 1928, Kamm et al (2) separated two active fractions from the posterior pituitary. These had been extracted in 0.25% acetic acid, they were heated to 95°C, cooled and filtered. The filtrate was concentrated at low temperature. Extraction with water instead of dilute acid led to loss of activity.

The extracts contained low molecular weight substances, proteins and active 'principles'. Proteins and active material were precipitated with ammonium sulfate. The active material was then solubilized with glacial acetic acid. The active principles were stable at room temperature for

several days when left in glacial acetic acid.

Oxytocic activity was removed from the mixture in glacial acetic acid by precipitation with ether. Pressor activity was precipitated with acetone.

At every step fractions were assayed in two ways. Oxytocic activity was assayed on strips of uterus from virgin Guinea pigs by the method of Daile and Laidlaw (3). Kamm proposed a pressor assay which measured increases in blood pressure.

Only 10% oxytocic activity/100% pressor activity was found in the pressor fraction. 4% pressor activity/ 100% oxytocic activity was found in the oxytocic fraction.

These results provided strong evidence for the existence of two separate hormones in the posterior pituitary.

Structure of Oxytocin.

Livermore and du Vigneaud (4) prepared high potency oxytocic material using the Craig (5) counter-current distribution technique. The possibility of preparing high potency material opened the way to structural investigation. Amino acid composition was determined by the method of Stein and Moore (6,7-10). The amino acids in oxytocin were found

to be isoleucine (Ile), leucine (Leu), tyrosine (Tyr), proline (Pro), aspartic acid (Asp), glutamic acid (Glu), glycine (Gly), cysteine (Cys). The components were equimolar with respect to each amino acid with the exception of ammonia, of which there were three moles. Tyrosine was destroyed during hydrolysis and therefore could not be accurately estimated.

Elemental analysis revealed the following data: (11)

C	50.12%
H	6.8 %
N	16.12%
S	6.5 %

These values agreed closely with those calculated for a peptide containing one mole of each of the above mentioned amino acids. The molecular weight was estimated at 1025. The molecule was thought to contain two free amino groups and one free carboxyl.

Desulfurization of oxytocin (12) yields two alanine in place of cystine. The cystine was not terminal because no free alanine was found. Only one fragment was recovered by counter-current distribution implying a cyclic structure.

The amino acid sequence was determined by Tuppy (13)

The degradation involved partial hydrolysis of oxidized oxytocin with mineral acids and a proteolytic enzyme from Bacillus subtilis. The digest was fractionated in an ionophoresis cell. Two acidic fractions were found : $CySO_3H$-Tyr-Ile-Glu and Asp-$CySO_3H$-Pro-Leu, $CySO_3H$ and Asp were N terminal amino acids. Asp and Glu were found to be amides. A fragment consisting of Leu-Gly placed Gly at the end of the sequence Asn-$CySO_3H$-Pro-Leu. The N terminal sequence was $CySO_3H$-Tyr-Ile-Gln.

At the same time du Vigneaud (14) also sequenced oxytocin using partial hydrolysates of oxytocin, desulfurized oxytocin and the fragment yielded by treatment of performic acid oxidized oxytocin with bromine water (15). Edman degradations were also done.

These studies led to the proposed sequence:

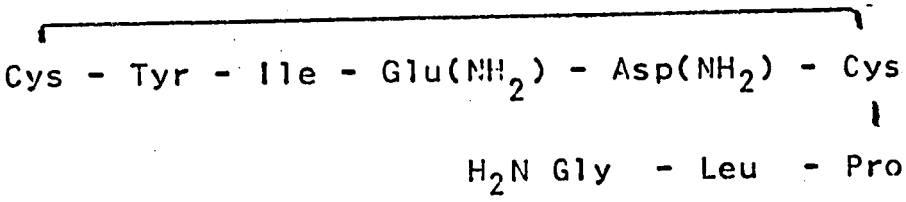

Further proof of the structure of oxytocin was obtained when du Vigneaud et al (16) synthesized a compound possessing all the physical, chemical and physiological

characteristics of natural oxytocin. This was the first synthesis of a polypeptide hormone.

Many different synthetic routes were later employed in the synthesis of oxytocin. Among the methods are those of Boissonnas et al (17), Rudinger et al (18), Villuz et al (19) Bodanszky and du Vigneaud (20).

Further Methods of Isolation and Purification.

Gel filtration provides a simple method of separating protein-bound hormones such as oxytocin and vasopressin (21). Hog pituitaries are extracted with 0.2 M pyridine - 0.05 M acetic acid buffer at pH 5.9. The supernatant is run through a G-25 Sephadex column. Two peaks are eluted, the first of which contains the active material. The eluate is evaporated and redissolved in 1M formic acid and heated at 70°C for ten minutes. The solution is again run on a G-25 Sephadex column in 1M formic acid. Three peaks are eluted; both oxytocic and vasopressor activities are recovered in the third peak.

Partition chromatography of natural and synthetic oxytocin gives material assaying at 500 U/mg

(22). A two phase solvent system similar to that used for counter-current distribution is employed. Sephadex G-25 is packed into columns and equilibrated with 0.2 N acetic acid. The aqueous phase of the solvent system is then used to equilibrate the column. This is followed by the organic phase. The hormone is then chromatographed. The column is later discharged of the two phase system and the uneluted material. After washing the column with 0.2 N acetic acid it is ready for use again.

Oxytocin and vasopressin have been separated by binding to neurohypophyseal proteins called neurophysins. This eliminates low molecular weight contaminants. The binding is highly specific and will be discussed later.

Structure of Vasopressin.

Vasopressin has been purified and characterized in a manner similar to oxytocin. Bovine vasopressin prepared by the Kamm (2) procedure could be partially purified by chromatography on Amberlite IRC-50. Better separation was obtained by counter-current distribution in water - sec. butanol. Another system consisting of sec. butanol - 0.05 M aqueous acetic acid was also used. The last two methods yielded material assaying

at 200 U/mg. The best system was n-butanol- p- toluene-sulfonic acid (0.10 M). The acid was removed on an Amberlite IR-4B column. The product of this separation assayed at 300 U/ mg (23).

The amino acids found in vasopressin were phenylalanine (Phe), tyrosine (Tyr), proline (Pro), glutamic acid (Glu), aspartic acid (Asp), arginine (Arg), glycine (Gly) and cysteine (Cys). These amino acids were in a 1:1 mole ratio to each other. The ammonia content was three times as high as that of any amino acid.

Counter-current distribution of hog vasopressin (24) in solvent systems used for bovine vasopressin demonstrated a difference in partition coefficients for the two vasopressins. Amino acid analysis showed that lysine was replaced by arginine. All preparations of lysine vasopressin were less active than arginine vasopressin. Further purification of hog pituitary extracts by electrophoresis on cellulose and counter-current distribution gave material with an activity of 250 U/mg. The mole ratios of all constituent amino acids was 1:1 and that of ammonia was 3:1.

The structure of arginine vasopressin (25,26) was elucidated by degradative studies similar to those performed on oxytocin by du Vigneaud. The sequence

of this hormone is:

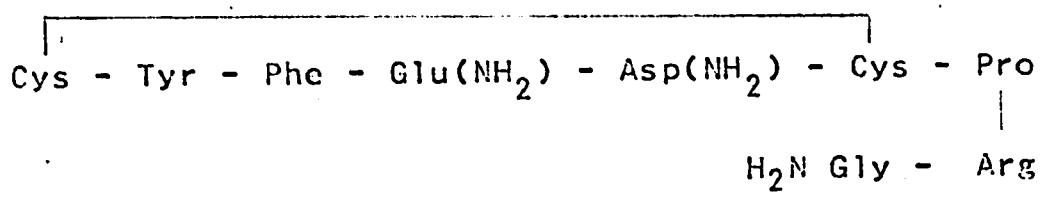

The sequence of lysine vasopressin was determined in a similar fashion. Lysine vasopressin has lysine in the place of arginine.

Synthesis of these hormones has been effected by various methods (27-30) and has proven the proposed structures.

Further Methods for Isolating and Purifying Vasopressins.

Columns of Amberlite can be used to purify vasopressins, as mentioned earlier. The material is dissolved in 0.02 M ammonium acetate buffer at pH 6.0 and applied to the column. Elution is done with a gradient to 0.2 M ammonium acetate at pH 7.0 (31).

Mixtures of oxytocin and vasopressin can also be separated on Amberlite IRC-50 (32). The column, equilibrated with 0.01 m ammonium acetate pH 4.6, is loaded and elution proceeds with a gradient from 0.02 M ammonium acetate pH 6.0 to 0.2 M ammonium acetate pH 7.0.

Oxytocin and vasopressin can be separated on Sephadex columns (G-25, G-50 and DEAE-25). Effectiveness of separation is significantly increased by limiting the swelling of the gels with high concentrations of acetic acid and pyridine (acetic acid : pyridine : water, 60:15:25)(33).

Studies of the hypothalamus and posterior pituitary (34) have shown the presence of α and β-melanocyte stimulating hormone (MSH) in preparations of vasopressin. The hormones are polypeptides and migrate with vasopressin in many types of extraction. Gel filtration on Sephadex G-25, G-50 and G-75 using pyridine : acetic acid : water (15:55:30) allows separation of α-MSH and lysine vasopressin. Sephadex G-25 equilibrated with 1 M acetic acid also resolves the mixture.

Function of Neurohypophyseal Hormones.

Synthesis.

The formation of oxytocin and vasopressin was thought to occur directly in the pituicytes of the neurohypophysis under the influence of nerve fibres of the supra-optico hypophyseal tract.

Today it is largely believed that neurohypophyseal hormones are actually formed in the supra-optico and paraventricular nuclei of the hypothalamus, transported along cell axons and deposited in granular form in the nerve endings of the neurohypophysis. These nerve endings are in direct apposition with the neurohypophyseal capillaries.

Neurohypophyseal hormones, including oxytocin, vasopressin α-MSH and β-MSH, have been detected and separated from canine and porcine hypothalami by Guillemin et al (35) and Schally et al (36).

Labelled neurohypophyseal hormones have been isolated from rat neural lobes after intra-cisternal injection of tritiated tyrosine (37). At various times after injection rats were decapitated and the neurohypophysis removed. Oxytocic and vasopressor activites were separated by column chromatography. The labelled peptides were similar to those, unlabelled, isolated by other methods in migration on paper chromatography and performic acid oxidation. The labelled peptides began to arrive in the neural lobes two hours after injection of tritiated tyrosine into the cisterna magnum . Incubation of neural lobes for four hours

with tritiated tyrosine did not lead to any incorporation of radioactivity into the hormones. This implies that biosynthesis does not occur in the isolated neurohypophysis.

Similar studies by Roux (38) with ^{35}S-methionine showed an accumulation of activity in the supra-optic nuclei as well as the paraventricular nuclei with subsequent transport to the neurohypophysis.

Roux (39) has recently questioned this hypothesis by finding that radioactive arginine is incorporated to a larger extent in the neurohypophysis than in the supra-optic nuclei. Loss of radioactivity in dehydrated animals is higher than in normal animals, this led him to believe that the radioactive material was incorporated into antidiuretic hormone. Antidiuretic material, vasopressin, was not isolated however. Roux believed the pituicytes were not necessarily devoid of synthetic activity as the present day theory implies.

Storage of Neurohypophyseal Hormones in Granules.

Differential gradient centrifugation of homogenates of rabbit neurohypophysis has shown that oxytocin and vasopressin are situated in membrane bound granules

measuring approximately 1,300 Å in diameter (40). These granules resemble those found in electron micrographs of neural swellings of rabbit neurohypophysis. The sedimentation properties of the granules are similar to those of mitochondria but resolution can be achieved by critical control of centrifugal force. It has been suggested that oxytocin and vasopressin are carried by diffrent granules. Density gradient centrifugation has shown that oxytocin is associated with lighter particles than vasopressin; isolated granules preferentially release one or the other hormone.

Protein Bound Neurohypophyseal Hormones.

Van Dyke et al (41) in 1942, isolated an apparently pure protein from the posterior pituitary which demonstrates vasopressor, antidiuretic, oxytocic and lactogenic properties. This was supported by the finding that many mammalian species have a vasopressin to oxytocin ratio approaching one and in many cases stimulation of the hypothalamus leads to simultaneous release of both hormones. The molecular weight of this protein was estimated to be 30,000.

The protein contained no cysteine, no hydroxyproline, no methionine and no tryptophan (42,43).

The Van Dyke protein was later shown to contain three units: a protein, oxytocin and vasopressin (44). Acetone dried powders of posterior pituitary glands were extracted with 0.1 N sulfuric acid (pH 4.5). The supernatant (pH 3.9) precipitated with NaCl. The salt was removed from the precipitate by dialysis against water. The desalted precipitate was dissolved in acetic acid - sodium acetate buffer (pH 3.9), reprecipitated, centrifuged and desalted. The product was lyophilized.

Dialysis of the Van Dyke protein against water, ultrafiltration, NaCl precipitation do not separate oxytocic and vasopressor activities. Dialysis against dilute acid, electrodialysis, counter-current distribution and trichloroacetic acid precipitation separate the hormones from an inert protein. Finding a variable vasopressin to oxytocin ratio at different stages of rat growth argues against the presence of a unique neurohypophyseal hormone also (45).

This led to a new concept in the purification of oxytocin and vasopressin from bovine and porcine neurohypophysis (46 -48). The peptides can be selectively

precipitated along with the protein (called neurophysin) by addition of NaCl, thus eliminating a large fraction of the contaminating neurohypophyseal peptides. The protein is later precipitated by trichloroacetic acid leaving the hormones in solution. These can be separated by ion exchange chromatography. It is also possible to isolate oxytocin and vasopressin from one species by precipitation with neurophysin from another (49).

More recent work has demonstrated that neurophysin is a heterogeneous protein. Preparations usually yield at least three distinct units capable of binding hormones (50 - 57).

The hormone binding properties of neurophysin have been studied in spite of heterogeneity (58). Maximum binding of hormone to protein occurs between pH 5.2 and 5.9 but precipitation of complexes occurs at pH 3.2. It was thought that physiological release of hormone could be mediated by pH changes. The relation between pH and binding is consistent with ionic association between a free NH_2 of the cysteine residue and a free carboxyl group of the protein.

The purified neurophysins can be crystallized when bound to hormones (59). A number of research

groups have studied the hormone binding properties of neurophysin. Ginsburg et al (60) estimated a molecule of porcine neurophysin could bind fourteen molecules of oxytocin and bovine neurophysin could bind seven molecules of oxytocin or four of vasopressin (61). Later estimates were that one mole of vasopressin would bind per 13,000 M.W. Hollenberg's Neurophysin-M (62) bound three moles of vasopressin alone or two moles of vasopressin and one mole of oxytocin. In subsequent work (63) bovine Neurophysin I (M.W. 19,000) bound three molecules of oxytocin or vasopressin and Neurophysin II (M.W. 20,000) bound two molecules of either hormone. Neurophysin III (57) binds one molecule of oxytocin or vasopressin per 10,000 M.W. Breslow and Abrash (50) measured two moles of oxytocin per 25,000 gm bovine protein and found vasopressin to be competitive. It was also found that analogues such as deamino vasopressin were not bound to neurohypophyseal protein.

Evidence has been presented that oxytocin and vasopressin are bound to diffrent neurohypophyseal fractions in diffrent neurosecretory granules (64) and can be released independently of each other depending on the stimulus.

Release of Hormones into the Blood Stream

The release of hormones from the neurohypophysis is under the control of nerve impulses arising in the anterior hypothalamus. The cells in the hypothalamus respond to the osmolarity of the blood bathing them. These cells secrete vasopressin in response to osmotic pressure changes. Electrical impulses to the anterior hypothalamus also cause oxytocin release. Ginsburg (65) has studied the molecular aspects of release of neurohypophyseal hormones from the carrier protein neurophysin. Ca^{++} influences the release of hormones from the neurohypophysis (66,67). There is evidence that the membrane enclosing the neurohypophyseal granules is not impermeable to the hormone and that accumulation within the granules is dependent upon protein binding. Calcium has been found to inhibit binding of lysine vasopressin to neurophysin (66). It has been proposed that calcium acts in the following manner: free and bound hormone can exist in granular and extra-granular sites. Neurophysin is highly concentrated in the granules. No gradient exists between free hormone in the granules and the cytoplasm. Nerve depolarization and the presence of calcium causes the

release of hormone from the extragranular neurophysin. Upon return to the resting state, hormones migrate from intragranular neurophysin and become bound to extragranular neurophysin. This however is only a model at present and awaits furter study.

The fate of neurophysin after release of hormone is not known. Neurosecretory granules take up less stain after release of large quantities of hormone but no chemical evidence is available yet. The hormones are released into the circulation via the capillaries apposed to the nerve cells.

Physiological Effects of Neurohypophyseal Hormones.

Oxytocin causes uterine contractions, it exerts an electrophysiological action on the endometrium (68). Vasopressin acts on the collecting tubules of the kidney and causes reabsorption of water while permitting electrolytes to pass into the urine. Vasopressin also increases blood pressure but the quantity required is pharmacological rather than physiological. In dogs, injection of vasopressin produces an increase in arterial blood pressure and pronounced bradycardia (slowing of heart rate) (69). In vasopressin-induced antidiuresis, net tubular reabsorption of sodium increases while that of potassium decreases (70). It is believed that

vasopressin affects the permeability of cells to sodium rather than the active transport mechanism (71). Vasopressin seems to exert its effects specially on the granular cells of the toad urinary bladder (72).

6.2. NMR Studies of Neurohypophyseal Hormones.

Molecular Conformation of Neurohypophyseal Hormones.

Nuclear magnetic resonance spectroscopy was judged a suitable technique for investigating the structure of neurohypophyseal hormones. It was first decided to study oxytocin and vasopressin conformations as individual molecules. The next step would be to isolate neurophysin and study the changes which occur in the hormone spectra upon binding to neurophysin.

Material and Methods.

Lysine vasopressin isolated from porcine hypothalami was a gift from the National Institutes of Health, Bethesda Maryland. The sample arrived in 70 1 ml bottles each containing 20 units vasopressor activity. The quoted activity was 260 U (units)/mg, essentially pure material. The samples were calculated to yield approximately five milligrams of dry powder.

The only possible contaminant quoted was α-MSH (less than 0.1%). The solution was at pH 3.5. The contents of the vials were lyophilized, redissolved in 0.01 M ammonium acetate pH 4.5 and relyophilized. The dry sample would not dissolve completely in water at pH 5.0. Acetic acid was added until the pH reached 3.2, the solution was still turbid. It was passed through a 1.0 u nylon Millipore filter. The sample was lyophilized. and redissolved in 0.5 ml D_2O at pD 3.3. The undissolved particles were removed by centrifugation in a 1 ml tube. The supernatant was used to obtain the NMR spectrum. Amino acid analysis revealed only the expected amino acids in the correct ratio. (73)

Synthetic oxytocin was purchased as a dry powder from Sigma Chemical Company. Quoted activity was 10 units/mg. Maximum oxytocic activity is 500 units/mg. Samples were purified by the method of Manning et al (74). Oxytocin is dissolved in 50% acetic acid, chromatographed on Sephadex G-15 and lyophilized. The lyophilized powder is redissolved in 0.2 N acetic acid and re-chromatographed to remove dissolved Sephadex. Such a procedure is mainly useful for removing inorganic salts and dimers. Synthetic oxytocin purified in this manner has an activity of $\simeq$480 units/mg (74). A 90 x 1.5 cm column was used. Flow rates were 8 - 10 ml/hr. Two ml fractions were collected.

Amino acid analysis showed the amino acids found in oxytocin were in equimolar amounts. 13.0 mg of oxytocin purified in this way were dissolved in 0.5ml D_2O, the pD was adjusted to 3.3 using deuterated acetic acid.

Oxytocin and vasopressin were also isolated during the purification of neurophysin (described later in this CHAPTER) but quantities were insufficient for NMR study.

Spectra were run on a Varian HA-100 spectrometer. External hexamethyldisiloxane (HMS) or internal 3-(trimethylsilyl)-propane sulfonic acid sodium salt (DSS) were used as references. The resonance signals were weak on a single scan. A Varian C-1024 computer of average transients (C.A.T.) was used to accumulate successive scans and thereby improve the signal to noise ratio (S/N). Signal to noise increases as the square root of the number of scans. Usually between 100 and 500 scans were recorded.

Results.

Base-Stacking in Lysine Vasopressin.

It was not possible to assign the resonances observed in the aliphatic region of the oxytocin and vasopressin spectra to the individual amino acids.

The aromatic region however proved to contain useful information. Vasopressin contains two aromatic amino acids, tyrosine and phenylalnine. Oxytocin has only tyrosine, the phenylalanine is replaced by an isoleucine. Comparing the chemical shifts of the aromatic protons in vasopressin with those of the individual amino acids (Fig. 6.1) showed an upfield shift of the resonances in vasopressin. Such an upfield shift was not seen in oxytocin. Samples of 4-Pro,8-Ile oxytocin and 4-Pro,8Gln oxytocin synthesized by Dr. Manning (Medical College of Toledo, Ohio) were made available to us by Dr. L.Benoiton (University of Ottawa). The samples were dissolved in D_2O and the spectra taken in order to see how the tyrosine resonances behaved in these compounds (Fig. 6.1). The tyrosine resonances did not demonstrate any upfield shifts, they occured in the same positions as in the free amino acid (Fig. 6.1). The upfield shifts in vasopressin were attributed to stacking of the aromatic rings.

Aromatic rings, as mentioned in CHAPTER 1, have delocalized π electrons and when placed in a magnetic field produce local magnetic fields. The induced local magnetic field reinforces or decreases the effect of the applied magnetic field at various

Figure 6.1

100 MHz NMR spectra of the aromatic protons of tyrosine and phenylalanine as free amino acids, in hormone and hormone analogues. Solutions were in D_2O and spectra were taken at 25°C.

Tyrosine	.002 M
Phenylalanine	.01 M
Lysine vasopressin	.01 M
Oxytocin analogues	.01 M

All spectra were time averaged (100 to 500 scans).

TYROSINE in D_2O

PHENYLALANINE in D_2O

Cys - Tyr - Phe - Gln - Asn - Cys - Pro - Lys - Gly NH_2

LYSINE VASOPRESSIN

Cys - Tyr - Ileu - Pro - Asn - Cys - Pro - Ileu - Gly NH_2

4-Pro, 8-Ileu, OXYTOCIN

Cys - Tyr - Ileu - Pro - Asn - Cys - Pro - Gln - Gly NH_2

4-Pro, 8-Gln, OXYTOCIN

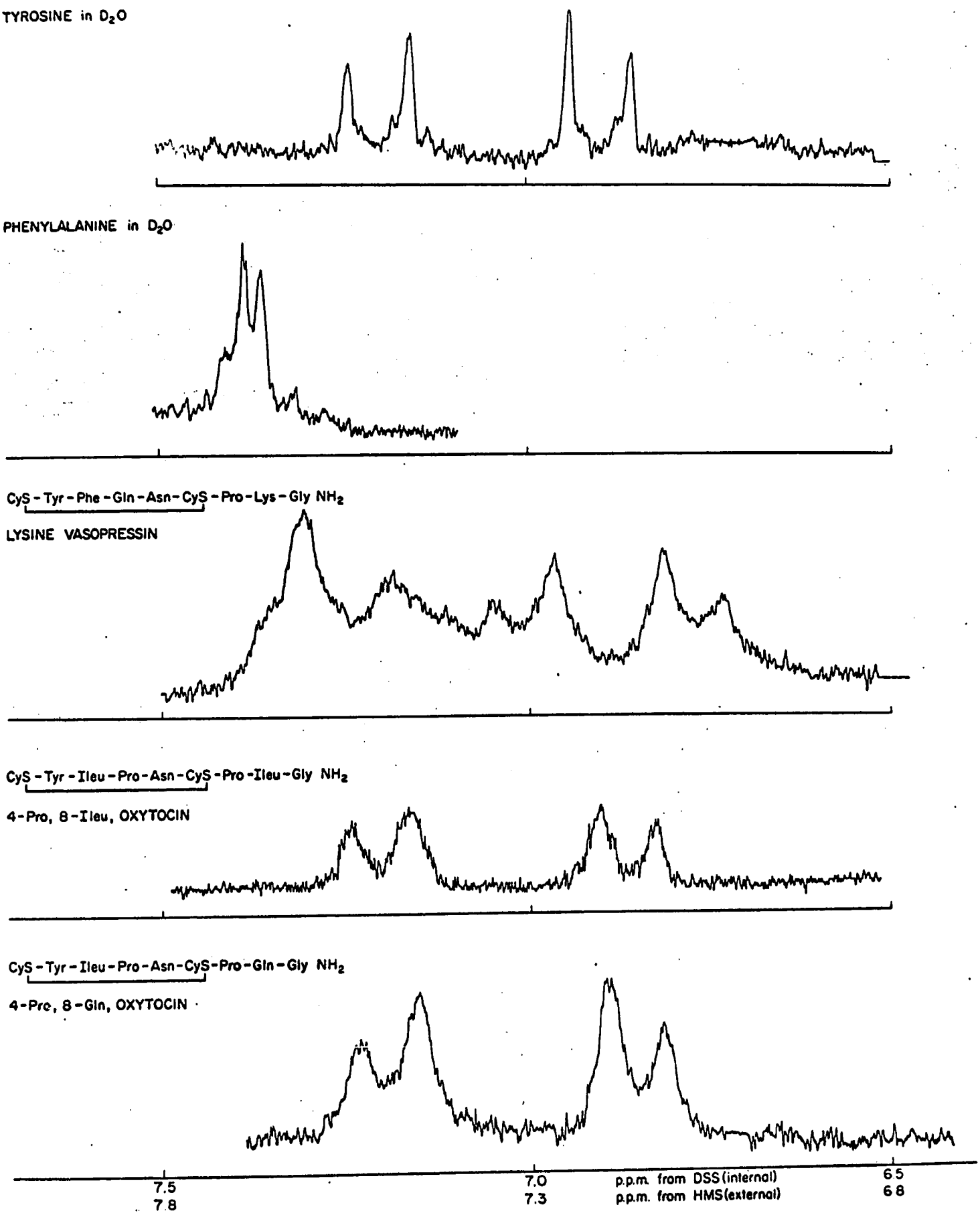

regions in space. Protons above and below the plane of the ring are shielded. Protons in the same plane as the ring are deshielded. These facts and the observed upfield shifts of the aromatic ring protons indicate that the tyrosine and phenylalanine rings are stacked. The magnitude of the upfield shifts of the aromatic protons are not all the same. From the 220 MHz spectrum (Fig. 6.2) it is possible to measure the magnitude of the upfield shifts for various groups of protons. The aromatic ring of tyrosine should give rise to an AA'BB' spectrum containing twenty four observable lines. Unfortunately the observed spectrum is 'deceptively simple' and appears to be an AB spectrum (this is the most common appearance for the aromatic region of tyrosine). For this reason it is impossible to do a complete analysis and measure chemical shift changes accurately. The same applies to phenylalanine which should give an AA'BB'C spectrum.

In lysine vasopressin the high field tyrosine resonances are shifted upfield by 0.07 p.p.m., the low field resonances are shifted upfield by 0.16 p.p.m. In tyrosine the high field resonances are those from the protons ortho to the hydroxyl group and the low field resonances are those from the protons meta

Figure 6.2

220 MHz spectrum of the aromatic region of lysine vasopressin in D_2O.

CyS – Tyr – Phe
|
CyS – Asn – Gln
|
Pro – Lys – Gly NH_2

LYSINE VASOPRESSIN

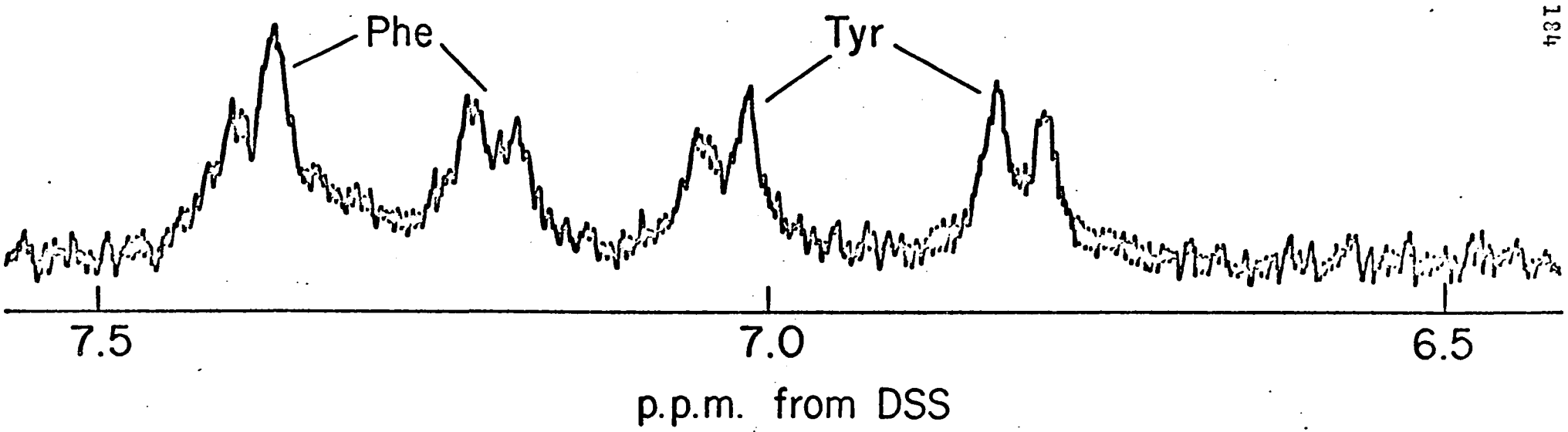

to the hydroxyl group. The high field resonances in phenylalanine are shifted upfield by 0.12 p.p.m. but the low field resonances only move upfield by 0.01 p.p.m. (Table 6.1).

Base-Stacking in Aromatic Dipeptides.

In order to see if base-stacking occured normally in dipeptides a number of aromatic dipeptides were examined. L-tyrosyl-L-tyrosine, L-tyrosyl-L-phenylalanine, L-phenylalanyl -L-phenylalanine and L-phenylalanyl-L-tyrosine were purchased from Miles-Yeda Ltd. and used without further purification. The peptides were dissolved in D_2O and the solutions adjusted to pD 6.8. The concentrations of solutions were varied up to 0.025 M when solubility permitted. In all spectra examined the aromatic region of tyrosine remained an AB quartet and comparisons could be made with the resonances in tha amino acid and in the hormone. The aromatic protons of phenylalanine in the dipeptides gave rise to more complex spectra. The two main groups of resonances previously observable were no longer present, spreading of lines occurred to high and low field. There were however not enough lines to allow a detailed analysis of the spectrum. As a consequence of this spreading of lines, comparison

Table 6.1

Resonance positions of tyrosine and phenylalanine as free amino acids, in hormones and in hormone analogues.

RESONANCE POSITIONS OF TYROSINE AND PHENYLALANINE

	TYR	PHE	LVP	OXYT	4PRO 8ILE OXYT	4PRO 8GLN OXYT
TYROSINE	6.90		6.83	6.89	6.87	6.87
	7.19		7.03	7.22	7.19	7.19
PHENYLALANINE		7.32	7.20			
		7.38	7.37			

TYR	tyrosine
PHE	phenylaalanine
LVP	lysine vasopressin
OXYT	oxytocin
4PRO 8ILE OXYT	4 proline 8 isoleucine oxytocin
4PRO 8GLN OXYT	4 proline 8 glutamine oxytocin

Spectra were run at 100 MHz in D_2O at pD 6.8

All values are reported w.r.t. internal DSS.(in ppm)
Tyrosine was a saturated solution (0.002M), all other samples were 0.01 M.
All spectra were time averaged (100 - 500 scans).

Positions reported are not chemical shifts, these could not be obtained from the deceptively simple spectra of tyrosine and phenylalanine.
The phenylalanine spectrum consisted of two major lines, these are the values reported here.
Tyrosine gave an AB type spectrum.The centre of each half of the AB spectrum was measured and reported. This was judged sufficient because the apparent

J_{AB} is the same in all spectra.

could not be made between the dipeptide, the free amino acid and the hormones. The best that could be done was to note the maximum upfield shifts which occured.

A pH study showed that the position of the resonances of the aromatic ring protons were pH dependent. This effect is probably greater in dipeptides than in polypeptides because the ring protons are near the the ionizable terminal groups (Table 6.2).

Comparing the resonance positions of the aromatic ring protons in the dipeptides with the free amino acid (or a peptide containing a single aromatic residue) should give an estimate of ring-stacking. This has been done using the data in Table 6.3. The maximum upfield shifts observed for tyrosine are approximately 0.08 p.p.m. This shows that aromatic rings of dipeptides tend to form stacks. The maximum upfield shift observed is smaller than some of the shifts observed in lysine vasopressin and therefore it seems that the nature of the stacking in vasopressin is at least partially determined by the peptide backbone if not by the presence of a ring closed by a disulfide link. The lack of an upfield shift in the hormone as large as that in the dipeptide for certain resonances also argues for a type of

Table 6.2

pH dependance of resonances from ring protons in aromatic dipeptides.

Peptide concentration was 0.01 M

Reference was external HMS

All spectra were time averaged (100 to 500 scans).

RESONANCES OF AROMATIC PROTONS IN DIPEPTIDES

	pD	PHENYLALANINE	TYROSINE
PHENYLALANINE	6.8	7.71 7.68 7.66	
TYROSINE	6.8		7.53 7.45 7.23 7.16
TYR-TYR	3.1		7.43 7.35 7.16 7.14 7.07 7.05
	6.5		7.46 7.37 7.19 7.17 7.11 7.08
	9.9		7.26 7.18 7.15 7.07
TYR-PHE	3,4	7.71 7.65 7.62 7.57 7.55	7.50 7.47 7.39 7.16 7.09
	6.9	7.63 7.61 7.59 7.57 7.54	7.46 7.38 7.18 7.10
	10.2	7.66 7.61 7.49 7.44	7.40 7.32 7.17 7.09
PHE-TYR	3.1	7.82 7.77 7.75 7.68 7.65	7.56 7.48 7.27 7.19
	6.9	7.70 7.67 7.65 7.62 7.58 7.55 7.51	7.48 7.39 7.37 7.15 7.13 7.07 7.05
	9.5	7.68 7.63 7.53 7.49	7.42 7.34 7.16 7.08
PHE-PHE	3.1	Broad unresolved line centered at 7.61	
	6.9	7.70 7.65 7.62 7.58 7.54 7.50	

Table 6.3

Resonances of ring protons in aromatic dipeptides.

RESONANCES OF AROMATIC PROTONS IN DIPEPTIDES.

	PHENYLALANINE		TYROSINE	
	Resonance	Relative intensity	Resonance	Relative intensity
PHE	771.3	5.3		
	768.7	14.3		
	768.3	13.8		
	766.0	11.3		
TYR			753.4	7.7
			745.0	9.1
			723.4	10.5
			715.8	7.4
PHE-PHE	770.0	3.2		
	764.8	8.6		
	762.0	9.8		
	758.4	9.8		
	754.2	5.6		
	749.9	3.0		
PHE-TYR	769.6	4.0	747.7	7.9
	767.2	9.5	739.3	9.8
	765.1	12.3	(736.6)	(2.2)
	762.4	5.7	715.3	9.8
	758.5	7.5	(713.2)	(2.5)
	754.9	6.0	707.2	6.2
	750.7	4.0	(704.8)	(1.2)
TYR-PHE	763.2	7.2	746.4	5.5
	761.4	8.8	738.0	7.0
	759.0	5.2	717.9	6.7
	756.9	6.7	709.8	4.5
	753.6	4.7		
TYR-TYR			745.8	6.0
			737.2	10.0
			719.3	8.0
			717.2	8.8
			711.0	4.8
			708.4	4.8

Resonance lines are given in Hz from external HMS.
Solutions of peptides were 0.01 M, pD was 6.8
Spectra were taken at 100MHz.
All spectra are time averaged (100 - 500 scans).
Relative intensities were measured directly on spectra, measurements are in cm and are given only to indicate the relative importance of each peak.
Tyrosine was a saturated solution.

stack which is particular to the hormone.

An additional source of upfield shifts which must be mentioned for the aromatic dipeptides is intermolecular ring-stacking. This type of stacking is minimized when solutions are very dilute.The usual manner by which such interactions are measured is to study the effect of concentration on the shifts, In view of the insolubility of most of the dipeptides used such studies are almost impossible.

Having observed upfield shifts of the ring protons in lysine vasopressin one should be able to propose a model of the stacked bases. Johnson and Bovey (75) have calculated the shielding effects produced by ring currents in benzene rings. Figure 6.3 (taken from reference 75) shows the effect of the benzene ring current on the chemical shifts of a nucleus at various positions around the benzene ring. In lysine vasopressin shieldings range between 0 and 0.20 p.p.m. Assuming the Johnson and Bovey calculations apply to systems such as aromatic dipeptides, one must place the tyrosyl ring protons in a plane between the 0 and +0.20 p.p.m. shieldings. Because it was impossible to assign the resonances in phenylalanine to particular ring protons one cannot determine which

Figure 6.3

Calculated shielding effects produced by ring currents in benzene.

Effect of benzene ring current on the chemical shift of a given nucleus at various positions around a benzene ring.

Z and ρ are units of ring radii (1.39 Å)

The origin of the axes is the center of the plane of the benzene ring.

The quadrant shown passes normally through the center of the ring.

(From reference 75).

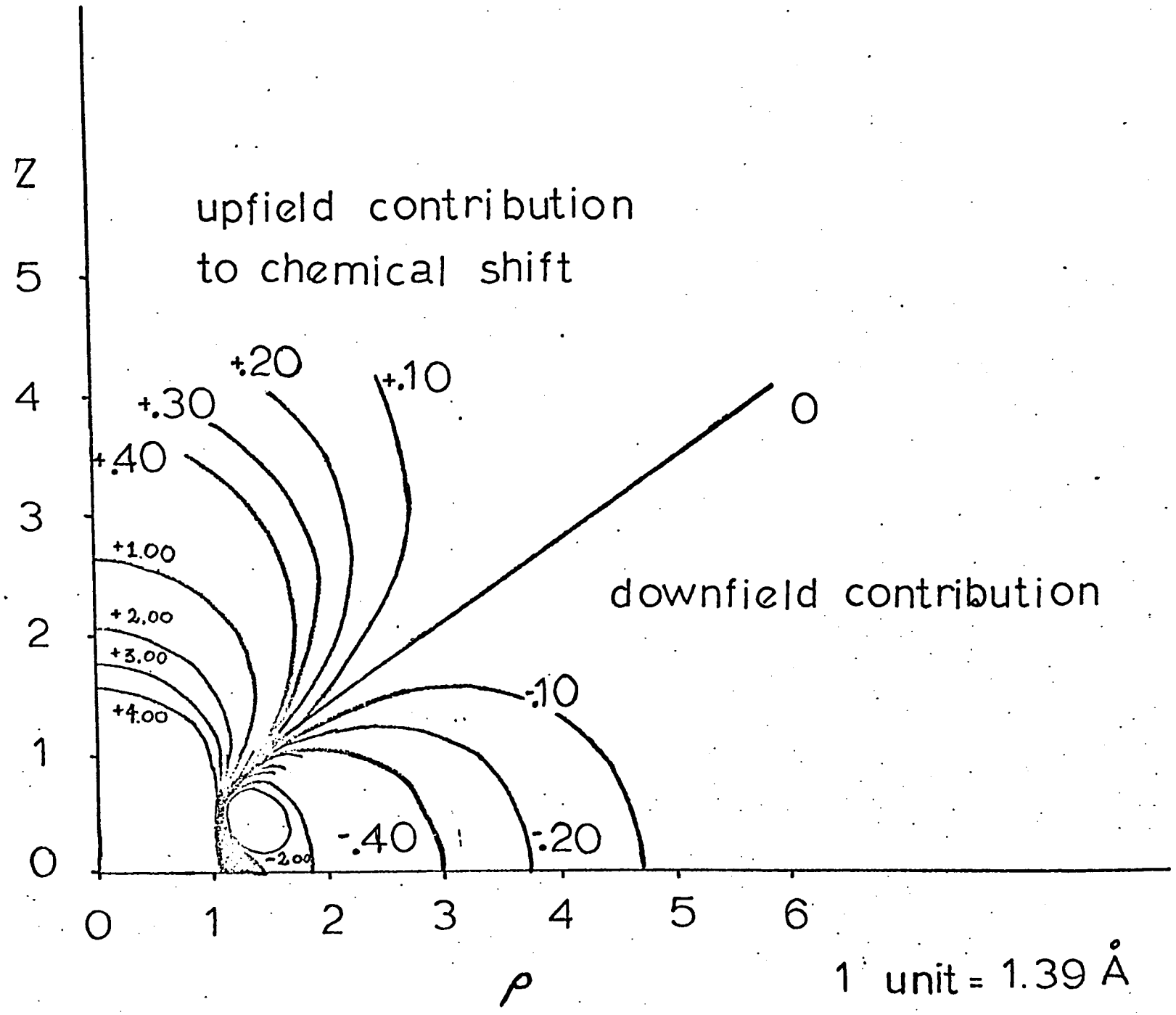
upfield contribution
to chemical shift
downfield contribution
Z
ρ
0
1
2
3
4
5
6
+.20
+.10
+.30
+.40
+1.00
+2.00
+3.00
+4.00
-.10
-.40
-.20
-2.00
1 unit = 1.39 Å

protons in phenylalanine have shifted upfield. This leads to ambiguity for a stacking model.However upon examination of the spectrum in Figure 6.2 it can be seen (from the relative areas under the peaks) that in lysine vasopressin three phenylalanine protons are shifted upfield by the same amount and two other protons are shifted upfield by another amount. From this one can construct a qualitative model which is shown in Figure 6.4

In order to test the applicability of Johnson and Bovey type calculations for use in the study of base-stacking of aromatic rings in amino acids it would be necessary to study rigid model peptides in which the degree of stacking is known. This could prove useful in the study of proteins by NMR techniques since the aromatic regions are relatively clear and changes can be easily seen.

Figure 6.4 -

Qualitative model of the stacking of the aromatic rings of tyrosine and phenylalanine in lysine vasopressin in aqueous solution.

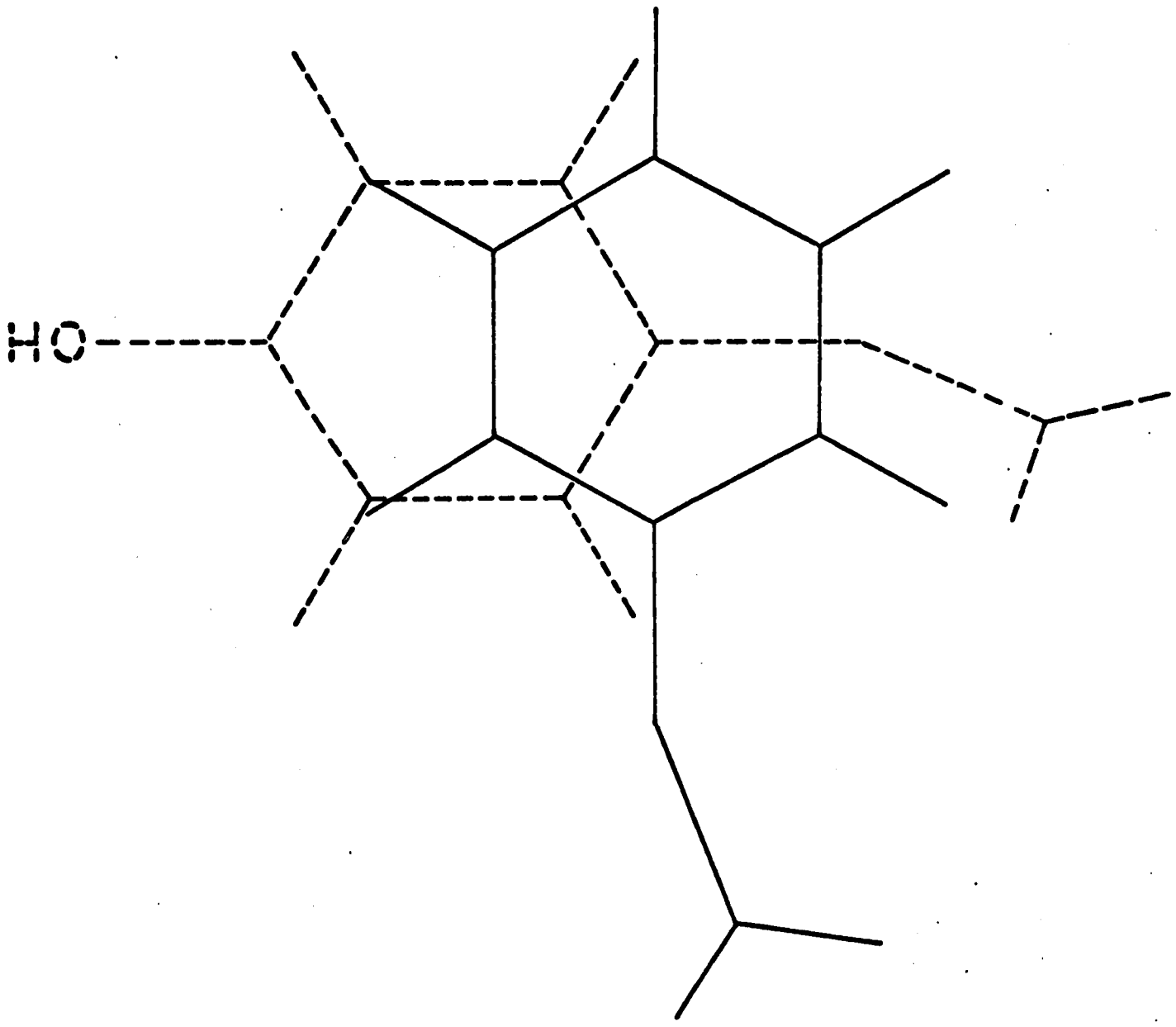
HO

Related NMR Studies.

Shortly after the previously mentioned series of experiments, a publication appeared containing the spectral assignment at 220 MHz and conformational analysis of oxytocin (Figure 6.5) in dimethyl sulfoxide (76). The use of dimethyl sulfoxide as solvent allowed observation of the NH resonances. This is not possible in D_2O because the protons in NH groups exchange at various rates, for deuterium. Proton homonuclear spin decoupling showed which NH, C^{α} and C^{β} protons belonged to the same amino acid residue. The resonances of the amino acids in the terminal tripeptide were assigned by taking the spectrum of Z-Pro-Leu-GlyNH_2. In order to assign the resonances of the cyclic moiety the spectra of the pentapeptides Z-Asp-Cys(Bzl)-Pro-Leu-GlyNH_2 and Z-Val-Cys(Bzl)-Pro-Leu-GlyNH_2 were taken. The magnitude of the couplings between the N and C^{α} protons was between 6.0 and 7.5 Hz (except for Ile which was 4.0 Hz). This led the authors to conclude that the dihedral angle between H-N-C^{α} and N-C^{α}-H was small.

The secondary structure of oxytocin was determined at 220 MHz in a mixture of dimethyl sulfoxide and

Figure 6.5

The structure of oxytocin.

OXYTOCIN

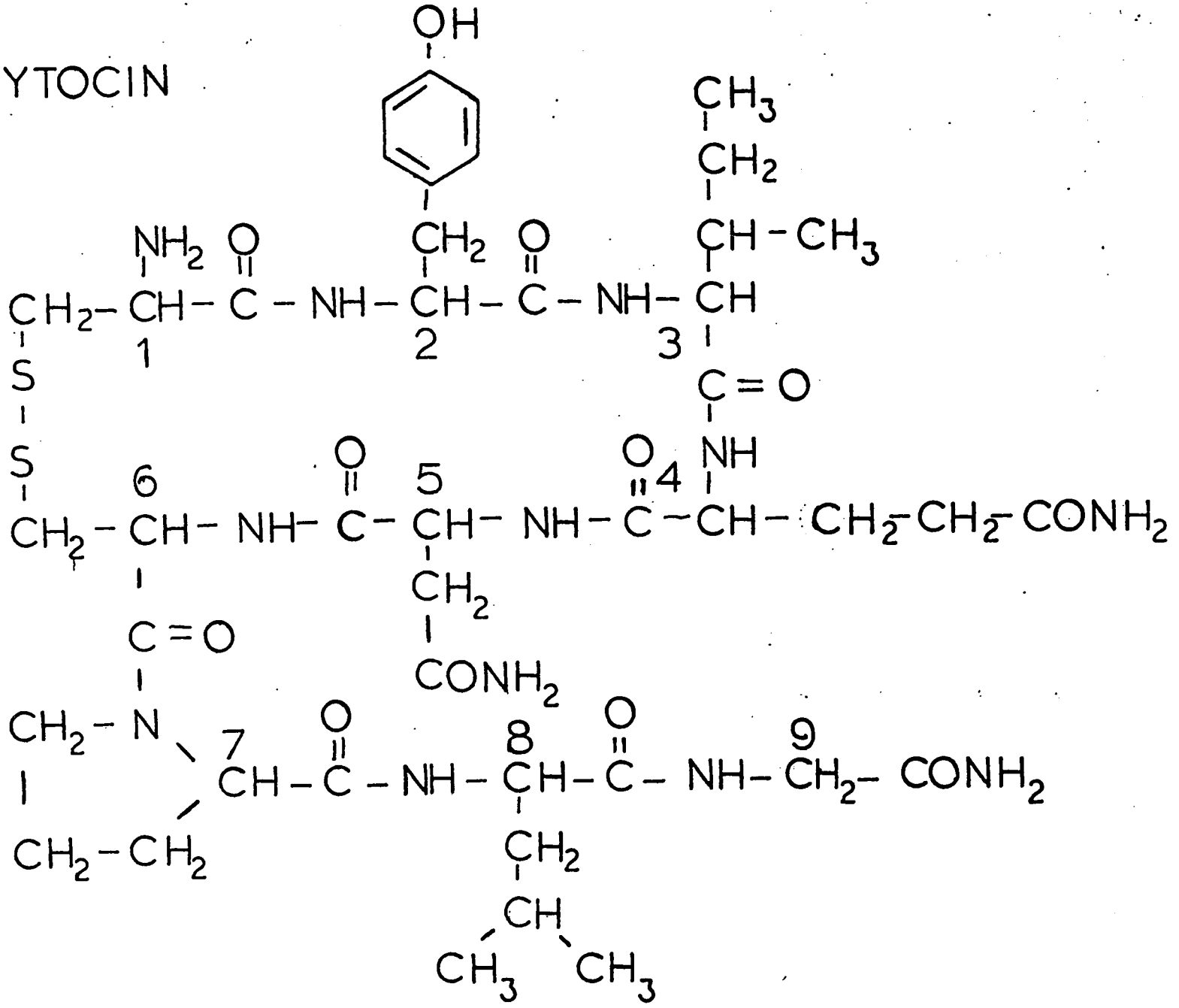

methanol (77). These studies involve the temperature dependence of amide proton chemical shifts in order to determine hydrogen bonded amide protons. An amide proton exposed to solvent has a larger temperature coefficient than an intramolecularly hydrogen bonded amide in the above mentioned solvent mixture. β turns in peptides are characterized by small $J_{CH,NH}$ for i + 1 residues and large $J_{CH,NH}$ for i + 2 residues. Hydrogen bonds form between the carbonyl of the i residue and the amide proton of the i + 3 residue. The amide proton resonance of the i + 3 residue is shielded by the end peptide moiety in the β turn and therefore appears at higher field than other amide proton resonances. Making use of these facts Urry et al (77) found that oxytocin contains a β turn. This β turn comprises the Tyr-Ile-Gln-Asn sequence. The observations which support this statement are as follow. The NH proton shifts of asparagine and tyrosine showed a low sensitivity to temperature changes. The amide proton resonance of asparagine was found at high field (the i + 3 residue). The α CH-NH coupling for isoleucine was small (the i + 1 residue). The α CH-NH coupling for glutamine was large (the

i + 2 residue). In this β turn, the carbonyl of tyrosine and the amide proton of asparagine are hydrogen-bonded. A second hydrogen bond between the amide proton of tyrosine and the carbonyl group of asparagine was likely in deamino oxytocin.

A second β turn was later proposed (78) to involve the Cys-Pro-Leu-GlyNH_2 residues at the C terminal end of oxytocin. The side chain carbonyl of asparagine is hydrogen-bonded to the amide proton of the leucine residue. The terminal tripeptide is proposed to be folded back on the ring; in this manner the carbonyl group of glycineamide is in an appropriate position to interact with the N-terminal amino group. In DMSO:D_2O solutions, the carbonyl group of cysteine in position 6 closes the second β-turn, the amide proton of glycine is its counterpart. X-ray studies on the C-terminal tetrapeptide of oxytocin (79) have demonstrated a hydrogen bond between the amino nitrogen of glycine (residue i + 3) and the carboxyl group of cysteine (residue i).

These studies have opened the way to study of the structure-activity relationships in neurohypophyseal hormones (80,81).

Studies on lysine vasopressin indicate a backbone

conformation similar to that of oxytocin in DMSO (71). The terminal tripeptide in lysine vasopressin appears to have more conformational freedom than in oxytocin. Stacking of the aromatic rings of tyrosine and phenylalanine was suggested to be important in hormone-receptor interactions. The structure of lysine vasopressin in DMSO has also been analysed by Von Dreele et al (82) and only one hydrogen bond was detected. The amide proton of asparagine is hydrogen-bonded to the carbonyl group of tyrosine.

Spectra of oxytocin and lysine vasopressin in aqueous solutions have recently been published (83). H_2O was used instead of D_2O in order to observe NH resonances. This causes a loss of information in the α CH region due to the presence of a large H_2O peak. NH proton resonances were assigned by comparison with dipeptides. Temperature coefficients were measured for the shifts of the NH proton resonances. None of the temperature coefficients were judged to be sufficiently small to indicate hydrogen-bonding. Observed resonances were not assigned to individual amino acids.

The question of peptide conformation in dimethyl sulfoxide and water deserves further consideration. CHAPTER 7 contains the result of studies on oxytocin

and related peptides in DMSO by ^{13}C NMR spectroscopy. The purpose of these experiments was to relate the carbon chemical shifts from carbonyl groups to the presence or absence of hydrogen bonds.

Protein-Hormone Interactions.

Isolation of Porcine Neurophysin.

Lysine vasopressin and oxytocin are known to bind porcine neurophysin. In order to study the protein-hormone interaction by NMR it was necessary to isolate neurophysin. The method Hollenberg and Hope (56) developed for isolating bovine neurophysin was used to isolate porcine neurophysin (54). Acetone-dried powders of porcine posterior pituitary were purchased from Nutritional Biochemicals Corporation.

Preparation of Protein-Hormone Complex.

In a typical run 10 grams of acetone-dried powder were dissolved in 400 ml of 0.1 M HCl. The solution was stirred in the cold-room at $4^{o}C$ overnight. Insoluble material was removed by a 10 minute centrifugation at 16,300 gmax in a Sorvall RCB-2 refrigerated centrifuge at $3^{o}C$. The supernatant was stored at $4^{o}C$. The insoluble material was re-extracted at $4^{o}C$ in 200 ml of 0.1 N HCl for twenty hours and centrifuged. The insoluble material was discarded. The second supernatant was combined with the first one. The pH was 1.7. The solution was then neutralized with 5N NaOH. The cloudy solution was centri-

fuged 15 minutes at 27,300 gmax (at 3°C.). The supernatant (≃ 575 ml) was decanted and acidified with 3 N HCl to pH 3.9. 10 g. of NaCl were added per 100 ml of supernatant. The solution was left overnight at 4°C in order to precipitate the crude protein-hormone complex.

The protein-hormone complex was centrifuged 15 minutes at 27,300 gmax (at 3°C.). The supernatant was discarded. The sediment was washed with 100 ml H_2O. The protein-hormone complex was desalted by dialysis against water (3 x 6 litres at 4°C, for 24 hours) using 18/32 Visking tubing.

The contents of the dialysis bags were collected and the residue dissolved with several drops of glacial acetic acid. The solution was lyophilized overnight. 863 mg of crude protein-hormone complex were recovered.

Column Chromatography.

Gel Filtration on Sephadex G-25.

100 grams of Sephadex G-25 superfine were stirred in 1000 ml of 0.1 N formic acid overnight. Another 1000 ml of 0.1 N formic acid were added to the Sephadex and poured into a 100 x 2.5 cm Sephadex column. The column was washed overnight with 0.1 N formic acid.

Approximately 100 mg. of crude protein-hormone complex were dissolved in 2 ml of 0.1 N formic acid and applied to the column. The column was eluted with 0.1 N formic acid at a flow rate of 20 ml/hr. Fractions were collected every 20 minutes. Effluent was monitored for protein content by measuring transmission at 254 nm with an LKB Uvicord. Two peaks were isolated (Figure 6.6), the first contained the proteins while the second contained the low molecular weight peptides vasopressin and oxytocin (54,56). 80% of the weight of material placed on the column was recovered.

Gel Filtration on G-75 Sephadex.

60 grams of G-75 Sephadex were stirred overnight in 2 litres of 0.1 N formic acid. The next day a 100 x 2.5 cm Sephadex column was packed. The column was washed overnight with 0.1 formic acid. The void volume was 140 ml as measured with Blue Dextran. Approximately 100 mgs of crude protein were dissolved in 2 ml 0.1 N formic acid and applied to the column. The column was eluted with 0.1 N formic acid at a flow rate of 8 ml/hr. Fractions were collected every hour. Three peaks were resolved (Figure 6.7). The first emerged with the void volume (A), the second after approximately 320 ml (B-I) and the third after approximately 380 ml (B-II) of

Figure 6.6

Separation of crude protein-hormone complex on G-25 Superfine Sephadex column (100 x 2.5 cm) in 0.1 N formic acid.

Flow rate 20 ml/hr.

Fractions were collected every 20 minutes.

Optical density was measured at 280 nm.

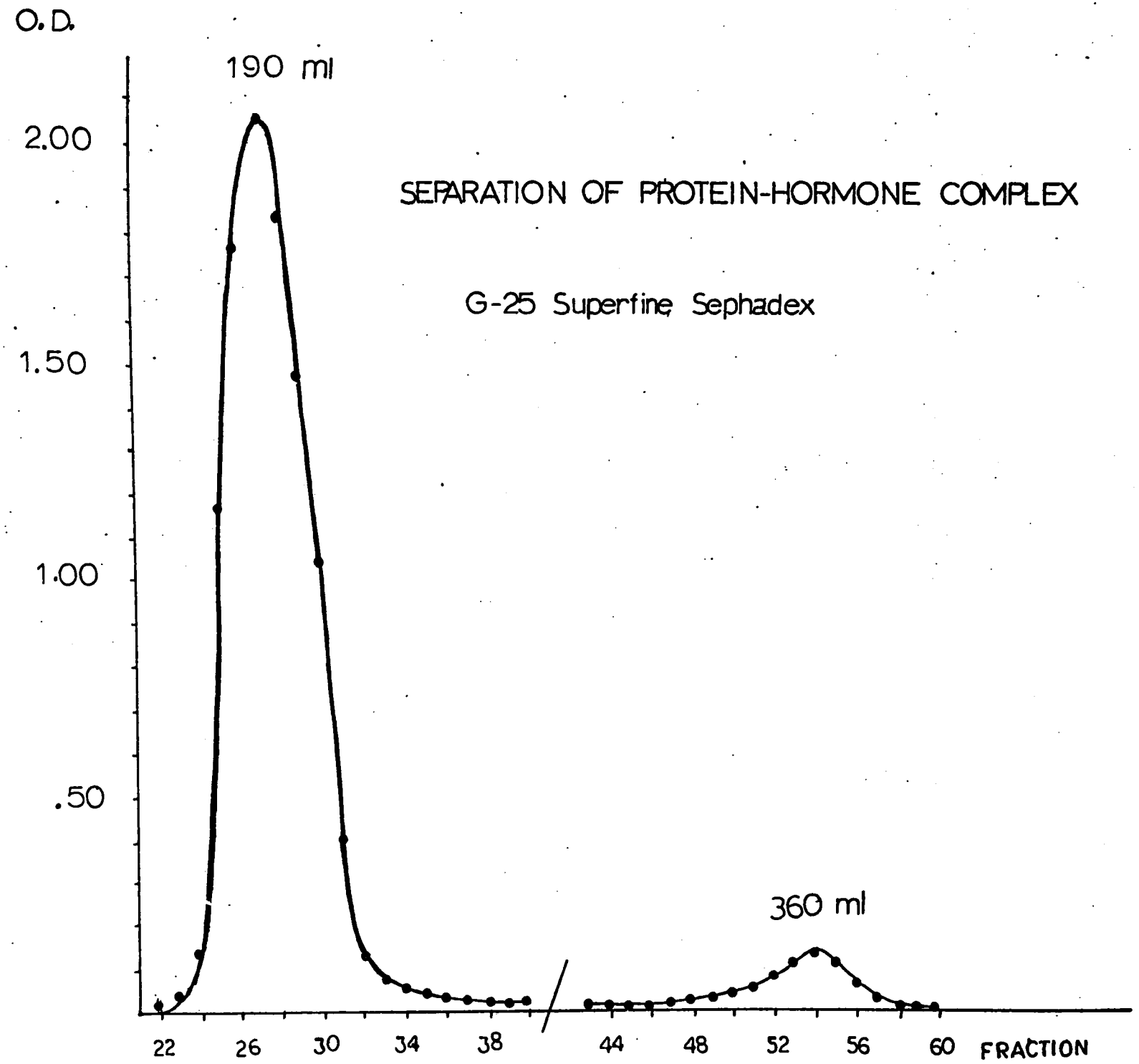
O.D.
190 ml
2.00
1.50
1.00
.50
SEPARATION OF PROTEIN-HORMONE COMPLEX
G-25 Superfine Sephadex
360 ml
22
26
30
34
38
44
48
52
56
60
FRACTION

Figure 6.7

Separation of porcine neurophysins from high molecular weight proteins.
G-75 Sephadex column (100 x 2.5 cm)
Flow rate 8 ml/hr
Fractions collected every hour.
Optical density measured at 254 nm and later tubes read at 280 nm.

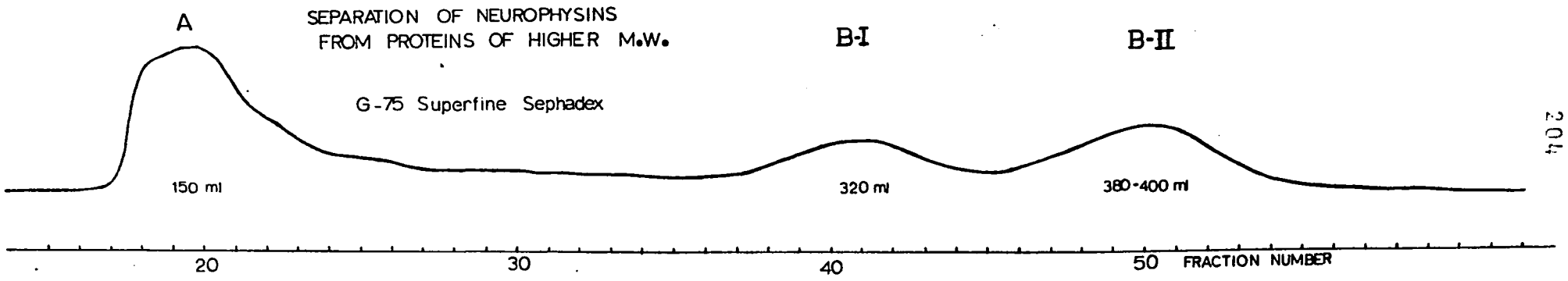
A
SEPARATION OF NEUROPHYSINS
FROM PROTEINS OF HIGHER M.W.
B-I
B-II
G-75 Superfine Sephadex
150 ml
320 ml
380-400 ml
20
30
40
50
FRACTION NUMBER

eluant. The neurophysins are found in the B peaks. Recovery from the column was 75%, each peak contained about one third of the material recovered.

Large Scale Preparation of Neurophysin.

Because it was not possible to separate the two bound hormones, oxytocin and vasopressin, on the G-25 column I decided to eliminate this step and start immediately with a G-75 column. This gave four peaks as expected. The first was the high molecular weight protein, the second two were the neurophysins and the third contained small peptides (Figure 6.8).

In an effort to obtain larger amounts of protein a 100 x 5 cm G-75 Sephadex column was run in 0.1 N formic acid at a flow rate of 25 ml/hr. Usually 500 mg of crude protein-hormone complex were run at one time. This procedure led to slightly less resolution of the B-I and B-II peaks. On disc electrophoresis B-I appeared as one diffuse band whereas B-II showed at least two bands. 700 mg. of B-II were reapplied to the same column and again eluted with 0.1 N formic acid. This gave two incompletely resolved peaks (Figure 6.9). The smaller peak appeared first. By disc. electrophoresis the first peak was shown to migrate in the same manner

Figure 6.8

Separation of crude protein-hormone complex on a G-75 Sephadex column in 0.1 N formic acid.
Column measured 100 x 2.5 cm.
Flow rate 28 ml/hr.
Fractions collected every 40 minutes.
Optical density measured at 260nm. tubes were later read at 280nm.

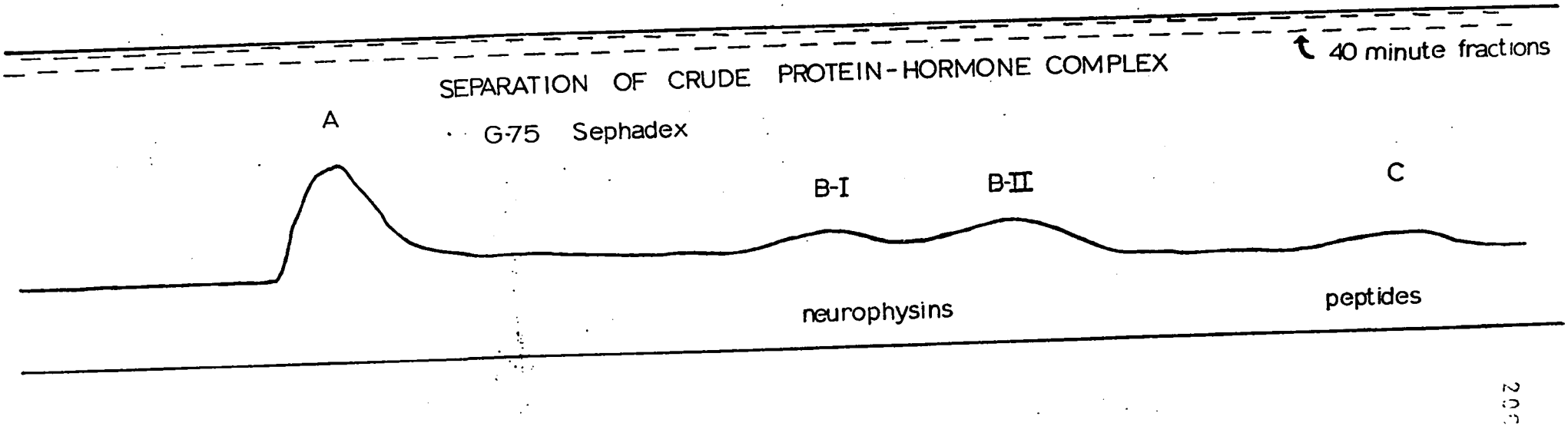
SEPARATION OF CRUDE PROTEIN-HORMONE COMPLEX
G-75 Sephadex
40 minute fractions
A
B-I
B-II
C
neurophysins
peptides

Figure 6.9

B-II proteins off G-75 Sephadex column rerun on same column (100 x 5 cm)

Eluant was 0.1 N formic acid.

Flow rate was 26 ml/hr.

Fractions were collected every 40 minutes.

Optical density was measured at 254nm

tubes were later read at 280 nm.

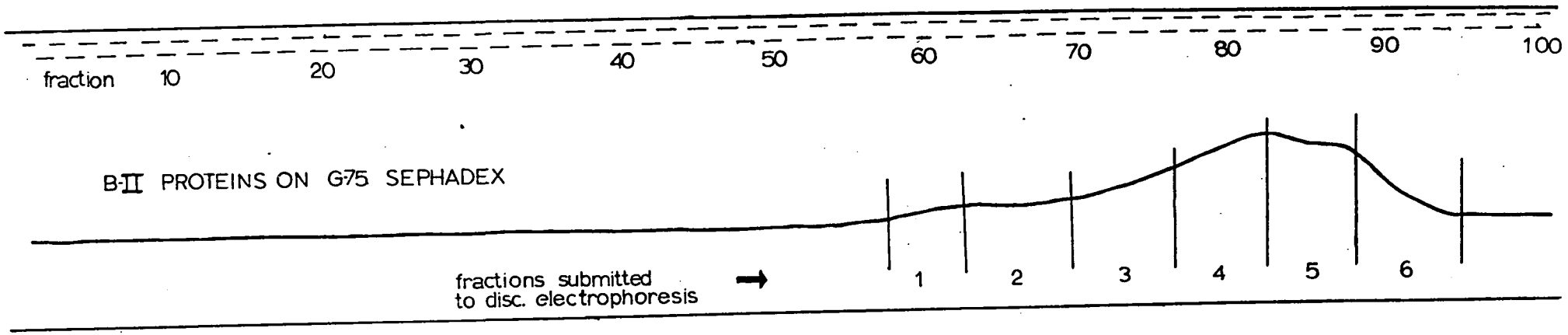
fraction 10 20 30 40 50 60 70 80 90 100
B-II PROTEINS ON G-75 SEPHADEX
fractions submitted to disc. electrophoresis
1 2 3 4 5 6

as did the B-I protein. Protein from the second peak gave two distinct bands. . . These results are in agreement with those of Uttental and Hope (84). These authors have shown that Neurophysin-II comes off the column first as did B-I. They also demonstrated that the second peak contains Neurophysin-I and Neurophysin-III. This accounts for the two bands seen in the polyacrylamide gel.

Ion-exchange Chromatography on CM-50 Sephadex.

Ion-exchange chromatography was done using CM-50 Sephadex on a 45 x 2.5 cm column. The column was equilibrated with sodium acetate buffer (ionic strength 0.1) at pH 4.5. Protein was dissolved in 0.2 N acetic acid and applied to the column. The column was eluted with 1.0 litre of sodium acetate buffer and a pH gradient was run between 4.5 and 5.0. Flow rate was 10 ml/hr. Fractions were collected every half hour. The fractions were pooled, dialyzed against water to remove salt and then lyophilized. B-II proteins were separated on this column and later submitted to disc. electrophoresis. This column did separate the two proteins, the results are shown in Figure 6.10.

B-I proteins were also run on this column,

Figure 6.10

Separation of B-II proteins on CM-50 Sephadex.
B-II proteins came off a G-75 Sephadex coulumn
(100 x 2.5 cm) run in 0.1 N formic acid.
CM-50 Sephadex column (45 x 2.5 cm) was run
in sodium acetate buffer (ionic strength 0.1)
A pH gradient was established between 4.5 and 5.0
Optical density was measured at 280 nm.

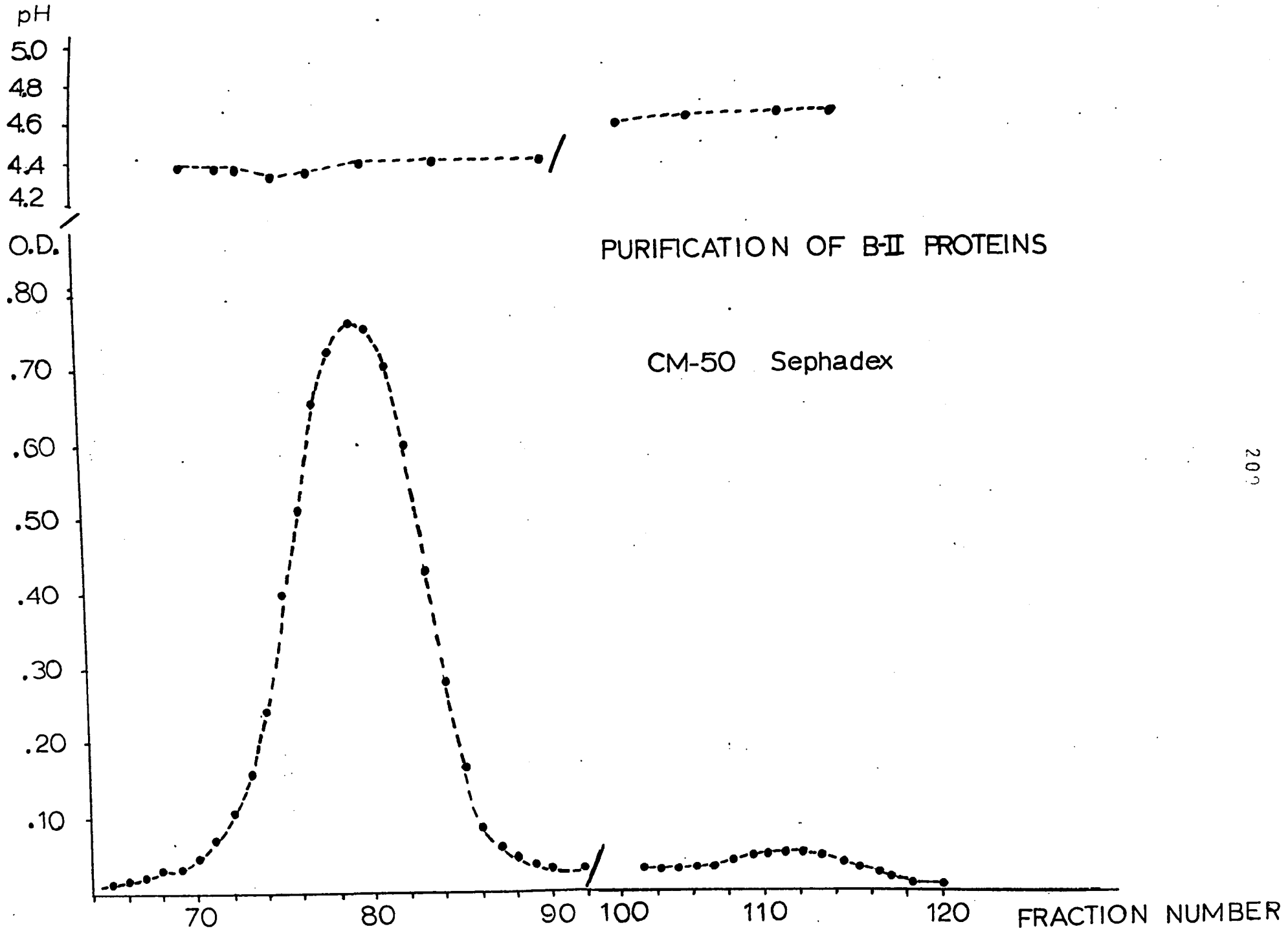
pH
5.0
4.8
4.6
4.4
4.2
O.D.
.80
.70
.60
.50
.40
.30
.20
.10
PURIFICATION OF B-II PROTEINS
CM-50 Sephadex
70
80
90
100
110
120
FRACTION NUMBER

the results are shown in Figure 6.11. Disc. electrophoresis showed a single band for B-I pk 2.

Disc. Electrophoresis.

Disc. electrophoresis, a method developed by Ornstein and Davis (85,86) has been used to study proteins of the posterior pituitary (87). Polyacrylamide gels were at pH 9.5. Solutions containing 5 mg /ml of protein were prepared, 20 µl were applied to each gel. 50 mV were applied for 30 minutes, the voltage was then raised to 100 mV and applied for the next hour. Gels were stained with Amido Black for one hour. Destaining was done in 7% acetic acid at 100 mV for one hour.

Amino Acid Analysis.

Amino acid analyses was performed on an automatic amino acid analyser (Beckman/Spinco Model 120) using the method of Spackman,Stein and Moore (73). Samples of protein (5mg) were hydrolysed <u>in vacuo</u> in constant boiling HCl (88) at 110°C. Results of the analyses are shown in Table 6.4 along with those published subsequently by other research groups (89-92). Porcine

Figure 6.11

Separation of B-I proteins on CM-50 Sephadex column run in sodium acetate buffer.

A pH gradient was established between pH 4.5 and 5.0.

B-I proteins were off a G-75 Sephadex column (100 x 2.5 cm) run in 0.1 N formic acid.

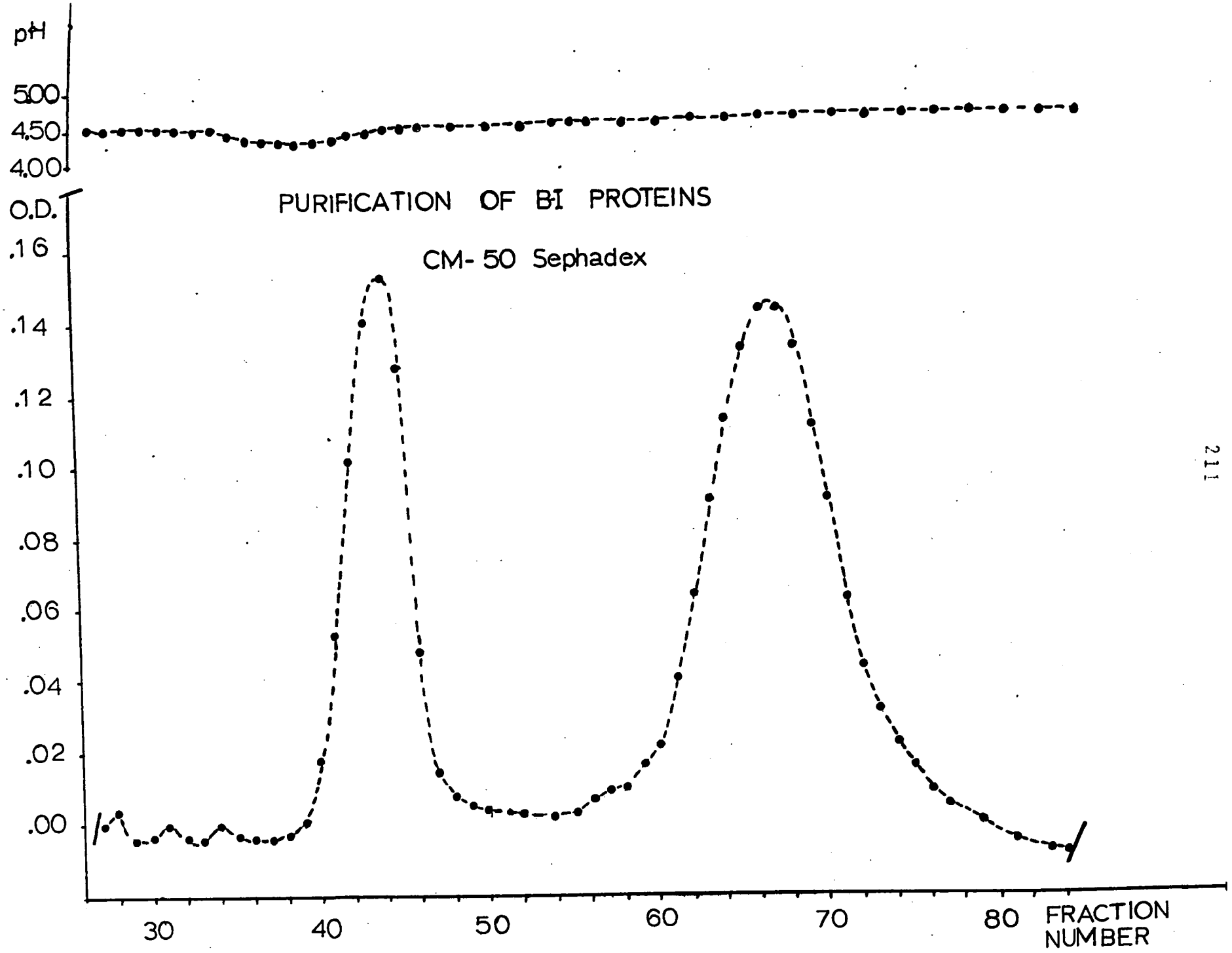
pH
5.00
4.50
4.00
PURIFICATION OF BI PROTEINS
CM-50 Sephadex
O.D.
.16
.14
.12
.10
.08
.06
.04
.02
.00
30
40
50
60
70
80
FRACTION NUMBER

Table 6.4

Amino acid composition of porcine neurophysins.

AMINO ACID COMPOSITION OF PORCINE NEUROPHYSINS.

TYPE	NP-I	NP-I	NP-I	B-II pk ①	NP-II	NP	B-I pk ②	NP-III
REFERENCE	90	91	89		89	92		89
LYSINE	2	2	2	2 (2.1)	4	6	6 (6.5)	2
HISTIDINE	-	-	tr	1	-	1	-	tr
ARGININE	5	5	5	5 (4.9)	6	6	8 (8.2)	6
CYSTINE (1/2)	12	14	12	12 (11.7)	18	14	18 (17.7)	12
ASPARTIC ACID	5	5	5	5 (5.2)	12	11	13 (13.0)	5
METHIONINE	1	1	1	1 (0.9)	-	1	tr (0.2)	1
THREONINE	2	2	2	2 (1.9)	3	4	3 (2.9)	2
SERINE	7	8	8	6 (5.6)	9	7	6 (6.0)	7
GLUTAMIC ACID	13	14	13	13 (12.6)	15	19	16 (15.6)	12
PROLINE	6	7	7	7 (7.3)	14	10	13 (13.1)	6
GLYCINE	14	15	14	15 (15.3)	20	19	22 (22.0)	13
ALANINE	7	8	7	8 (8.3)	12	11	14 (14.3)	8
VALINE	2	2	2	2 (2.1)	4	6	5 (4.7)	2
ISOLEUCINE	2	2	2	2 (2.1)	3	3	2 (2.4)	2
LEUCINE	7	7	7	7 (7,1)	9	9	10 (9.7)	7
TYROSINE	1	1	1	1 (1.0)	2	2	1 (1.4)	1
PHENYLALANINE	3	4	3	3 (3.2)	6	4	6 (6.4)	3
TOTAL	89	97	91		137	133		89
M.W.	9,170		9,356		14,020	13,000		9,214

NP : Neurophysin

tr : traces

Neurophysin-I has recently been sequenced (91).

Discussion and Conclusion.

Separation of B-II proteins was shown in Figure 6.11. The first and major peak eluted between pH 4.40 and 4.56. This was called B-II pk 1. The second, small, peak eluted at pH 4.60. This one was designated B-II pk 2. The B-II pk 1 fraction has the same elution profile as Porcine Neurophysin-I (89). Only this fraction has been submitted to amino acid analysis and corresponds well to Porcine Neurophysin-I. The B-II pk 2 fraction has not yet been analysed.

The B-I fraction eluted from the G-75 Sephadex column should contain Neurophysin-II (89). The B-I fraction off the G-75 Sephadex column (100 x 2.5 cm) was run on the CM-50 Sephadex column. Two peaks were eluted (Fig. 6.13). The first peak eluted between pH 4.40 and 4.56, as did Porcine Neurophysin-I. The second peak (2/3 of the total protein) eluted between pH 4.60 and 4,67. This fraction migrated as a single band on electrophoresis. The second peak was called B-I pk 2. A fraction of this was submitted to amino acid analysis and the results are shown in Table 6.4 It appears that there is less agreement about the

composition of porcine neurophysin with a molecular weight around 13,000-14,000 (89,92) than there is about Porcine Neurophysin-I (M.W. $\leq$ 10,000) (89 - 91).

These studies were undertaken to secure a supply of porcine neurophysin in order to study binding between neurophysin and neurohypophyseal hormones. When this series of experiments began little had been published on the composition of porcine neurophysins. I am pleased to see my findings agree with those of Uttenthal and Hope (89). Protein-hormone binding studies have been delayed due to difficulties associated with analysis of the hormone spectra. Hopefully these experiments will be undertaken in the future.

The NMR spectrum of Porcine Neurophysin-II has been taken. There appears to be little conformational information in the spectrum, lines are broad and the resonances for individual amino acids cannot be seen. This is expected from high molecular weight compounds such as proteins. A more fruitful approach is to study the changes in the hormone spectrum when it binds to the protein.

The model for the base stacking in lysine vasopressin has been published (93).

6.3 Conclusion.

Porcine Neurophysin I (91) Bovine Neurophysin II (94) have been sequenced. We now shall reconsider the results of neurophysin-hormone binding studies in the light of this data. The number of hormone molecules bound to neurophysin varies between one and fourteen (60,61) depending upon the experimental technique used. Two or three molecules of hormone bound per molecule of protein is the more usual estimate (62,63). Neurophysin is a relatively small protein. The molecular weights reported vary between 10,000 and 20,000 (57,63). The molecular weight of oxytocin and vasopressin is near 1,000. If three molecules of hormone are bound to one molecule of neurophysin this represents 3/20 to 3/10 of the M.W. of neurophysin. However, if 14 molecules are bound, this could represent 7/10 to 14/10 of the M.W. of neurophysin. The latter binding cannot be very specific. All hormone molecules cannot be bound to the same type of site. Binding could simply be due to non-specific ionic bonds. This is not a very appealing model. If only three molecules of hormone are bound per molecule of neurophysin, binding could occur at specific sites on the protein. This could be more similar to enzyme-substrate interaction at active

sites. Bovine Neurophysins I and II are reported to bind three and two molecules of oxytocin or vasopressin respectively. In this case binding sites in neurophysin are not exclusive to one hormone and binding of hormone analogues may be possible. Such studies could yield information on the type of binding sites found in neurophysin. Binding of three hormone molecules to a monomeric protein is unusual and it would be very relevant to find if all the sites are identical.

It may yet be demonstrated that each neurophysin binds only one molecule of each hormone. This would allow a highly specific interaction between neurophysin and oxytocin or vasopressin.

Many groups have examined binding properties of oxytocin and vasopressin to neurophysin, yet no one knows why this binding is necessary. Possibly the supra-optico and paraventricular nuclei cannot synthesize oxytocin and vasopressin at a rate which is fast enough to cope with changes in physiological conditions of the organism. Binding of the hormones to neurophysin in storage granules may be necessary to prevent degradation of the hormones in the cytoplasm of neurohypophyseal cells. Release of vasopressin and oxytocin from the neurohypophysis could occur along with neurophysin.

This could be a protective mechanism for the hormones. Regardless of where separation of the hormone-protein complex occurs, a specific release mechanism must exist. The receptor at the target organ could have a higher affinity for the hormone than does neurophysin and the target organ could cause release of hormone from neurophysin. Another possibility is that neurophysin begins to be degraded and release of the hormone ensues.

6.4 References.

1. J.J. Abel and M.C. Pincoffs, Proc, Natl, Acad. Sci. U.S.A. 3 507 (1917)

2. O. Kamm, T.B. Aldrich, I.W. Grote, L.W. Rowe and E.P. Bugbee, J. Amer. Chem. Soc. 50 573 (1928)

3. H.H. Daile and Laidlaw, J. Pharmacol. 4 75 (1912)

4. A.H. Livermore and V. du Vigneaud, J. Biol. Chem. 180 365 (1949)

5. L.C. Craig, J. Biol. Chem. 155 519 (1944)

6. J.G. Pierce and V. du Vigneaud, J. Biol. Chem. 182 359 (1950)

7. W.H. Stein and S. Moore, J. Biol. Chem. 176 337 (1948)

8. W.H. Stein and S. Moore, J. Biol. Chem. 176 367 (1948)

9. S. Moore and W.H. Stein, J. Biol. Chem. 178 53 (1949)

10. S. Moore and W.H. Stein, J. Biol. Chem. 178 79 (1949)

11. G.J. Pierce and V. du Vigneaud, J. Biol. Chem. 186 77 (1950)

12. R.A. Turner, J.G. Pierce and V. du Vigneaud, J. Biol. Chem. 193 359 (1951)

13. H. Tuppy, Biochim. Biophys. Acta 11 449 (1953)

14. V. du Vigneaud, C. Ressler and S. Tripett, J. Biol. Chem. 205 949 (1953)

15. C. Ressler, S. Tripett and V. du Vigneaud, J. Biol. Chem. 204 861 (1953)

16. J.M. Mueller, J.G. Pierce and V. du Vigneaud, J. Biol. Chem. 204 857 (1953)

17. R.A. Boissonnas, S. Guttman, P.A. Jacquenoud and J.P. Waller, Helv. Chim. Acta 38 5688 (1959)

18. J. Rudinger, J. Honzl and M. Zaoral, Coll. Czech. Chem. Comm. 21 202 (1956)

19. L. Velluz G. Amiard, J. Bart, B. Goffinet and R. Heymes, Bull. Soc. Chim. de France 1464 (1956)

20. Bodanszky and V. du Vigneaud, J. Amer. Chem. Soc. 81 5688 (1959)

21. E.B. Linder, A. Elmqvist and J. Porath, Nature 184 1565 (1959)

22. D. Yamashiro, Nature 201 76 (1964)

23. R.A. Turner, J.G. Pierce and V. du Vigneaud, J. Biol. Chem. 191 21 (1951)

24. D.N. Ward and V. du Vigneaud, J. Biol. Chem. 222 951 (1956)

25. E.A. Popenoe and V. du Vigneaud, J. Biol. Chem. 205 133 (1953)

26. E.A. Popenoe and V. du Vigneau, J. Biol. Chem. 206 353 (1954)

27. V. du Vigneaud, M.F. Bartlett and A. Johl, J. Amer. Chem. Soc. 79 5572 (1957)

28. V. du Vigneaud, D.T. Gish, P.T. Katsoyannis and G.P. Hess, J. Amer. Chem. Soc. 80 3355 (1958)

29. R.A. Boissonnas and R.L. Huguenin, Helv. Chim. Acta 43 182 (1960)

30. R.O. Studer, Helv. Chim. Acta 46 421 (1963)

31. D.N. Ward and R. Guillemin, Proc. Soc. Exptl. Biol. Med. 96 568 (1957)

32. A.V. Schally, H.S. Lipscomb and R. Guillemin, Biochim. Biophys. Acta 31 252 (1959)

33. J. Porath and E.B. Linder, Nature 191 69 (1961)

34. J. Porath and A.V. Schally, Andocrin. 70 738 (1962)

35. P. Guillemin, A.V. Schally, H.S. Lipscomb, R.N. Anderson and J.M. Long, Endocrin. 70 471 (1962)

36. A.V. Schally, H.S. Lipscomb, J.M. Long, W.E. Dear and R. Guillemin, Endocrin. 70 478 (1962)

37. B.T. Pickering and C.W. Jones, J. Endocrin. 46 vi (1970)

38. M. Roux, Arch. Anat. Microsc. Morphol. Exp. t 54 965 (1965)

39. M. Roux, Comptes Rendus des Seances de Soc. de Biol. 163 1593 (1970)

40. R. Barer, H. Heller and K. Lederis, Proc. Roy Soc. Ser. B 158 388 (1963)

41. H.B. Van Dyke, B.F. Chow, R.O. Greep and A. Rothen, J. Pharmacol. Exptl. Therap. 74 190 (1942)

42. R.T. Block and H.B. Van Dyke, Nature 165 975 (1950)

43. H.B. Van Dyke, Arch. Bioch. Biop. 36 1 (1953)

44. R. Acher, J. Chauvet and G.O. Olivry, Biochim. Biophys. Acta 22 421 (1956)

45. R. Acher, J. Chauvet and G.O. Olivry, Biochim. Biophys. Acta 22 428 (1956)

46. R. Acher, A. Light and V. du Vigneaud, J. Biol. Chem. 233 116 (1958)

47. A. Light, R.O. Studer and V. du Vigneaud, Arch. Biochem. Biophys. 83 84 (1959)

48. B.T.B. Frankland, M.D. Hollenberg, D.B. Hope and B.A. Schacter, Brit. J. Pharmacol. 26 502 (1966)

49. J. Chauvet, M.T. Lenci and R. Acher, Biochim. Biophys. Acta 38 266 (1960)

50. E. Breslow and L. Abrash, Proc. Natl. Acad. Sci. 56 640 (1966)

51. K. Jayasena and P.J. Thomas, J. Physiol. 183 45 P (1966)

52. D.B. Hope and M.D. Hollenberg, Biochem. J. 99 5 P (1966)

53. M.D. Hollenberg and D.B. Hope, Biochem. J. 104 122 (1967)

54. L.O. Uttental, Y. Ishida and D.B. Hope, Biochem. J. 105 36 C (1967)

55. C.M. Dean, M.D. Hollenberg abd D.B. Hope, Biochem. J. 104 8 C (1968)

56. M.D. Hollenberg and D.B. Hope, Biochem. J. 106 557 (1968)

57. R. Rauch, M.D. Hollenberg and D.B. Hope, Biochem. J. 115 473 (1969)

58. M. Ginsburg and M. Ireland, J. Physiol. 169 15 P (1963)

59. M.D. Hollenberg and D.B. Hope, J. Physiol. 185 5 P (1966)

60. M. Ginsburg, K. Jayasena and P.J. Thomas, J. Physiol. 184 387 (1966)

61. M. Ginsburg and M. Ireland, J. Endocrin. 32 187 (1965)

62. M.D. Hollenberg and D.B. Hope, Biochem. J. 105 921 (1967)

63. M.D. Hollenberg and D.B. Hope, Biochem. J. 106 557 (1968)

64. C.R. Dean and D.B. Hope, Biochem. J. 106 565 (1968)

65. M. Ginsburg, Proc. Roy. Soc. Ser. B 170 27 (1968)

66. H. Lesnik, J.W. Grezek and W.Z. Traczyk, J. Endocrin. 45 83 (1969)

67. N.A. Thorn and J. Warburg, Acta physiol. scand. 76 31 A (1969)

68. A.L. Kleinhaus and R.Y. Kao, J. Gen. Physiol. 53 758 (1969)

69. S. Varma, B.P. Jaju and K.P. Bhargana, Circ. Res. 24 787 (1969)

70. M. Barraclough, J. Gerignard, N.F. Jones, C. Knight, M. Muirhead-Allwood and M. Reid, J. Physiol. 203 71 P (1969)

71. J. Rider and S. Thomas, J. Physiol. 203 72 P (1969)

72. D.R. Di Bona, N.C. Civan and A. Leaf, J. Memb. Biol. 1 79 (1969)

73. D.H. Spackamnn, W.H. Stein and S. Moore, Anal. Chem. 30 1190 (1958)

74. M. Manning, T.C. Wuu and J.W.M. Baxter, J. Chromatog. 38 396 (1968)

75. C.E. Johnson and F.A. Bovey, J. Chem. Phys. 29 1012 (1958)

76. L.F. Johnson, I.L. Schwartz and R. Walter, Proc. Natl. Acad. Sci. 64 1269 (1969)

77. D.W. Urry, M. Ohnishi and R. Walter, Proc. Natl. Acad. Sci. 66 111 (1970)

78. D.W. Urry and R. Walter, Proc. Natl. Acad. Sci. 68 956 (1971)

79. A.D. Rudko, F.M. Lovell and B.W. Low, Nature New Biology 232 18 (1971)

80. R. Walter, I.L. Schwartz, J.H. Darnell and D.W, Urry, Proc. Natl. Acad. Sci. 68 1355 (1971)

81. R. Walter, Structure-Activity Relationships of Proteins and Polypeptide Hormones. Part I p.181 Excerpta Medica 1971.

82. P.H. Von Dreele, A.I. Brewster, H.A. Scheraga, M.F. Ferger and V. du Vigneaud, Proc. Natl. Aced. Sci. 68 1028 (1971)

83. J. Feeney, G.C.K. Roberts, J.H. Rockey and A.S.V. Burgen, Nature New Biology 232 108 (1971)

84. L.O. Uttental and D.B. Hope, Biochem. J. 116 899 (1970)

85. L. Ornstein, Ann. N.Y. Acad. Sci. 121 321 (1969)

86. B.J. Davis, Ann. N.Y. Acad. Sci. 121 404 (1964)

87. M.L. Rennels, Endocrin. 78 659 (1966)

88. A.M. Crestfield, S. Moore and W.H. Stein, J. Biol. Chem. 238 622 (1963)

89. L.O. Uttental and D.B. Hope, Biochem. J. 116 899 (1970)

90. T.C. Wuu, S. Crumm and M. Saffran, J. Biol. Chem. 244 482 (1969)

91. T.C. Wuu, S. Crumm and M. Saffran, J. Biol. Chem. 246 6043 (1971)

92. M. Ginsburg and P.J. Thomas, J. Physiol. 201 181 (1969)

93. R. Deslauriers and I.C.P. Smith, Biochem. Biophys. Res. Comm. 40 171 (1970)

94. R. Walter, D.H. Schlesinger, I.L. Schwartz and J.D. Capra, Biochem. Biophys. Res. Comm. 44 293 (1971)

CHAPTER 7

^{13}C NMR STUDIES ON OXYTOCIN AND RELATED PEPTIDES.

CHAPTER 7.

^{13}C NMR STUDIES ON OXYTOCIN AND RELATED PEPTIDES.

7.1 Introduction

Only recently has ^{13}C NMR spectroscopy been used to study the structure and conformation of biomolecules. The main reason for this is the low natural abundance of ^{13}C (1.1%). Another reason is the low sensitivity of ^{13}C (1.59×10^{-2}) as compared to ^{1}H (1.00), at the same field strength. This is due to the small magnetogyric ratio of ^{13}C.

Advances in commercially available instrumentation have contributed to widespread use of ^{13}C NMR spectroscopy in organic chemistry. ^{13}C NMR spectroscopy (cmr) is an attractive method for conformational studies because direct observation of the backbone carbons in organic molecules is possible.

Pulse Fourier transform NMR spectroscopy has greatly reduced the time required to obtain spectra of compounds containing only natural abundance ^{13}C. A good textbook on pulse and Fourier transform NMR spectroscopy has been written by T. Farrar and E.D. Becker (1).

^{13}C NMR spectroscopy is proving useful in

In structural identification of large molecules. This is because ^{13}C resonances occur over 200 ppm whereas ^{1}H resonances generally range over 10 ppm. This means resonances of macromolecules will be more widely spaced in ^{13}C spectra than in ^{1}H spectra.

A number of techniques used in obtaining ^{13}C spectra differ from those used in ^{1}H NMR spectroscopy. This results in ^{13}C spectra which differ from ^{1}H spectra in certain characteristic ways. Because ^{13}C-^{1}H geminal couplings are very large (100-250 Hz) a great extent of overlap in the various ^{13}C multiplets occurs. In order to simplify spectra, all the protons are simultaneously decoupled. This results in a single resonance line for each nonequivalent ^{13}C nucleus and it also increases the sensitivity. The intensity of the resonance lines increases further by a so called nuclear Overhauser effect (2). This effect is the result of a change in the ^{1}H spin populations caused by the decoupling field. Relaxation of the ^{1}H nuclei changes the spin populations of the ^{13}C nuclei by dipole-dipole interaction and this leads to an increase in the ^{13}C resonances of nuclei which are bonded to protons.

^{13}C-^{13}C couplings are not seen in spectra of compounds with natural abundance ^{13}C because the probability of having two ^{13}C nuclei side by side is only 0.01%.

Information about the number of protons coupled to each ^{13}C nucleus can be obtained by 'off-resonance' decoupling. This eliminates long-range and vicinal couplings. The geminal couplings decrease to 10 - 50 Hz. The spectrum appears to be first order. It is important to mention that the separation between the lines of a multiplet in this case is <u>not</u> a measure of the coupling constant.

A number of review articles and textbooks have appeared which explain these principles and deal with applications of ^{13}C NMR. These are listed in references 3 - 5 at the end of this chapter.

^{13}C NMR is being used to study biosynthetic pathways (6), biological systems such as erythrocyte membranes (7) and biomolecules, with varying degrees of success. The spectra of carbon-13 enriched chlorophylls a and b (8) have been obtained and many of the resonances assigned. Tentative assignment of some of the peaks in the natural abundance ^{13}C spectrum of ribonuclease (9) have been made. Carbon-13 enrichment of amino acids at specific sites in peptides has been used as a means of placing reporter groups in synthetic peptides (10). The use of ^{13}C NMR in structural studies of oligosaccharides has been investigated (11,18).

^{13}C NMR is being used for conformational analysis of nucleic acids and their constituents (12-17).

The ^{13}C spectrum of the decapeptide antibiotic gramicidin S-A in methanol and dimethyl sulfoxide has been analysed by Gibbons et al (19). Assignment of peaks was based on comparison of peak positions with the ^{13}C chemical shifts of the N-acetyl amino acid methyl esters. The peaks in the monomeric spectra were assigned by comparison with those observed for amino acids (20,21) and calculated by Grant's rules (22,23). The carbonyl resonances fell within too narrow a range to be assigned unambiguously. Unfortunately this type of approach can lead to ambiguities if the chemical shift changes when going from monomer to cyclic peptide. Furthermore, little conformational analysis is possible.

Ohnishi et al (24) have analysed the spectra of some free and potassium ion complexed antibiotics. In valinomycin, the carbonyl resonances directly coordinating the potassium ion shift downfield 4 ppm when the complex is formed. Smaller shifts are also observed for the carbons away from the binding site. This is the first observation of the influence of conformational rearrangements on the chemical shift of carbon atoms in peptides.

Our studies were undertaken in order to test the usefulness of ^{13}C NMR spectroscopy in conformational studies on biologically active molecules. It was hoped that hydrogen-bonding and changes in secondary structures could be detected by this form of NMR spectroscopy.

A model for the conformation of oxytocin in DMSO-d_6 solution has been proposed. (This was discussed in detail in 6.2.2) A number of hydrogen bonds are involved in determining the conformation, among these a hydrogen bond has been found between the carbonyl group of cysteine in position 6 and the amide proton of glycine. In this way the terminal tripeptide is folded back onto the ring portion of the molecule.

In these conformational studies it was first essential to assign the resonance peaks of the carbons in the individual amino acids. The next step was to build up an oxytocin molecule from peptides. Changes in spectra, which could not be attributed to the effect of adding an extra amino acid, were sought for conformational information. Large differences in spectra were expected upon ring closure for instance.

7.2 ^{13}C Studies on Oxytocin and Protected Peptides.

Material and Methods.

In order to positively identify all the resonances in oxytocin, protected precursor peptides were examined. Oxytocin, deamino lysine vasopressin and the protected peptides were a gift from Dr. R. Walter (Mt Sinai School of Medecine, City University of New York, N.Y.)

The following peptides were studied:

Z-Pro-Leu-Gly-OEt (I)
97 mg dissolved in 0.4 ml DMSO-d_6

Z-Pro-Leu-Gly-NH_2 (II)
52 mg dissolved in 0.2 ml DMSO-d_6

Z-Cys(Bzl)-Pro-Leu-Gly-NH_2 (III)
98 mg dissolved in 0.4 ml DMSO-d_6

Z-Asn-Cys(Bzl)-Pro-Leu-Gly-NH_2 (IV)
56 mg dissolved in 0.2 ml DMSO-d_6

Z-Gln-Asn-Cys(Bzl)-Pro-Leu-Gly-NH_2 (V)
76 mg dissolved in 0.2 ml DMSO-d_6

Z-Ile-Gln-Asn-Cys(Bzl)-Pro-Leu-Gly-NH_2 (VI)
80 mg dissolved in 0.2 ml DMSO-d_6

Z-Tyr(Bzl)-Ile-Gln-Asn-Cys(Bzl)-Pro-Leu-Gly-NH_2 (VII)
100 mg dissolved in 0.2 ml DMSO-d_6

Z-Cys(Bzl)-Tyr-Ile-Gln-Asn-Cys(Bzl)-Pro-Leu-Gly-NH_2 (VIII)
50 mg dissolved in 0.2 ml DMSO-d_6

Cys-Tyr-Ile-Gln-Asn-Cys-Pro-Leu-Gly-NH_2 (Oxytocin)

40 mg dissolved in 0.2 ml DMSO-d_6

1-deamino
Cys-Tyr-Phe-Gln-Asn-Cys-Pro-Lys-Gly-NH_2 (1-deamino lysine vasopressin)

40 mg dissolved in 0.2 ml DMSO-d_6

Abbreviations

Z	benzyloxycarbonyl
OEt	O-ethyl
Bzl	benzyl
Gly-NH_2	glycinamide
Leu	leucine
Pro	proline
Cys	cysteine
Asn	asparagine
Gln	glutamine
Ile	isoleucine
Tyr	tyrosine
Phe	phenylalanine
Lys	lysine
Cys Cys	cystine

All amino acids are L isomers.

^{13}C spectra were run on a Varian XL-100 spectrometer operating at 25.16 MHz. Spectra were recorded using the pulsed Fourier transform (FT) mode of operation. Dimethyl sulfoxide-d_6, purchased from Merck, Sharp and Dohme of Canada Ltd, was dried over molecular sieves (Linde 3A)

prior to use. Chemical shifts are reported in parts per million (ppm) downfield from external TMS. The computers used in these studies (Varian 620-i and Varian 620-L) allowed acquisition of 4,096 and 8,192 output data points respectively in the transformed spectra. Spectra were obtained with complete proton decoupling.

Results and Discussion.

7.2.1 Amino Acids.

In view of the insolubility of the free amino acids in dimethyl sulfoxide assignment of the ^{13}C resonances from individual amino acids in the tripeptides was done by comparison with the resonance positions from amino acids in neutral D_2O (21,31) and protected amino acids in DMSO-d_6 (30,31).

7.2.2 Peptides.

The assignments of the resonances in peptides I to VIII are given in tables 7.1 to 7.8. A resume of these tables is in table 7.11.

A. Z-Pro-Leu-Gly-OEt (I) and
Z-Pro-Leu-Gly-NH_2 (II)

In peptide I, assignment of the ^{13}C resonances was done by comparison with the chemical shifts observed for individual amino acids in neutral D_2O (21,

31) and protected amino acids in DMSO-d_6 (31). There was no ambiguity in the assignments. When peptide I is converted to peptide II the major changes in chemical shift are in the glycine residue. The α CH_2 group shifts downfield 1.0 ppm while the carbonyl resonance moves downfield 1.2 ppm. This is expected, amino groups exert little effect on the carbonyl shielding whereas formation of a methyl ester causes an upfield shift in the carbonyl shielding (5). The shifts can be as large as 7.0 ppm, the magnitude of the effect does however depend on the solvent (5).

An interesting phenomenon is visible in the proline ^{13}C resonances. Two lines appear for each of the α CH, β CH_2 and δ CH_2 carbons. The γ CH_2 resonance is close to the δ CH_3 resonance of Leu and a second line may or may not be present under the δ CH_3 of Leu. This occurs in both peptides I and II. The presence of two resonances for each carbon suggests a <u>cis</u>-<u>trans</u> isomerism about the NZ-Pro bond. Peptide II has been studied in DMSO-d_6 by Hruby <u>et al</u> (25), using 220 MHz proton magnetic resonance spectroscopy. It was found that <u>cis</u> and <u>trans</u> isomers about the NZ-Pro bond were equally favoured. A 100 MHz proton spectrum was taken of peptide II, it was similar to that reported by

Hruby *et al* (25).

B. Z-Cys(Bzl)-Pro-Leu-Gly-NH_2 (III)
Z-Pro-Leu-Gly-NH_2 (II)

Only one resonance for each carbon of Pro is visible in peptide III. This implies disappearance of *cis-trans* isomerism about the Cys-Pro bond. Hruby *et al* (25) found resonances characteristic of *cis* and *trans* isomers in the peptide SBz-Cys-Pro-Leu-Gly-NH_2. The ratio of *cis* and *trans* isomers was 2:3. The 100 MHz proton NMR spectrum of peptide III showed a total lack of the resonances characteristic of the *cis* isomer.

Assignment of the ^{13}C resonances due to *cis* and *trans* isomers of Pro should be possible. Unfortunately peptides II and III are not the ideal model compounds because chemical shift changes occur when peptide II is converted into peptide III. Normally a 2.0 - 2.4 ppm upfield shift occurs in the α CH resonance as the benzyloxycarbonyl protecting group is replaced by an N terminal amino acid. This is not observed in Pro. Changes in the chemical shifts of the β CH_2 and γ CH_2 are larger than expected for this amino acid. This may reflect the greater conformational strain present in a Pro residue, as compared to an acyclic amino acid, when an amino acid is attached to the N terminus. It may however, in this case, represent a specific effect

due to addition of a Cys residue to the N terminus.

G. Levy and C. Nelson (26) have studied the ^{13}C spectra of aliphatic amides and found chemical shift differences between aliphatic carbons cisoid to the carbonyl group and those transoid to the carbonyl group. Spectra of neat N-N dimethylformamide reveal a 5.1 ppm difference between the two CH_3 resonances. The high field resonance is attributed to the CH_3 group cisoid to the carbonyl. In N-methylformamide, when the CH_3 group eclipses the carbonyl group it is 3.4 ppm to higher field than when it eclipses the formyl proton. In N,N-di-n-butylformamide, the resonances corresponding to the α, β, γ and δ carbons cisoid to the oxygen are upfield from those of the same carbons transoid to the oxygen.

Based on these findings, an α carbon cis to the carbonyl in Pro (trans Pro) would be to high field from an α carbon trans to the carbonyl (cis Pro). Following this argument a δ carbon trans to the carbonyl group in Pro (trans Pro) would be to low field from a δ carbon cis to the carbonyl (cis Pro). A cis α carbon and a trans δ carbon should occur in a trans Pro. A trans α carbon and a cis δ carbon will occur in a cis Pro. If a mixture of cis and trans Pro

occurs, there should be an equal amount of cis α and trans δ carbons. If the cis and trans carbons have the same relaxation times and equal nuclear Overhauser enhancement, the intensity of the ^{13}C resonance lines should give a measure of the rotamer populations.

Deber et al (27), using 220 MHz proton NMR spectroscopy, have found that α hydrogen nuclei in oligo and poly-L-proline chains give rise to seperate resonances for trans and cis peptide bonds. In polyproline, the low field peak of the two αCH resonances corresponds to the cis Pro (trans αCH-carbonyl). When polyproline in deuterochloroform or ethanol undergoes transition from the all cis to the all trans form, 220 MHz spectra not only show changes in the α proton region but also in the β, γ and δ proton regions. The β protons move upfield, the α and γ protons move downfield. This implies reverse assignments for α and β protons in cis and trans forms of Pro. Glycyl-proline (t-butyloxycarbonyl-Gly-Pro-OBz and t-butyl-oxycarbonyl-Gly-Pro-OH) in DMSO-d_6 is mainly in the trans form (70-80%). The upfield resonance of the α CH resonances corresponds to the trans Gly-Pro bond.(α carbon cis to the carbonyl group). Proline oligomers (dipeptide to hexapeptide) in chloroform were also studied. The di-, tri- and tetrapeptides contain

appreciable amounts of both cis and trans peptide bonds. In the pentapeptide, all residues except the N terminus are entirely trans. The same phenomenon is present in the hexamer.

Based on the above findings a tentative assignment of the Pro resonances is as follows: the high field α CH proton and the low field δ CH_2 resonance are from the trans Pro, the low field β CH_2 resonance may be from the trans Pro (this assignment is more speculative than the other two.)

It has been postulated (25) that an interaction occurs between the lone pair on the sulfur and the carboxamide $-NH_2$ in the tetrapeptide. Since no changes, other than in the Pro residue, are seen when going from peptide II to peptide III, the ^{13}C spectra provide no evidence for such interaction.

C. Z-Asn-Cys(Bzl)-Pro-Leu-Gly-NH_2 (IV)
Z-Cys(Bzl)-Pro-Leu-Gly-NH_2 (III)

When an Asn residue is added to III changes are seen in the Cys residue. The ^{13}C resonance of the carbonyl group in Cys moves upfield 0.5 ppm, the α carbon moves upfield 1.8 ppm. These changes are expected. Only one resonance for the the carbonyl carbons of Asn is observed, it is broader and more intense than the other carbonyl carbon resonances. The same phenomenon

occurs in the protected amino acid (31). In oxytocin (28), the γ carbonyl group is hydrogen-bonded to the Leu NH proton, this however may be present only in the cyclic nonapeptide.

D. Z-Gln-Asn-Cys(Bzl)-Pro-Leu-Gly-NH_2 (V)
and Z-Asn-Cys(Bzl)-Pro-Leu-Gly-NH_2 (IV)

The Asn residue in V has undergone the largest changes. The α carbon moves upfield 2.0 ppm, the β carbon moves upfield 0.3 ppm and the carbonyl carbon moves downfield 0.2 ppm. The Gln residue, unlike the Asn, shows two peaks in the carbonyl region. The low field peak is assigned to the δ carbonyl carbon. Again this is not unexpected, Asn free amino acid (in D_2O) carbonyl resonances are separated by 1.2 ppm while the carbonyl resonances in Gln (free amino acid in D_2O) are separated by 3.6 ppm.

E. Z-Ile-Gln-Asn-Cys(Bzl)-Pro-Leu-Gly-NH_2 (VI)
and Z-Gln-Asn-Cys(Bzl)-Pro-Leu-Gly-NH_2 (V)

The α carbon on Gln in peptide moves upfield 2.4 ppm and the β carbons moves downfield 0.3 ppm. No changes are seen in the Gln carbonyl carbon resonances. The carbonyl carbons of Asn move back upfield 0.2 ppm.

F. Z-Tyr(Bzl)-Ile-Gln-Asn-Cys(Bzl)-Pro-Leu-Gly-NH_2 (VII)
and Z-Ile-Gln-Asn-Cys(Bzl)-Pro-Leu-Gly-NH_2 (VI)

In VII, the α carbon of Ile moves upfield 2.4 ppm. The β CH_2 and the δ CH_2 move downfield 0.1 ppm. The carbonyl carbon shifts downfield 0.3 ppm. It appears that one of the Asn carbonyl carbon resonances moves upfield 0.3 ppm. In oxytocin (28), the NH of Asn is hydrogen bonded to the oxygen of the carbonyl group in Tyr. In 1-deamino oxytocin (29), the oxygen of the carbonyl group in Asn is hydrogen-bonded to the NH of Tyr. Again this type of interaction may require the constraints produced by ring closure of the nonapeptide.

G. Z-Cys(Bzl)-Tyr-Ile-Gln-Asn-Cys(Bzl)-Pro-Leu-Gly-NH_2 (VIII)
and Z-Tyr(Bzl)-Ile-Gln-Asn-Cys(Bzl)-Pro-Leu-Gly-NH_2 (VII)

The α CH resonance of Tyr moves upfield 2.4 ppm A number of changes occur in the carbonyl region and only tentative line assignments can be made, however specific amino acid substitution or ^{13}C enrichment of the nonapeptide would permit unambiguous assignment. The largest shifts in the carbonyl region are about $\pm$ 0.2 ppm.

These studies on protected peptides have shown that lines can be assigned to individual carbons in amino acids by building up peptides one residue at a time. When an N terminal amino acid is added to an NZ

protected peptide the largest changes in chemical shift occur in the penultimate amino acid. The α carbon resonance usually shifts upfield 2.0 to 2.4 ppm. No changes were seen in the other amino acids. Cis and trans isomers of Pro can be seen. Pro was anomalous with respect to the α carbon chemical shift upon addition of a Cys residue, it did not shift upfield.

7.2.3 Oxytocin and Deamino Lysine Vasopressin.(Fig. 7.1, 7.2)

When the protected nonapeptide (VIII) is deprotected and cyclized to form oxytocin a number of spectral changes are seen, the largest being in the α carbon and carbonyl carbon resonances.(Tables 7.9 and 7.11)

The α carbon resonances in the ring move downfield while the β carbon resonances move upfield. This is not the case for either the Leu or Gly residues of the terminal tripeptide. Changes in the Pro resonances are less than 0.2 ppm. The amino acids most affected by ring closure are Cys, Gln and Ile. In Gln and Ile, the α carbon resonances are shifted downfield 1.8 and 1.9 ppm while the β carbon resonances are shifted upfield 1.2 and 0.6 ppm respectively. Asn and Tyr show smaller but significant shifts. In these amino acids, th the α carbon resonances shift upfield 0.7 and 0.6 ppm. The β-carbon resonances shift downfield 0.2 and 0.8 ppm respectively.

The β carbon resonances of Cys appear to move downfield as the ring is closed (4.4 ppm). The ^{13}C signal of the β carbon of Cys in glutathione shifts downfield 13 ppm upon oxidation to cystine in oxidized glutathione (in D_2O). The α carbon shifts upfield 3 ppm in this compound (30). In oxytocin, the α carbon of Cys-6 moves

Figure 7.1

CMR spectrum of oxytocin taken at 25.2 MHz

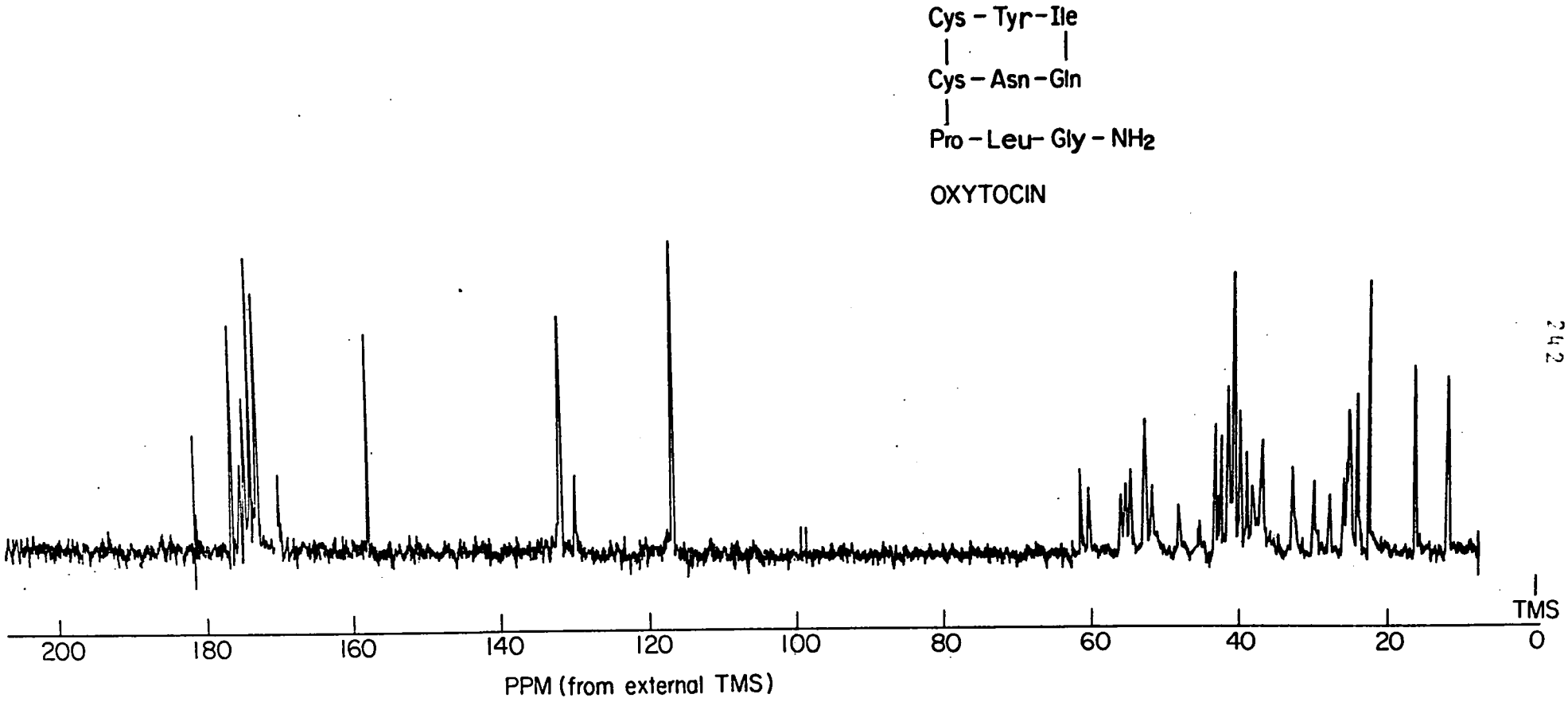
Cys – Tyr – Ile
Cys – Asn – Gln
Pro – Leu – Gly – NH2
OXYTOCIN
TMS
200
180
160
140
120
100
80
60
40
20
0
PPM (from external TMS)

downfield 2.7 ppm and that of Cys-1 moves upfield 4.6 ppm.

It is not possible to assign all the carbonyl carbon resonances of oxytocin using the above approach. It can be seen that the carbonyl carbon of Cys-6 moves upfield 1.1 ppm upon ring closure. The δ carbonyl carbon of Gln did not change. In general, the carbonyl region in oxytocin is similar to that of the protected nonapeptide except that two resonances have moved to lower field. This type of shift is expected when hydrogen bonds occur but until studies are made on oxytocin analogues no definite conclusions can be drawn.

Deamino Lysine Vasopressin. (Fig. 7.2) (Tables 7.10 and 7.11)

The spectrum of deamino lysine vasopressin was taken and compared with that of oxytocin in order to assign the resonances of amino acids common to both compounds. The other resonances were assigned by comparison with the free amino acid resonances and are therefore more subject to error than the resonances in oxytocin. In the cyclic moiety little difference is observed in the α carbon resonances of Gln (-0.1 ppm) and Tyr residues (-0.2 ppm) in both compounds, nor in the β CH_2 resonances of Asn. The Asn α CH moves downfield 0.5

Figure 7.2

CMR spectrum of 1-deamino lysine vasopressin taken at 25.2 MHz.

H Cys – Tyr – Phe
| |
Cys – Asn – Gln
|
Pro – Lys – Gly – NH_2

1-DEAMINO LYSINE VASOPRESSIN

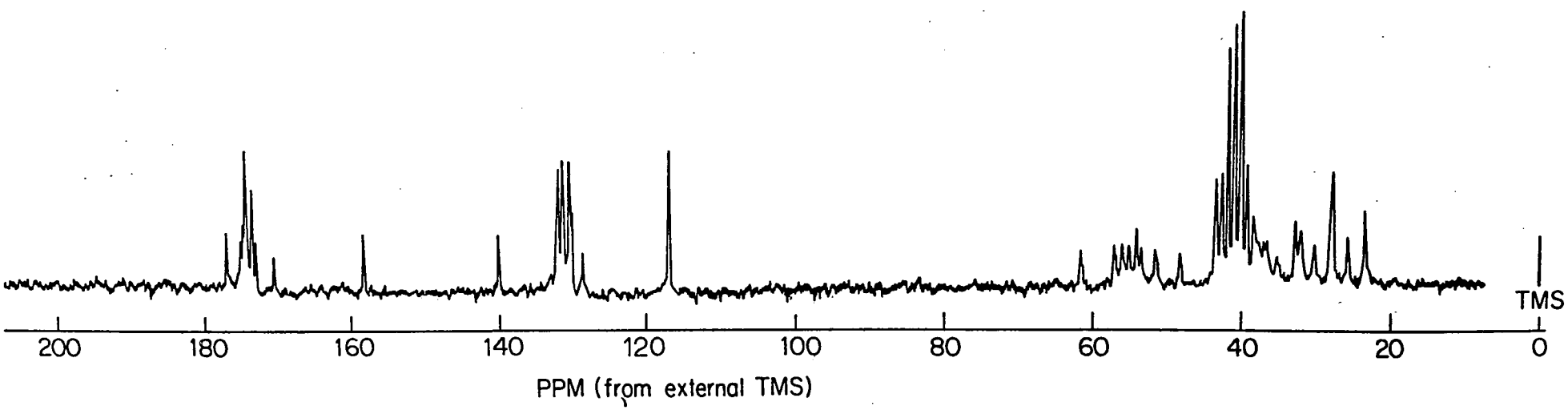

ppm and the Cys-6 α CH moves upfield 0.8ppm. In deamino vasopressin, the α carbon of Cys-1 is to high field of that in oxytocin due to absence of an N terminal amino group. This group is more similar to a γ CH_2 group in Gln and the α CH_2 of Cys-1 is found near the γ CH_2 of Gln.

7.4 Conclusion.

In linear peptides, ^{13}C resonance lines can be assigned to individual amino acids by building up peptides residue per residue. In protected peptides the largest changes caused by addition of an N terminal amino acid occur in the α carbon of the penultimate amino acid. The α carbon resonance usually moves upfield 2.0 - 2.4 ppm. Small changes also occur in the β carbon resonances. Cis and trans isomers of Pro give rise to distinct ^{13}C resonances.

When a protected linear peptide corresponding to the oxytocin sequence is deprotected and cyclized to form oxytocin a number of changes are seen in the α carbon resonances. The α carbon resonances of the cyclic moiety shift downfield and the β carbons move upfield slightly. Only small changes (less than 0.2 ppm) are seen in the resonances of the Pro residue. No changes are seen in the Leu and Gly-NH_2 resonances. The ^{13}C spectrum of oxytocin does not therefore show any conformational change in the terminal tripeptide when going from the acyclic protected nonapeptide to oxytocin.

In oxytocin, cis:trans isomers can occur about the Cys-Pro amide bond. Only the trans isomer occurs in oxytocin. Only the trans isomer is present in all

protected peptides larger than 11.

Oxidation of Cys residues produces dramatic changes in the ^{13}C spectra of the α and β carbon resonances (30). Similar changes are seen when 2 Cys(Bzl) are linked to form a Cys-Cys residue.

The Pro and Gly-NH_2 residues of the terminal tripeptide have the same chemical shifts in oxytocin and deamino lysine vasopressin, ^{13}C NMR does not reveal any difference in the conformation of the tri-terminal tripeptides in the two hormones.

Unambiguous assignment of the carbonyl resonances in cyclic peptides will require the study of cyclic analogues. The major differences in the carbonyl regions of the protected nonapeptide and oxytocin occur in only two resonances which are shifted downfield slightly. In deamino lysine vasopressin only one resonance is at lower field.

Continuing this series of investigations, it would be of interest to study deprotected water-soluble peptides. This could yield information about conformation differences or similarities in precursor peptides and hormones such as oxytocin and vasopressin.

Preliminary studies on hydrogen-bonded base pairs of cytidine and guanosine in dimethyl sulfoxide have shown only small changes in the hydrogen-bonded carbonyl

carbons.(+0.4 ppm). Small changes can also be seen in the other base carbons, these changes may prove useful in determining the absence or presence of hydrogen bonds in nucleosides. In order to measure hydrogen bonds in peptides it would be necessary to make accurate assignments of the carbonyl carbons in view of the magnitude of the shifts seen in nucleosides.

Tables 7.1

7.2

7.3

7.4

7.5

7.6

7.7

7.8

Chemical shift and line assignments of the ^{13}C resonances of protected precursor peptides of oxytocin in DMSO. Spectra were taken at 25.2 MHz using the Fourier transform mode of operation. The ^{13}C-^{1}H couplings have been removed by noise-decoupling. Data is taken from 5 KHz scans, 1 KHz scans were taken in the carbonyl region. Chemical shifts are reported in ppm downfield from external TMS. Probe temperature was 37°C. Samples were run in 5 mm tubes. Usually 15,000 transients were sufficient to obtain spectra with more than 3:1 signal-to-noise ratios.

Table 7.1

Z-Pro-Leu-Gly-OEt (I)

Chemical Shift	Intensity	Assignment	
174.09	63	Leu	C=O
173.20	15	Pro	C=O
171.13	51	Gly	C=O
138.59	52	NZ	C_1
129.77	55	NZ	Aromatic
128.97	42	NZ	Aromatic
128.48	25	NZ	Aromatic
68.37	42	NZ	CH_3
61.88	77	OEt	CH_2
61.47	21	Pro	α CH
60.69	30	Pro	α CH
52.34	71	Leu	α CH
48.69	24	Pro	δ CH_2
48.17	15	Pro	δ CH_2
42.81	21	DMSO	CH_3
42.53	57	Gly	α CH_2
42.33	101	Leu	β CH_2
42.01	35	DMSO	CH_3
41.22	26	DMSO	CH_3
40.34	28	DMSO	CH_3
39.55	13	DMSO	CH_3
32.79	30	Pro	β CH_2
31.47	18	Pro	β CH_2
25.64	90	Leu	γ CH
25.23	11	Pro	γ CH_2
24.44	75	Leu	δ CH_3
23.13	100	Leu	δ CH_3
15.58	88	OEt	CH_3

Table 7.2

Z-Pro-Leu-Gly-NH_2 (II)

Chemical Shift	Intensity	Assignment	
173.97	48	Pro	C=O
173.77	106	Leu	C=O
172.38	62	Gly	C=O
155.40	15	NZ	C=O
138.51	63	NZ	C_1
129.85	120	NZ	Aromatic C_2, C_6
129.05	102	NZ	Aromatic C_3, C_5
128.46	60	NZ	Aromatic C_4
67.47	64	NZ	CH_2
61.61	41	Pro	α CH
60.61	48	Pro	α CH
53.06	179	Leu	α CH
48.69	59	Pro	δ CH_2
48.17	44	Pro	δ CH_2
43.52	146	Gly	α CH_2
42.81	27	DMSO	CH_3
42.01	108	DMSO	CH_3
41.73	60	Leu	β CH_2
41.41	42	DMSO	CH_3
40.34	52	DMSO	CH_3
39.55	15	DMSO	CH_3
32.67	56	Pro	β CH_2
31.48	35	Pro	β CH_2
25.72	183	Leu	γ CH
25.52	62	Pro	γ CH_2
24.52	214	Leu	δ CH_3
23.13	160	Leu	δ CH_3

Table 7.3

Z-Cys(Bz)-Pro-Leu-Gly-NH_2 (III)

Chemical Shift	Intensity	Assignment	
173.69	26	Leu	C=O
173.09	22	Pro	C=O
172.38	34	Gly	C=O
171.10	41	Cys	C=O
139.98	40	SBz	C_1
138.51	15	NZ	C_1
130.44	133	SBz	Aromatic
129.96	209	NZ, SBz	Aromatic
129.52	135	NZ	Aromatic
128.38	51	NZ	Aromatic
128.18	12	SBz	Aromatic
67.25	63	NZ	CH_2
61.49	67	Pro	αCH
54.13	47	Cys	αCH
53.06	75	Leu	αCH
48.49	52	Pro	δ CH_2
43.60	84	Gly	α CH_2
42.93	14	DMSO	CH_3
42.01	46	DMSO	CH_3
41.73	71	Leu	β CH_2
41.22	41	DMSO	CH_3
40.34	33	DMSO	CH_3
39.55	16	DMSO	CH_3
37.36	93	Cys	β CH_2
34.28	58	SBz	CH_2
30.41	57	Pro	β CH_2
26.03	79	Pro	γ CH_2
25.84	112	Leu	γ CH
24.52	61	Leu	δ CH_3
23.13	117	Leu	δ CH_3

Table 7.4

Z-Asn-Cys(Bzl)-Pro-Leu-Gly-NH_2 (IV)

Chemical shift	Intensity	Assignment	
173.69	79	Leu	C=O
173.09	55	Pro	C=O
172.77	65	Asn	C=O
172.50	37	Gly	C=O
170.59	39	Cys	C=O
157.27	32	NZ	C=O
139.98	56	SBz	C_1
138.51	43	NZ	C_1
130.56	200	SBz	Aromatic
129.85	209	NZ, SBz	Aromatic
129.17	93	NZ	Aromatic
128.38	86	NZ, SBz	Aromatic
67.17	79	NZ	CH_2
61.49	61	Pro	α CH
53.34	53	Asn	α CH
53.06	72	Leu	α CH
52.27	55	Cys	α CH
48.57	40	Pro	δ CH_2
43.60	83	Gly	α CH_2
42.80	28	DMSO	CH_3
42.01	60	DMSO	CH_3
41.81	74	Leu	β CH_2
41.14	55	DMSO	CH_3
40.34	63	DMSO	CH_3
39.55	25	DMSO	CH_3
39.03	54	Asn	β CH_2
37.24	89	Cys	β CH_2
34.18	46	SBz	CH_2
30.84	54	Pro	β CH_2
26.03	80	Pro	γ CH_2
25.85	107	Leu	γ CH_2
24.52	111	Leu	δ CH_3
23.13	149	Leu	δ CH_3

Table 7.5

Z-Gln-Asn-Cys(Bzl)-Pro-Leu-Gly-NH_2 (V)

Chemical shift	Intensity	Assignment	
175.48	30	Gln	δ C=O
173.69	40	Leu	C=O
173.17	38	Pro	C=O
172.97	56	Asn	C=O
172.50	41	Gly	C=O
172.30	18	Gln	C=O
170.59	27	Cys	C=O
140.10	26	SBz	C_1
138.51	24	NZ	C_1
130.56	110	SBz	Aromatic
129.97	153	NZ,SBz	Aromatic
129.25	74	NZ	Aromatic
128.38	45	NZ,SBz	Aromatic
67.17	53	NZ	CH_2
61.61	26	Pro	α CH
56.12	29	Gln	α CH
53.06	35	Leu	α CH
52.34	27	Cys	α CH
51.27	30	Asn	α CH
48.57	21	Pro	δ CH_2
43.60	44	Gly	α CH_2
42.81	25	DMSO	CH_3
42.01	45	DMSO	CH_3
41.81	32	Leu	β CH_2
41.14	42	DMSO	CH_3
40.34	49	DMSO	CH_3
39.55	15	DMSO	CH_3
38.63	28	Asn	β CH_2
37.24	56	Cys	β CH_2
33.98	24	SBz	CH_2
33.07	52	Gln	γ CH_2
30.48	31	Pro	β CH_2
29.29	30	Gln	β CH_2
26.03	42	Pro	γ CH_2

Table 7.5 (continued)

Chemical shift	Intensity	Assignment
25.83	55	Leu γ CH
24.52	80	Leu δ CH_3
23.13	78	Leu δ CH_3

Table 7.6

Z-Ile-Gln-Asn-Cys(Bzl)-Pro-Leu-Gly-NH_2 (VI)

Chemical shift	Intensity	Assignment	
176.56	16	Gln	C=O
173.69	38	Leu	C=O
173.09	24	Pro	C=O
172.77	66	Asn	C=O
172.50	52	Ile	C=O
172.50	52	Gly	C=O
172.30	47	Gln	C=O
170.59	34	Cys	C=O
157.67	15	NZ	C=O
140.10	26	SBz	C_1
138.59	30	NZ	C_1
130.56	126	SBz	Aromatic
129.97	129	NZ,SBz	Aromatic
129.25	65	NZ	Aromatic
128.38	49	NZ,SBz	Aromatic
67.05	33	NZ	CH_2
61.61	32	Pro	α CH
60.89	32	Ile	α CH
53.74	22	Gln	α CH
53.06	42	Leu	α CH
52.30	32	Cys	α CH
51.27	28	Asn	α CH
48.57	25	Pro	δ CH_2
43.60	61	Gly	α CH_2
42.81	34	DMSO	CH_3
42.01	66	DMSO	CH_3
41.41	18	Leu	β CH_2
41.14	66	DMSO	CH_3
40.34	64	DMSO	CH_3
39.55	27	DMSO	CH_3
38.63	37	Asn	β CH_2
38.04	42	Ile	β CH
37.24	64	Cys	β CH_2
34.06	24	SBz	CH_2

Table 7.6 (continued)

Chemical shift	Intensity	Assignment
32.99	28	Gln γ CH_2
30.48	36	Pro β CH_2
29.61	17	Gln β CH_2
26.03	84	Pro α CH_2
26.03	84	Ile α CH_2
25.83	72	Leu α CH
24.52	93	Leu δ CH_3
23.13	85	Leu δ CH_3
16.97	42	Ile γ CH_3
12.52	53	Ile δ CH_3

Table 7.7

Z-Tyr(BzO)-Ile-Gln-Asn-Cys(BzO)-Pro-Leu-Gly-NH_2 (VII)

Chemical shift	Intensity	Assignment	
175.68	31	Gln	C=O
173.69	31	Leu	C=O
173.47	32	Pro	C=O
172.89	31	Asn*Tyr*	C=O
172.57	63	Asn*Gly	C=O
172.30	30	Gln	C=O
172.30	30	Ile	C=O
170.75	18	Cys	C=O
158.59	27	Tyr	C_4 (para)
140.10	17	SBz	C_1
138.59	22	NZ	C_1
131.83	78	Tyr	C_2, C_6 (ortho)
130.56	81	SBz	Aromatic
129.97	152	SBz, NZ	Aromatic
129.17	124	NZ	Aromatic
128.97	59	Tyr	C_1
128.38	34	NZ, SBz	Aromatic
115.94	53	Tyr	C_3, C_5 (meta)
70.83	36	OBz	CH_2
66.85	27	NZ	CH_2
61.61	16	Pro	α CH
58.50	23	Ile	α CH
57.90	13	Tyr	α CH
53.98	14	Gln	α CH
53.06	21	Leu	α CH
52.46	16	Cys	α CH
51.35	17	Asn	α CH
48.57	11	Pro	δ CH_2
43.72	26	Gly	α CH_2
42.81	22	DMSO	CH_3
41.93	49	Leu	β CH_2
41.14	54	DMSO	CH_3
40.34	39	DMSO	CH_3
39.43	22	DMSO	CH_3
38.63	24	Asn	β CH_3

Table 7.7 (continued)

Chemical shift	Intensity	Assignment	
38.24	36	Ile	CH_2
38.24	36	Tyr	CH_2
37.36	38	Cys	CH_2
34.06	19	SBz	CH_2
33.07	30	Gln	CH_2
30.48	17	Pro	CH_2
29.61	20	Gln	CH_2
26.03	48	Ile	CH_2
26.03	48	Pro	CH_2
25.83	51	Leu	CH
24.52	58	Leu	CH_3
23.13	60	Leu	CH_3
16.97	53	Ile	CH_3
12.60	33	Ile	CH_3

* Indicates only a tentative assignment.

Table 7.8

Z-Cys(Bzl)-Tyr-Ile-Gln-Asn-Cys(Bzl)-Pro-Leu-Gly-NH_2 (VIII)

Chemical shift	Intensity	Assignment
175.68	34	Gln δ C=O
173.89	34	Leu C=O
172.89	67	Pro, Tyr C=O
172.50	95	Asn, Ile C=O
172.30	68	Gly, Gln C=O
171.74	17	Cys-1 C=O
170.51	34	Cys-6 C=O
157.39	27	Tyr C_4 (para)
139.90	29	SBz C_1
138.51	35	NZ C_1
131.76	61	Tyr C_2, C_6 (ortho)
130.44	133	SBz Aromatic
129.97	255	SBz, NZ Aromatic
129.37	56	NZ Aromatic
129.17	95	Tyr C_1
128.38	113	NZ, SBz Aromatic
116.45	54	Tyr C_3, C_5 (meta)
67.17	51	NZ CH_2
61.47	32	Pro α CH
58.67	18	Ile α CH
55.52	27	Tyr α CH
53.85	28	Gln α CH
53.06	17	Leu α CH
52.27	19	Cys-6 α CH
51.35	19	Asn α CH
50.27	29	Cys-1 α CH
48.57	18	Pro δ CH_2
43.60	45	Gly α CH_2
42.81	42	DMSO CH_3
41.93	61	DMSO CH_3
41.93	61	Leu β CH_2
41.14	99	DMSO CH_3
41.34	70	DMSO CH_3
39.43	33	DMSO CH_3
38.75	25	Asn β CH_2

Table 7.8 (continued)

Chemical shift	Intensity	Assignment
38.18	49	Ile βCH_2
38.18	49	Tyr βCH_2
37.24	67	Cys-6 βCH_2
37.04	75	Cys-1 βCH_2
35.17	37	SBz CH_2
34.06	30	SBz CH_2
33.07	46	Gln βCH_2
30.29	40	Pro βCH_2
29.61	33	Gln γCH_2
25.61	67	Leu γCH
25.61	67	Ile γCH_2
24.52	25	Leu δCH_3
23.13	25	Leu δCH_3
16.97	60	Ile δCH_3
12.60	67	Ile δCH_3

Table 7.9

CMR spectrum of oxytocin (40 mg dissolved in 0.2 ml DMSO). Spectrum was recorded at 25.2 MHz, with proton noise-decoupling. Data is taken from a 5 KHz scan, 1 KHz scans were recorded in the carbonyl region. 84,000 transients were accumulated prior to Fourier transformation. Sample was run in a 5 mm tube. Chemical shifts are reported in ppm downfield from external TMS. The spectrometer was operating at 37°C.

Table 7.9

Cys-Tyr-Ile-Gln-Asn-Cys-Pro-Leu-Gly-NH_2 (Oxytocin)

Chemical shift	Intensity	Assignment	
175.76	86	Gln	δ C=O
174.56	33		
174.15	58		
173.77	41		
173.29	111		
172.97	15		
172.50	98		
172.18	37		
171.90	10		
169.40	29	Cys-6	C=O
169.12	11		
157.39	82	Tyr	C_4 (para)
131.64	86	Tyr	C_2, C_6 (ortho)
129.45	27	Tyr	C_1
116.53	115	Tyr	C_3, C_5 (meta)
61.69	28	Pro	α CH
60.61	20	Ile	α CH
56.24	18	Tyr	α CH
55.64	22	Gln	α CH
54.93	28	Cys-6	α CH
53.06	47	Leu	α CH
52.07	22	Asn	α CH
48.49	14	Pro	α CH
45.69	10	Cys-1	α CH
43.62	44	Gly	α CH_2
43.12	15	Cys-6	β CH_2
42.81	40	DMSO	CH_3
41.93	58	Leu	β CH_2
41.61	33	DMSO	CH_3
41.41	17	Cys-1	β CH_2
41.14	101	DMSO	CH_3
40.34	55	DMSO	CH_3
39.43	34	DMSO	CH_3
38.53	38	Asn	β CH_2
37.56	20	Ile	β CH_2

Table 7.9 (continued)

Chemical shift	Intensity	Assignment
37.36	38	Tyr β CH_2
33.19	28	Gln γ CH_2
30.40	21	Pro β CH_2
28.42	17	Gln β CH_2
26,51	24	Ile γ CH_2
26.03	30	Pro γ CH_2
25.72	50	Leu γ CH_2
24.64	55	Leu δ CH_3
23.13	98	Leu δ CH_3
17.09	66	Ile δ CH_3
12.79	61	Ile δ CH_3

Table 7.10

CMR spectrum of 1-deamino lysine vasopressin (40 mgs dissolved in 0.2 ml DMSO). Spectrum was recorded at 25.2 MHz with proton noise-decoupling. Data is taken from a 5 KHz scan, 1 KHz scans were recorded in the carbonyl region. 112,000 transients were recorded prior to Fourier transformation. Sample was run in a 5 mm tube. Chemical shifts are reported in ppm downfield fron external TMS. The spectrometer was operating at 37°C.

Table 7.10

1-deamino

Cys-Tyr-Ile-Gln-Asn-Cys-Pro-Lys-Gly-NH_2 (1-deamino lysine vasopressin)

Chemical shift	Intensity	Assignment
175.75	22	Gln δ C=O
173.89	19	Lys C=O
173.57	26	Phe* C=O
173.22	53	Asn* C=O
173.22	53	Pro* C=O
172.38	38	Gln* C=O
172.38	38	Gly C=O
171.90	19	Cys-1 C=O
169.40	13	Cys-6 C=O
157.39	22	Tyr C_4 (para)
139.30	21	Phe C_1
131.36	45	Tyr C_2, C_6 (ortho)
130.76	48	Phe C_2, C_6 (ortho)
129.85	48	Phe C_3, C_5 (meta)
129.57	30	Tyr C_1
127.98	13	Phe C_4 (para)
116.53	53	Tyr C_3, C_5 (meta)
61.61	15	Pro αCH
57.11	17	Lys αCH
56.04	16	Tyr αCH
55.13	17	Phe αCH
54.13	22	Cys-6 αCH
53.54	15	Gln αCH
51.55	15	Asn αCH
48.37	13	Pro δCH_2
43.60	41	Gly αCH_2
43.12	13	Cys βCH_2
42.73	43	DMSO CH_3
41.93	90	DMSO CH_3
41.14	100	DMSO CH_3
40.22	104	DMSO CH_3
40.22	104	Lys ϵCH_2
39.43	47	DMSO CH_3
38.54	28	Asn* βCH_2

Table 7.10 (continued)

Chemical shift	Intensity	Assignment
37,84	18	Phe* β CH_2
37.24	17	Cys* β CH_2
36.74	17	Tyr* β CH_2
35.43	12	Cys-1 α CH_2
32.99	26	Gln γ CH_2
32.27	22	Lys β CH_2
30.49	17	Pro β CH_2
28.10	44	Gln β CH_2
28.10	44	Lys δ CH_2
26.03	19	Pro γ CH_2
23.72	31	Lys γ CH_2

* Indicates that only a tentative assignment can be made based on the chemical shifts of amino acids and amino acid derivatives.

Table 7.11

This table summarizes the data contained in Tables 7.1 to 7.10 inclusively.

Table 7.11

Peptide		I	II	III	IV	V	VI	VII	VIII	Oxyt.	1d-LVP
Gly	αCH_2	42.53	43.52	43.60	43.60	43.60	43.60	43.72	43.60	43.62	43.60
	C=O	171.18	172.42	172.46	172.46	172.46	172.46	172.50	172.50*		172.42
Leu	α CH	52.34	53.06	53.06	53.06	53.06	53.06	53.06	53.06	53.06	
	βCH_2	42.33	41.73	41.73	41.81	41.81	42.01	41.93	41.93	41.93	
	γ CH	25.64	25.72	25.84	25.85	25.83	25.83	25.83	25.91	25.72	
	δCH_3	24.44	24.52	24.52	24.52	24.52	24.52	24.52	24.52	24.64	
	δCH_3	23.13	23.13	23.13	23.13	23.13	23.13	23.13	23.13	23.13	
	C=O	174.09	173.77	173.65	173.65	173.69	173.65	173.65	173.89	173.77	
Pro	α CH	61.47 60.69	61.61 60.61	61.49	61.49	61.61	61.61	61.61	61.47	61.69	61.61
	βCH_2	32.79 31.47	32.67 31.48	30.41	30.48	30.48	30.48	30.48	30.29	30.40	30.49
	γCH_2	25.23	25.52	26.03	26.03	26.03	26.03	26.03	25.91	26.03	26.03
	δCH_2	48.69 48.17	48.69 48.17	48.49	48.57	48.57	48.57	48.57	48.57	48.49	48.37
	C=O	173.29	173.09	173.13	173.13	173.17	173.13	173.13	173.01*		173.22
Cys	α CH			54.13	52.27	52.34	52.36	52.46	52.27	54.93	54.13
	βCH_2			37.36	37.24	37.24	37.24	37.36	37.24	41.61	43.12
	C=O			171.06	170.63	170.59	170.59	170.63	170.51	169.40	169.43
Asn	α CH				53.35	51.27	51.27	51.35	51.35	52.07	51.55
	βCH_2				39.03	38.63	38.63	38.63	38.75	38.53	38.54
	γ C=O				172.85	173.01	172.85	173.01*	172.50*		
	C=O				172.85	173.01	172.85	172.81*	172.89*		173.22

Table 7.11 (continued)

Peptide		I	II	III	IV	V	VI	VII	VIII	Oxyt	1d-LVP
Gln	α CH					56.12	53.74	53.74	53.85	55.64	53.54
	β CH_2					29.29	29.61	29.61	29.61	28.41	28.10
	γ CH_2					33.07	32.99	33.07	33.07	33.19	32.99
	δ C=O					175.52	175.56	175.76	175.60	175.76	175.65
	C=O					172.34	172.30	172.30	172.30		172.34*
Ile	α CH						60.89	58.50	58.67	60.61	
	β CH						38.04	38.24	38.16	37.56	
	γ CH_2						26.03	26.03	25.91	26.01	
	γ CH_3						16.97	16.97	16.97	17.09	
	δ CH_3						12.53	12.60	12.60	12.79	
	C=O						172.54	172.81	172.38*		
Tyr	α CH							57.90	55.52	56.24	56.04
	β CH							38.24	38.16	37.36	36.74
	C_4							158.59	157.39	157.39	157.39
	C_2, C_6							131.83	131.76	131.64	131.36
	C_1							128.97	129.17	129.45	129.57
	C_3, C_5							115.94	116.45	116.53	116.53
	C=O							173.25	173.13*		
Cys	α CH								50.27	45.69	35.43
	β CH_2								37.04	41.41	42.73
	C=O								171.74		171.94*
Lys	α CH										57.11
	β CH_2										32.27
	γ CH_2										23.72
	δ CH_2										28.10
	ε CH_2										40.22
	C=O										173.89

Table 7.11 (continued)

Peptide		I	II	III	IV	V	VI	VII	VIII	Oxyt	1d-LVP
Phe	α CH										55.13
	C_1										139.30
	C_2, C_6										130.76
	C_3, C_5										129.85
	C_4										127.08
	C=O										173.57
NZ	C_1	138.59	138.51	138.51	138.51	138.51	138.58	138.59			
	C_2, C_6	129.77	129.85	129.52	129.85	129.97	129.97	129.97			
	C_3, C_5	128.97	129.05	128.38	129.17	129.25	129.25	129.17			
	C_4	128.48	128.46	128.18	128.38	128.38	128.38	128.38			
	CH_2	68.37	67.45	67.25	67.17	67.05	66.85	67.17			
SBz	CH_2			38.38	34.18	33.98	34.06	34.06	34.06		
	Arom			139.98	139.98	140.10	140.10	140.10			
	Arom			130.44	130.56	130.56	130.56	130.56			
	Arom			129.96							
OEt	CH_2	61.88									
	CH_3	15.58									
DMSO		42.81	41.81	42.93	42.81	42.81	42.81	42.81	42.81	42.81	42.93
		42.01	42.01	42.01	42.01	42.01	42,01	41.93	41.93	41.93	41.93
		41.22	41.14	41.14	41.14	41.14	41.14	41.14	41.14	41.14	41.14
		40.34	40.34	40.34	40.34	40.34	40.34	40.34	40.34	40.34	40.22
		39.55	39.55	39.55	39.55	39.55	39.55	39.43	39.43	39.43	39.43

Table 7.11 (continued)

Peptide		I	II	III	IV	V	VI	VII	VIII	Oxyt	1d-LVP
OBz	CH_2							70.83			
SBz	CH_2								35.17		

7.4 References.

1. T.C. Farrar and E.D. Becker, Pulse and Fourier Transform NMR. Introduction to Theory and Methods, Academic Press, N.Y., 1971.

2. J.H. Noggle and R.E. Schrimer, The Nuclear Overhauser Efffect, Chemical Applications, Academic Press, N.Y., 1971.

3. P.S. Pregosin and E.W. Randall, C-13 Magnetic Resonance Spectroscopy, in Determination of Organic Structures by Physical Methods. Vol 3. ed. F.C. Nachod and J.J. Zuckerman, Academic Press, N.Y. 1972.

4. E. Breitmaier, G. Jung and W. Voelter, Angew. Chem. internat. Edit. 10 673 (1971)

5. J.B Stothers, Carbon-13 NMR Spectroscopy, A.T. Blomquist and H. Wasserman Eds, Academic Press, N.Y., 1972

6. M. Tanabe, H. Seto and L.R. Johnson, J. Amer. Chem. Soc. 92 2157 (1970).

7. J.C. Metcalfe, N.J.M. Birdsall, J. Feeney, A.G. Lee, Y.K. Levine and P. Partington, Nature 233 199 (1971)

8. C.E. Strouse, V.H. Kollman and N.A. Matwiyoff, Biochem. Biophys. Res. Comm. 46 328 (1972)

9. A. Allerhand, D.W. Cochran and D. Doddrell, Proc. Natl. Acad. Sci. U.S.A. 67 1093 (1970)

10. M.H. Freedman, J.S. Cohen and I.M. Chaiken, Biochem. Biophys. Res. Comm. 42 1148 (1971)

11. D.E. Dorman and J.D. Roberts, J. Amer. Chem. Soc. 93 4463 (1971)

12. A.J. Jones, M.W. Winkley, D.M. Grant and R.K. Robins, Proc. Natl. Acad. Sci. U.S.A. 65 27 (1970)

13. D.E. Dorman and J.D. Roberts, Proc. Natl. Acad. Sci. U.S.A. 65 19 (1970)

14. A.L. Jones, D.M. Grant, M.W. Winkley and R.K. Robins, J. Amer. Chem. Soc. 92 4079 (1970)

15. A.R. Tarpley Jr. and J.H. Goldstein, J. Amer. Chem. Soc. 93 3573 (1971)

16. R.U. Lemieux, T.L. Nagabhushan and B. Paul, in press

17. H.H. Mantsch and I.C.P. Smith, Biochem. Biophys. Res. Comm. 46 808 (1972)

18. E. Breitmaier, G. Jung and W. Voelter, Chimia 25 362 (1971)

19. W.A. Gibbons, J.A. Sogn, A. Stern, L.C. Craig, L.F. Johnson, Nature 227 840 (1970)

20. W.J. Horsley and H.J. Sternlicht, J. Amer. Chem. Soc. 90 3738 (1968)

21. W.J. Horsley, H. Sternlicht and J. Cohen, J. Amer. Chem. Soc. 92 680 (1970)

22. D.M. Grant and E.G. Paul, J. Amer. Chem. Soc. 86 2984 (1964)

23. K.F. Kuhlmann and D.M. Grant, J. Amer. Chem. Soc. 90 7355 (1968)

24. M. Ohnishi, M.C. Fedarko, J.D. Baldeschwieler and L.F. Johnson, Biochem. Biophys. Res. Comm. 46 312 (1972)

25. V.J. Hruby, A.I. Brewster and J.A. Glasel, Proc. Natl. Acad. Sci. U.S.A. 68 450 (1971)

26. G.C. Levy and G.L. Nelson, in press

27. C.M. Deber, F.A. Bovey, J.P. Carver and E.R. Blout, J. Amer. Chem. Soc. 92 6191 (1970)

28. D.W. Urry and R. Walter, Proc. Natl. Acad. Sci. U.S.A. 68 956 (1971)

29. R. Walter, in Structure-Activity Relationships of Protein and Polypeptide Hormones, Part I, Excerpta Medica, M. Margoulies and F.C. Greenwood Eds. p.181 1971.

30. G. Jung, E. Breitmaier, W. Voelter, T. Keller and C. Tanzer, Angew. Chem. internat. Edit 9 894 (1970)

31. W. Voelter, G. Jung, E. Breitmaier and E. Bayer, Z. Naturforsch. 26b 213 (1971)

CONCLUSION

This work has provided an opportunity to evaluate the overall uses of NMR spectroscopy in elucidating the conformations of biologically active molecules. From the range of compounds studied a number of conclusions can be drawn concerning the NMR technique itself.

Small molecules such as amphetamines and nucleosides give rise to second-order spectra which can yield information about their conformations in solution.

Complete conformational analysis of large peptides is not often possible by NMR due to the complexity and lack of resolution observed in such spectra. NMR has given information on peptides from chemical shift changes. Hydrogen-bonding in peptides dissolved in non-aqueous solvents, such as DMSO-d_6, can be detected by downfield shifts in the NH resonances. Intramolecular, NH···O=C, hydrogen bonds are detected by lack of change in the chemical shift of NH groups as the temperature is varied. Upfield and downfield shifts in various resonances can be induced by diamagnetic ring currents in aromatic residues. Upfield shifts are usually attributed to stacking of residues.

The study of proteins by NMR is more complex than that of peptides. It is often necessary to study 'reporter' groups. Histidine residues, which are low field shifted,

can serve as such 'reporter' groups. NMR can be used to determine the pK's of the individual histidines in proteins. Changes in Tyr, Phe and Trp residues can be followed when proteins are denatured, if there are few such residues in the molecule under study.

CMR is now proving useful in conformational studies of peptides. It has been shown that chemical shift changes occur upon cyclization of a protected nonapeptide to form oxytocin. It may be possible to detect hydrogen bonds in peptides by observing the carbonyl resonances. Changes in the carbonyl resonances occur upon cyclization of oxytocin and assignment of some of the resonances awaits the study of oxytocin analogues. Experiments are now under way along these lines.